

1997

A Theory of Cortical Neural Processing.

David Timothy Young

Louisiana State University and Agricultural & Mechanical College

Follow this and additional works at: https://digitalcommons.lsu.edu/gradschool_disstheses

Recommended Citation

Young, David Timothy, "A Theory of Cortical Neural Processing." (1997). *LSU Historical Dissertations and Theses*. 6534.

https://digitalcommons.lsu.edu/gradschool_disstheses/6534

This Dissertation is brought to you for free and open access by the Graduate School at LSU Digital Commons. It has been accepted for inclusion in LSU Historical Dissertations and Theses by an authorized administrator of LSU Digital Commons. For more information, please contact gradetd@lsu.edu.

INFORMATION TO USERS

This manuscript has been reproduced from the microfilm master. UMI films the text directly from the original or copy submitted. Thus, some thesis and dissertation copies are in typewriter face, while others may be from any type of computer printer.

The quality of this reproduction is dependent upon the quality of the copy submitted. Broken or indistinct print, colored or poor quality illustrations and photographs, print bleedthrough, substandard margins, and improper alignment can adversely affect reproduction.

In the unlikely event that the author did not send UMI a complete manuscript and there are missing pages, these will be noted. Also, if unauthorized copyright material had to be removed, a note will indicate the deletion.

Oversize materials (e.g., maps, drawings, charts) are reproduced by sectioning the original, beginning at the upper left-hand corner and continuing from left to right in equal sections with small overlaps. Each original is also photographed in one exposure and is included in reduced form at the back of the book.

Photographs included in the original manuscript have been reproduced xerographically in this copy. Higher quality 6" x 9" black and white photographic prints are available for any photographs or illustrations appearing in this copy for an additional charge. Contact UMI directly to order.

UMI

**A Bell & Howell Information Company
300 North Zeeb Road, Ann Arbor MI 48106-1346 USA
313/761-4700 800/521-0600**

**A THEORY OF CORTICAL
NEURAL PROCESSING**

A Dissertation

**Submitted to the Graduate Faculty of the
Louisiana State University and
Agricultural and Mechanical College
in partial fulfillment of the
requirements for the degree of
Doctor of Philosophy**

in

The Department of Electrical and Computer Engineering

by

David T. Young

B.S., Louisiana State University, 1987

M.S., Louisiana State University, 1989

August 1997

UMI Number: 9808791

**UMI Microform 9808791
Copyright 1997, by UMI Company. All rights reserved.**

**This microform edition is protected against unauthorized
copying under Title 17, United States Code.**

UMI
300 North Zeeb Road
Ann Arbor, MI 48103

ACKNOWLEDGMENTS

The author wishes to thank his advisor, Professor Subhash Kak, for patience and guidance throughout all the hard work done for this dissertation. Professor Kak's invaluable assistance has been greatly appreciated. The author would also like to thank Professors Donald Kraft, Jerry Trahan, Jagnathan Ramanujam, Manju Hegde and Mark Davidson for serving on his committee.

Special thanks go to the author's colleagues and friends whose moral support has been a great help. Finally, the author would like to, but can not adequately, express his deep appreciation for the love and encouragement of his parents.

TABLE OF CONTENTS

ACKNOWLEDGMENTS	ii
LIST OF TABLES	v
LIST OF FIGURES	vi
ABSTRACT	x
CHAPTER	
1 INTRODUCTION	1
1.1 Background	3
1.1.1 Neuroscience Background	5
1.1.2 Neural Network Background	7
1.2 Dissertation Overview	11
2 A FRAMEWORK FOR CORTICAL MODELING	13
2.1 The Representation of Uncertainty	14
2.1.1 Chaotic Instability	15
2.1.2 Previous Methods of Representing Uncertainty	17
2.2 Theory Formulation	19
2.2.1 Chaotic Base Condition	20
2.2.2 Stability Bubbles	22
2.2.3 Confined Activation	23
2.3 Cortical Architecture	24
2.3.1 Formulation of the Interconnection Structure	25
2.3.2 Local Cortical Circuits	29
2.4 The Function of the Cerebral Cortex	32
2.4.1 Selective Attention	33
2.4.2 Dynamic Binding	35
2.4.3 Hierarchical Memory	36
2.5 Summary	38
3 CHAOTIC NEURODYNAMIC NETWORKS	39
3.1 Cortical Behavior Modeling	40
3.1.1 Characterization of Behavior	40
3.1.2 The Computational Role of Chaos	41
3.2 Simulated Laminar Structure	43
3.2.1 Lateral Interaction Function	44

3.2.2	Simulation of Chaotic Base Condition	46
3.2.3	Response to Stimuli	47
3.3	Summary	49
4	SELF PARTITIONING CORTICAL STRUCTURES	50
4.1	Cortical Cluster Formation	52
4.1.1	Threshold Variation Study	58
4.1.2	Function Variation Study	60
4.2	Disordered Boolean Circuits	61
4.3	A Developmental Model of the Striate Cortex	66
4.4	Summary	70
5	CONFINED ACTIVATION	74
5.1	Traditional Pattern Completion	75
5.2	Information Driven Dynamics	80
5.2.1	The Preservation of Uncertainty	81
5.2.2	Quiet Neurons	86
5.2.3	Energy as an Estimate of Entropy	88
5.2.4	Collective and Individual Uncertainties	90
5.3	The IDD Model	93
5.3.1	Small Network Examples	97
5.3.2	Larger Simulations	101
5.4	Feature Based Retrieval	103
5.5	Summary	107
6	CONCLUSIONS	108
6.1	Discussion	109
6.2	Future Research	112
	BIBLIOGRAPHY	113
	A SIMULATIONS OF THE LAMINAR STRUCTURE MODEL	118
	B FUNCTION VARIATION : COMPLETE	123
	C FUNCTION VARIATION : REDUCED	132
	D SELF PARTITIONING ON WALSH PATTERNS	141
	E FEATURE BASED RETRIEVAL RESULTS	156
	VITA	159

LIST OF TABLES

2.1 Fractal Dimension of Selected Chaotic Systems	16
E.1 Probe Percent Correlations	157
E.2 Final Percent Correlations (Random)	157
E.3 Final Percent Correlations (FBR)	158

LIST OF FIGURES

1.1	Cortical Structure	6
1.2	Neuron as Threshold Logic Gate	8
1.3	Neural Network Architectures	9
2.1	Typical Neural Processing Task	18
2.2	Frequency Sensitive Connection	26
2.3	Large Scale Cortical Circuit	27
2.4	The Nested Structure	28
2.5	KI and KII Subsets	31
3.1	Lateral Interaction Function	45
3.2	Gain Matrix(Upper Right Quadrant)	46
3.3	Base Response ($y_{4,1}$ vs $y_{3,5}$) : $t=0,40$	47
3.4	Base Response ($y_{4,1}$ vs $y_{3,5}$) : $t=0,20$	48
4.1	Pericolumnar Inhibition	54
4.2	Cluster Formation A	55
4.3	Cluster Formation B : Part 1	57
4.4	Cluster Formation B : Part 2	58
4.5	Threshold Variation Study	59
4.6	Active Percent of Array	60
4.7	Number of Stable Clusters	61
4.8	Recurrent Synchronous Network	62

4.9	Forcing Structure of OR Gates	64
4.10	Another Forcing Structure	64
4.11	Boolean Network with Frozen Elements	66
4.12	Lateral Function for Ocular Dominance Model	69
4.13	Ocular Dominance Surface	70
4.14	Simulated Column Formation : Part 1	71
4.15	Simulated Column Formation : Part 2	72
5.1	The Hopfield Model	76
5.2	The Boltzmann Machine	77
5.3	Hopfield Pattern Completion	79
5.4	Training Set	79
5.5	Continuous Transfer Function	87
5.6	Energy and Entropy	90
5.7	Basic format of the IDD algorithm	95
5.8	Small Network Example	97
5.9	Oscillating Energy	98
5.10	Initial Entropy: Long Decay	99
5.11	Initial Entropy: Rapid Decay	99
5.12	Retrieval Dynamics	101
5.13	Memory Set	102
A.1	$\omega_1 = \omega_2 = \pi/25, \phi = 0, \text{ distance} = 1$	119

A.2	$\omega_1 = \pi/25, \omega_2 = \pi/22, \phi = 0, \text{ distance} = 3$	120
A.3	$\omega_1 = \omega_2 = \pi/25, \phi = \pi/4, \text{ distance} = 3$	121
A.4	$\omega_1 = \omega_2 = \pi/25, \phi = \pi, \text{ distance} = 3$	122
B.1	Complete Function : Set 1	124
B.2	Complete Function : Set 2	125
B.3	Complete Function : Set 3	126
B.4	Complete Function : Set 4	127
B.5	Complete Function : Set 5	128
B.6	Complete Function : Set 6	129
B.7	Complete Function : Set 7	130
B.8	Complete Function : Set 8	131
C.1	Reduced Function : Set 1	133
C.2	Reduced Function : Set 2	134
C.3	Reduced Function : Set 3	135
C.4	Reduced Function : Set 4	136
C.5	Reduced Function : Set 5	137
C.6	Reduced Function : Set 6	138
C.7	Reduced Function : Set 7	139
C.8	Reduced Function : Set 8	140
D.1	Walsh Pattern Response : Set 1	142
D.2	Walsh Pattern Response : Set 2	143

D.3 Walsh Pattern Response : Set 3	144
D.4 Walsh Pattern Response : Set 4	145
D.5 Walsh Pattern Response : Set 5	146
D.6 Walsh Pattern Response : Set 6	147
D.7 Walsh Pattern Response : Set 7	148
D.8 Walsh Pattern Response : Set 8	149
D.9 Walsh Pattern Response : Set 9	150
D.10 Walsh Pattern Response : Set 10	151
D.11 Walsh Pattern Response : Set 11	152
D.12 Walsh Pattern Response : Set 12	153
D.13 Walsh Pattern Response : Set 13	154
D.14 Walsh Pattern Response : Set 14	155

ABSTRACT

This dissertation puts forth an original theory of cortical neural processing that is unique in its view of the interplay of chaotic and stable oscillatory neurodynamics and is meant to stimulate new ideas in artificial neural network modeling. Our theory is the first to suggest two new purposes for chaotic neurodynamics: (i) as a natural means of representing the uncertainty in the outcome of performed tasks, such as memory retrieval or classification, and (ii) as an automatic way of producing an economic representation of distributed information. We developed new models, to better understand how the cerebral cortex processes information, which led to our theory. Common to these models is a neuron interaction function that alternates between excitatory and inhibitory neighborhoods. Our theory allows characteristics of the input environment to influence the structural development of the cortex. We view low intensity chaotic activity as the a priori uncertain base condition of the cortex, resulting from the interaction of a multitude of stronger potential responses. Data, distinguishing one response from many others, drives bifurcations back toward the direction of less complex (stable) behavior. Stability appears as temporary bubble-like clusters within the boundaries of cortical columns and begins to propagate through frequency sensitive and non-specific neurons. But this is limited by destabilizing long-path connections. An original model of the post-natal development of ocular dominance columns in the striate cortex is presented and compared to autoradiographic images from the literature with good matching results. Finally, experiments are shown to favor computed update order over traditional approaches for better performance of the pattern completion process.

CHAPTER 1

INTRODUCTION

This dissertation views cognitive tasks as often uncertain in their outcome and that this uncertainty is represented by a unique mechanism carried out by the cerebral cortex; the grey tissue making up the outermost layers of the brain. We propose that low intensity chaotic activity in the cerebral cortex represents the a priori uncertain base condition that exists before information is supplied by input. This view of our theory expresses a new interpretation of the role of chaotic oscillations in neurodynamic activity. Fundamental mechanisms underlying how the brain focuses its attention and organizes its memories in a hierarchical structure that binds together separate but related activity into a useful whole, are some of the important questions related to the oscillatory nature of cortical processing.

This dissertation also considers the representational form given information in the cerebral cortex to be important in the development of its structure. The aim of the developmental process is to partition computing resources in a hierarchical manner that is well adapted to the kinds of data represented by input patterns likely to be encountered. Our theory views cortical structures as being formed dynamically as well as developmentally and suggests a similar mechanism of lateral interaction is responsible for both. The long term influence of dynamic processes that respond quickly to input allow characteristics of the input environment to shape the developmental process that partitions computing resources of the cortex.

A recent trend in neurocomputing is toward physiologically realistic models of brain function [1, 5, 15, 37, 47, 48]. The oscillatory nature of brainwave activity is especially prominent in many of these new models and is a topic in neuroscience that receives a great deal of attention [12, 13, 18, 24, 29, 38, 39]. Chaotic neurodynamics, as well as oscillations in general, are being seen as likely ways to advance beyond present limitations.

The rest of our theory concerns itself with the formation of stable activity when information is applied by input and how this is automatically organized into a hierarchical structure. The final form of this structure is considered by our theory to be largely influenced by the content of the input data. This is consistent with some linguistics theories of Human language acquisition as well as with observations of the postnatal development of ocular dominance columns in the striate cortex [25].

The approach taken in our investigation of the cerebral cortex, which led to our theory, is to explore both the development of cortex structures as well as characteristics of its neurodynamic behavior. Therefore, we posed two questions: (i) "How does the cerebral cortex organize itself to process information?", and (ii) "How is information represented in the neurodynamics of the brain?" We believe these are related questions that are best examined together when attempting to formulate physiologically realistic models.

This dissertation draws on a physiological knowledge of the brain to address an important issue overlooked by traditional neural computing schemes. Specifically, traditional neural networks report results without any indication of the uncertainty with which they are reached. Without means of attaching a measure of uncertainty to the results, perfect reliability could be erroneously assumed. It is argued that

the utilization of uncertainty should be studied from the standpoints that its arbitrary elimination is not always advantageous and that its persistence is biologically plausible.

In addressing the representational form given data by traditional schemes, this dissertation expands on a recent interpretation of the usefulness to which chaotic dynamics may be employed [7, 8, 9, 47], while keeping it in context with the issue of utilizing uncertain results.

Understanding gained through modeling specific brain functions can help in the design of artificial neural networks which mimic those functions. Relating these functions together leads toward a more comprehensive understanding of the brain's ability to perform tasks that have, until now, evaded our best technological efforts.

1.1 BACKGROUND

A great deal of knowledge about the brain has already lead to much progress in neuroscience and artificial neural network modeling. But still, so much more about the brain is not well understood. From neurophysiology to neuropsychology, the many and diverse fields of neuroscience testify to the formidable task of understanding the brain. Some of this material will be reviewed briefly below, along with a background of neural network modeling, to provide the context and terminology used throughout this dissertation [6, 34, 44, 51].

Before doing this, we relate our work to the contributions of several leading views, including the organizing principle of Mountcastle [32], an oscillation based model of selective attention by Crick and Koch [4], the role of chaotic dynamics in olfactory perception proposed by Freeman [7, 8, 9, 10, 11], a nested structure

formulated by Sutton [48], and others. First we consider differences of our work in regard to those that study cortical processing from a neuroscience point of view, then in regard to some new physiologically realistic artificial neural network models.

Structures (minicolumns and microcolumns) that are smaller than the standard column-like structures of the cortex, and the mechanism of pericolumnar inhibition given to explain their existence, are concepts suggested by Mountcastle [32]. We pick up on the idea of cortical microcolumns but adapt pericolumnar inhibition in a different way that allows us to partition the cortex on the basis of stable oscillation versus chaotic activity. The mechanism for selective attention proposed by Crick and Koch [4], is based on observations of synchronized oscillations in the brain near 40 Hz. Our theory proposes a different mechanism responsible for synchronization among remote regions of the brain.

The physiologically realistic model of olfactory function developed by Freeman [7, 8, 9, 10, 11] provides an interpretation for how the brain might make use of chaotic oscillations. Our theory is different in that we view complex oscillation as produced by uncertainty instead of a way to represent more information than that captured in simple periodic oscillation. We describe Freeman's interpretation in more detail in Chapter 3 and discuss aspects of his model in Section 2.3.

In a model proposed by Sutton [48] neurons are organized in a series of clusters, one within another, to form a nested hierarchical structure based on different classes of neuron types determined by their respective connectivity patterns. We expand this somewhat by allowing neural activity as well as connectivity to be the basis of clusters formed and cast it within a developmental context. By contrast, Sutton suggests no mechanism for how clusters are formed.

The formation of clusters by agglomeration due to the operation of the so called “Mexican hat” function in a two dimensional array is well known and associated with Kohonen’s work on feature maps [23]. Our contribution is to consider the cortex as having several functions with different spatial resolutions that form the clusters suitable for hierarchical organization. As we model it, some form over a long period of cortical development while others are temporary and allow for dynamic reconfiguration.

Finally, a mechanism presented by Kauffman [22], disordered boolean circuits, illustrates how somewhat randomly constructed arrays of boolean logic gates can spontaneously form functionally isolated “islands” (clusters) of oscillating activity. Clusters in our theory are the result of the agglomeration of neurons and neural circuits with similar behavior. This makes our approach more responsive to order found in neural activity than one that relies on random connectivity. We believe that only in this way will the resulting structure be best adapted to process the kind of data it is likely to encounter.

1.1.1 NEUROSCIENCE BACKGROUND

Consider for a moment the coordinated electrochemistry of billions of specialized nerve cells, most of which are found in the cortex, and the highly organized and amazingly intricate interconnections between them that make up what is, without a doubt, the most complex structure known. The brain is remarkably efficient in its construction. It is estimated that the human cortex contains over 10 billion neurons that communicate with one another through more than 60 trillion neural connections (or synapses). Six identifiable layers can easily be distinguished within almost any

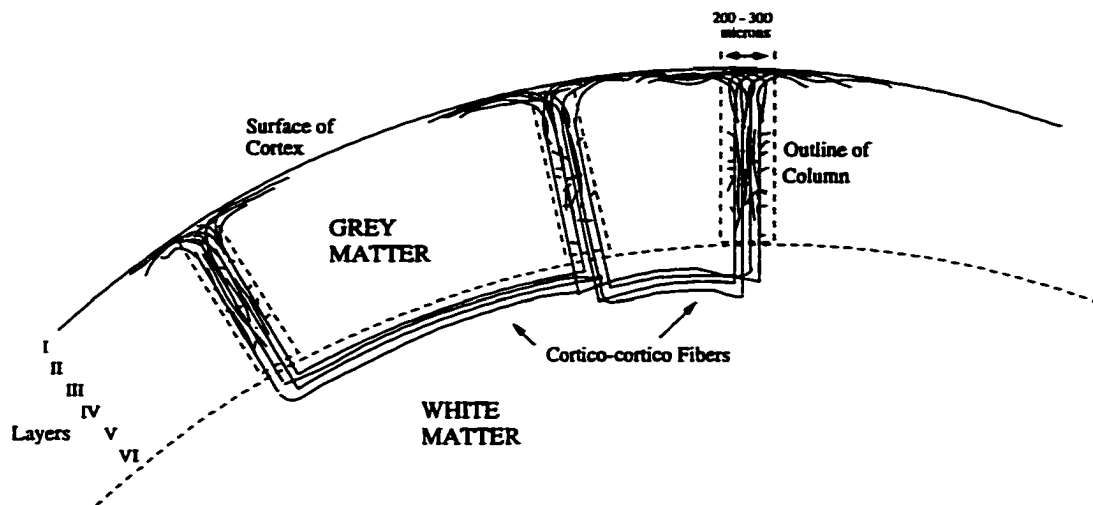


Figure 1.1: Cortical Structure

region of the cortex. These distinctions are mainly based on population distributions of the various types of nerve cells and their morphology. Most neurons within a given layer are connected to other nearby neurons of the same layer. However a special type of cell, known as the *pyramidal nerve cell* because of its shape, provides the cortex with connections that project down through the layers. Pyramidal cells sometimes help to form vertical structures referred to as *cortical columns*, as seen in Figure 1.1. These columns show that a high level of connectivity not only exists between nearby neurons of the same layer but also vertically, across layers through synapses predominately formed with pyramidal nerve cells.

Interaction among neurons occurs not only at the level of the local neuron assembly but also globally. Note that pyramidal cells also communicate between remote regions of the cortex through what are called *cortico-cortical fibers*. Not shown are the many additional indirect connections made by other pyramidal cells through brain structures such as the thalamus. Centrally located, the thalamus is distinct from the cortex and is thought to help globally coordinate cortical function.

Besides the vertical organization of the cortex, there is also an important lateral structure as well. It has been hypothesised for more than a century, and is now well known, that spatially distributed correlations exist within several cortical regions that relate to features in sensory input [23]. Visual, acoustical and tactile information are all examples of spatial mappings within cortical regions.

The efforts of neuroscientists necessarily include attempts to model biological neural systems through computer simulations. These efforts dovetail nicely with those of computer engineers who wish to push forward the state of the art of computer design. The next section provides an overview of some of these efforts using artificial neural network modeling [16].

1.1.2 NEURAL NETWORK BACKGROUND

The beginning of the modern era of neural networks is often associated with the 1943 publication of McCulloch and Pitts [28]. Interestingly, this corresponds to the same period of time in which von Neumann developed the first general purpose electronic computer, the ENIAC, during the years from 1943 to 1946. Today virtually every computer that the average person is likely to encounter can trace its architectural lineage back to the von Neumann model. While descendants of the ENIAC appeared rapidly in the years that followed its development, the alternative view of computing, through artificial neural networks, took longer to catch on. Contributions by Minsky [30], Rosenblatt [42] and others provided some important advances in the field during this time, but it was not until 1982 when J.J. Hopfield [17] published his idea of what became known as the Hopfield model that the field began to enjoy the popularity it sees now.

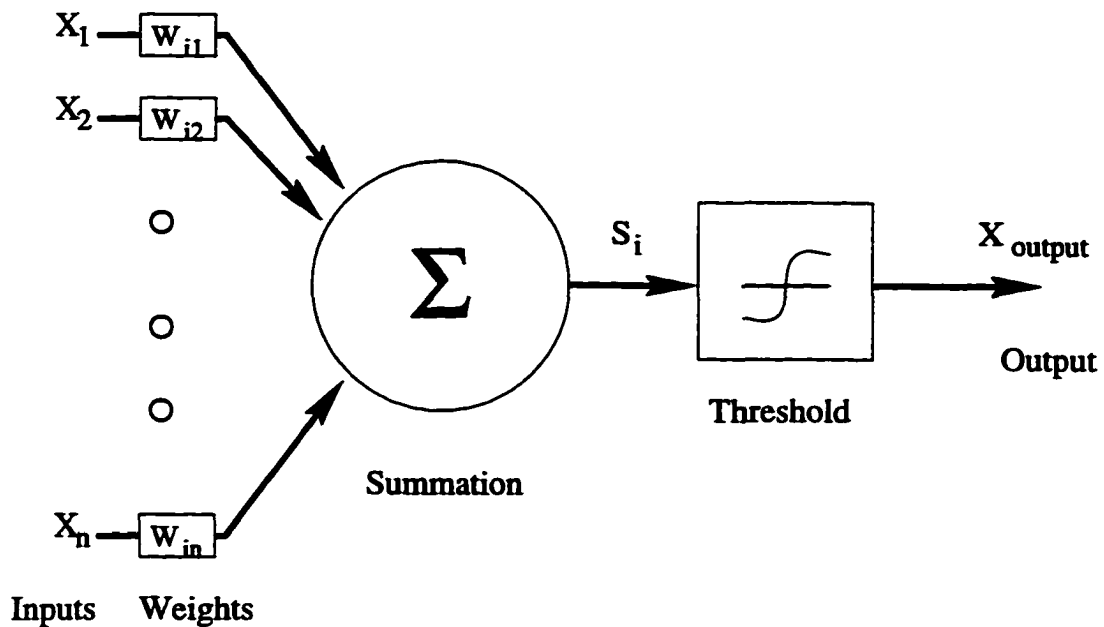


Figure 1.2: Neuron as Threshold Logic Gate

Important to physiologically realistic models is knowing how closely to follow the source of inspiration. As mentioned, the brain performs certain kinds of tasks with greater speed and efficiency than by any artificial means. But, oddly, it accomplishes this with neurons that are believed to operate many times slower (milliseconds verses nanoseconds) than the logic elements of typical electronic devices. Obviously, it would be meaningless to slow electrical components just to be realistic. After all the brain is a living tissue that does much more than perform its computational task. It grows, metabolizes nutrients and protects itself from diseases as well. Attempts to model the behavior of a neuron, therefore, inevitably assume some degree of simplification. Traditionally neurons are modeled as simple threshold logic gates such as the one depicted in Figure 1.2. This figure shows a nonlinear threshold function performed on the weighted sum of n binary inputs. The output X_i is also binary. Though crude, this binary model has been able to

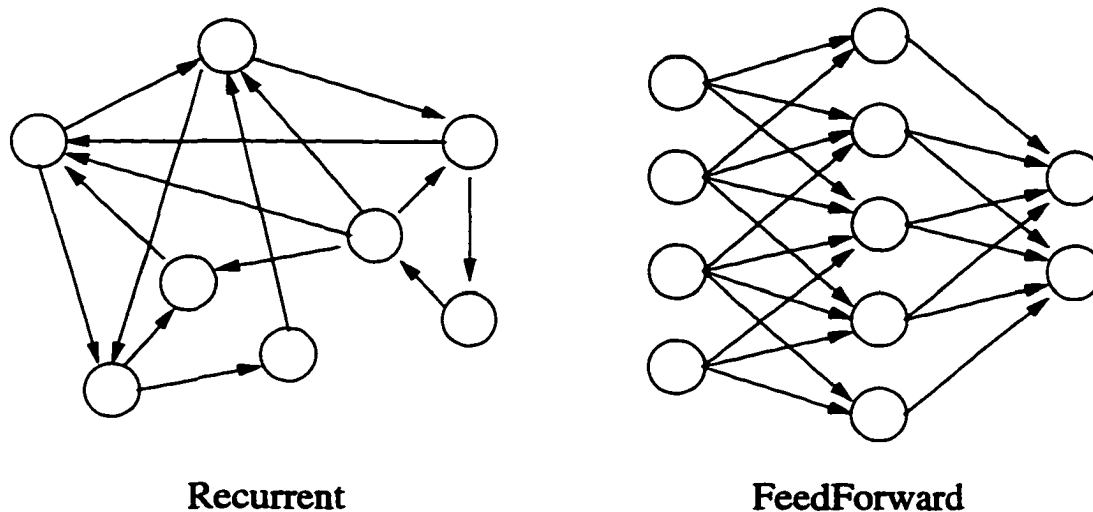


Figure 1.3: Neural Network Architectures

uncover methods for learning correlated relationships in devices such as the Perceptron [42]. Early concepts of brain function have also ascribed symbolic or abstract meaning to individual neurons. This gave way to the distributed representation of data which took form in feedforward and recurrent structures. A recurrent structure must include at least one feedback path, as illustrated in Figure 1.3. This introduced the important concept of stabilization to network dynamics. Stable patterns of activity can be associated with learned items or objects of memory in networks such as that made popular by J. J. Hopfield [17], which made such things as content addressable memory possible. At this point discrete valued network elements that were updated at discrete time intervals were adequate to capture this basic kind of behavior. Discrete systems are usually described by an equation of the form

$$X_{t+1} = \mathcal{F}(MX_t + bias), \quad (1.1)$$

where X_t is the system state vector at time t , M is a matrix of connection weights and $bias$ is a constant offset. But many unanswered questions remained that seemed to require another approach. Some limitations that emerged include the occurrence of spurious stable states and errors in recall. A spurious state is a stable condition of the system, as are memories. However, a spurious state corresponds to none of the intended learned memories of the system. It exists purely as an unwanted by-product of the learning procedure. Errors in recall, on the other hand, produce learned memories as the final result, only the memory recalled is not the correct one.

In addition to updates at discrete time intervals, system states may also be updated continuously. The following equation depicts a continuous system:

$$\frac{d^2Y}{dt^2} + \frac{AdY}{dt} + BY = \mathcal{G}(Y) + I(t), \quad (1.2)$$

where Y is the system state at time t , \mathcal{G} is a nonlinear operator and $I(t)$ is an input function. At first, Continuous time dynamic systems were mostly seen as an unnecessary complication of their discrete counterparts. Since the influence of a sigmoidal nonlinear operator on a real number is to discretize the value, the two approaches were essentially equivalent. Any attempt to model the individual action potentials, or spikes, of a biological neuron was thought to be even more unnecessary. It was believed that only the average rate that a neuron fired was of any importance. As it turns out, this is short-sighted. A number of results have since clearly shown that a great deal more information is encoded within a neural spike train [35, 40, 41]. Efforts to simulate this activity can be divided into those

dealing with periodic oscillators [14, 15, 33] and quasi-periodic and/or turbulent chaotic activity [7, 8, 9, 10, 11, 43, 46, 47, 52]. Not all oscillatory models simulate the neural spike train, as we shall see, but in any case the dynamic behavior is quite rich. These models now are beginning to demonstrate applications beyond that of mimicking, in general form, neural spike trains.

1.2 DISSERTATION OVERVIEW

The main contribution of this dissertation is a new theory of cortical neural processing that better captures some of the computational characteristics of the brain by providing a realistic interpretation of the interplay between chaotic and stable neurodynamics. The objective, from an engineering point of view, is to use this enhanced understanding to design new kinds of artificial neural networks. Our theory is summarized in Chapter 2 along with a discussion of the relevant issues.

In Chapter 3, our method of representation that expresses uncertainty as a *chaotic base condition* is presented. Two mechanisms that lead to neurodynamic instability (the tendency to depart from periodic oscillation) are described and two views of the computational role of chaos are discussed. A model is presented that simulates a *laminar structure* and attempts to duplicate the lateral interaction within a cortical column. It is used to demonstrate the *chaotic base condition* and the formation of *stability bubbles*.

Chapter 4 develops our theory further by investigating the agglomeration of neurons into clusters due to their lateral interaction along the cortex. Both transient and static clusters are considered. The operation of a two-dimensional spatial function is studied experimentally. It is used to model the receptive field of most cortical

neurons as well as the *pericolumnar inhibition* proposed by Mountcastle [32]. The response to several random and regular patterns of initial activity are considered. Next, a developmental model of the cortex is proposed to characterize the formation of ocular dominance columns in the striate cortex. The results of the model are compared with autoradiographic images found in the literature [25] of the actual developing tissue.

The task of presenting economic representations is examined in Chapter 5 by exploring the *limited activation* described by our theory. Our method of *Feature Based Retrieval* is cast as a means of identifying minimal representations of distributed memories. Experimental evidence showing improved performance of our method over that of another pattern completion method is presented. It is speculated that the chaotic base condition of our theory provides the necessary ensemble information to form economic distributed representations.

Finally, a summary and discussion of the work presented in this dissertation is provided in Chapter 6. Issues related to the performance of cognitive tasks are also discussed along with the opportunities for future research that our work has created.

CHAPTER 2

A FRAMEWORK FOR CORTICAL MODELING

In this chapter we put forth an original interpretation of how the cerebral cortex accomplishes key aspects of its function. Our theory of cortical neural processing brings together, in a novel way, issues relevant to the realistic modeling of brain function to formulate a useful view of the structure and behavior of the cerebral cortex. Cortical structure varies significantly from region to region, but in many ways similarities also exist among them. We consider only general structure and behavior features that we believe are commonly repeated throughout the cortex. The framework we present establishes a role for chaotic neural activity based on the need to represent the uncertainty of the outcomes of performed tasks. Our theory is not one specific model, though we develop models in later chapters to illustrate aspects of it. The ideas of our theory are meant to serve as a guide for a variety of future artificial neural network models.

Our theory has six parts: (i) we view low intensity chaotic activity as the a priori base condition of the cerebral cortex; (ii) we suppose that information supplied by input drives bifurcations back toward less complex (stable) oscillations; (iii) we suggest that transient stable activity agglomerates into temporary clusters; and (iv) we further suggest that stable oscillations spread to remote regions of the cortex, creating large scale synchronized activity; (v) we suppose that the spread of stable oscillations is limited by the destabilizing influence of long-path connections; finally, (vi) we believe that the long-term effect of repeated stable fragments of synchronized

activity, during early developmental growth, influences the final form of the cerebral cortex.

2.1 THE REPRESENTATION OF UNCERTAINTY

The neurodynamics of the brain describe a complex and ever changing pattern of oscillating electrochemical activity. It is well known that, at any given moment, the majority of the brain's neurons produce a low intensity non-periodic waveform. From the earliest recordings made of brainwaves to the most sophisticated micro-electrode and magnetic scanning techniques available today, this *background activity*, as it is called, has been interpreted as noise and filtered from stronger signal-like responses. In recent decades, interest in the mathematics of chaos has brought new tools and a broader understanding to the analysis of neural time series recordings. These tools have only now begun to lead theoretical studies toward new interpretations about the role of chaotic neurodynamics.

One concept takes a view completely opposite the conventional perspective that chaotic neural activity is noise. It supposes that the complexity of a chaotic neural response serves to encode signals, rich in information, coming from the body's many input receptors [7, 8]. According to this concept, chaos is actually believed not to be noise but the signal itself. Under this interpretation, a signal of high fractal dimension corresponds to a complex environmental stimulus. However, the signal measured to have highest dimension is in fact the so called background, which is of low intensity and generally does not evoke a response at all [47]. Our theory proposes a different interpretation of neural chaos. The view we suggest places the role of chaotic neurodynamics between the two extremes of signal and noise.

2.1.1 CHAOTIC INSTABILITY

We assert that the unstable nature of chaotic activity is the principle factor for its incorporation into the natural design of the brain. Our purpose is to relate the instability of chaotic neurodynamics to a natural means of measuring uncertainty. The more unstable a signal is, the less reproducible it will be, and therefore it is also less reliable. According to our theory, chaotic neural responses are understood as being produced because of uncertainty in the results of the tasks performed by the brain. This view comes from the fact that unpredictability in chaotic systems is a quantitatively measurable value. We begin by considering a measure known as *fractal dimension*, a quantitative property of a set of points in an n-dimensional space characterizing the motion of a chaotic system. Specifically, it measures the extent to which the points fill a subspace as the number of points becomes very large. One definition of fractal dimension is d_I , the well known information dimension [31],

$$d_I = \lim_{\epsilon \rightarrow 0} \frac{\sum_{i=1}^N P_i \log P_i}{\log \epsilon}. \quad (2.1)$$

To intuitively understand Equation 2.1, consider the set of N_0 points representing a trajectory of the chaotic motion of a selected system. Suppose we cover these points with a set of N cubes of size ϵ . The probability, P_i of finding a point in the i^{th} cube is given as

$$P_i = \frac{N_i}{N_0}, \quad (2.2)$$

where N_i is the number of points in the i^{th} cube, N_0 is the total number of points in the set and $\sum_{i=1}^N P_i = 1$.

We interpret Equation 2.1 by relating it to the information theoretic concept of *entropy*. Defined by Shannon [45], the *entropy* of a discrete random variable, x , with a range of N values is given by the expression

$$H(x) = - \sum_{k=1}^N p_k \log p_k. \quad (2.3)$$

Entropy is a measure of the average amount of information conveyed by the event $x = x_k$, where x_k is a particular value of the random variable x and p_k is the probability of the event. Comparing Equations 2.1 and 2.3, it is easy to see why this measure of fractal dimension (d_f) is called *information dimension*. The probability P_i is related to p_k of Equation 2.3 and a point in the i^{th} cube of size ϵ is considered as the random variable x having the value x_k . In other words, we are describing the information conveyed by finding a point in the i^{th} cube as its size, ϵ , goes to zero.

Fractal dimension is useful because it provides a way to compare the unpredictability (instability) of chaotic systems. Table 2.1 is from the literature and lists fractal dimensions of known chaotic systems based on a measure of *correlation dimension* [31].

Table 2.1: Fractal Dimension of Selected Chaotic Systems

Name of System	Dimension
Henon map	1.26
Logistic map	1.538
Lorenz Equations	2.06 ± 0.01

Just as there is more than one measure of fractal dimension (information, correlation, etc.), there are also more ways to quantify chaotic behavior. Phase diagrams

and Fourier transforms are used in most of the analyses we perform, but the information dimension is discussed here so that we may relate it to uncertainty.

Before the event $x = x_k$, there is an amount of uncertainty. After its occurrence, there is a gain in the amount of information. Therefore, information is related to uncertainty. From *instability* to *fractal dimension* to *information* to *uncertainty* we establish a clear motivation for a natural representation of uncertainty by chaotic instability.

2.1.2 PREVIOUS METHODS OF REPRESENTING UNCERTAINTY

Before presenting our approach, let us examine sources of uncertainty and existing ways to represent it in traditional artificial neural networks. We pose the simple problem of a content addressable memory (CAM) to represent a typical neural processing task as it is implemented by traditional artificial neural network schemes. The nature of the task is not important to this particular discussion and could, for example, be posed equally well in terms of the classification problem. What is more, the type of the neural structure and the way in which its connections are learned are also unimportant. Uncertainty of outcome is as relevant to feedforward structures as it is to fully connected recurrent structures, regardless of the learning algorithm employed.

Consider the diagram of Figure 2.1 depicting an artificial neural network which has learned M memories and produces a response to an applied probe. Ideally, the response will be a stable pattern of activity representing a memory most closely matched by the content of the probe. If the probe is ambiguous, in the sense that

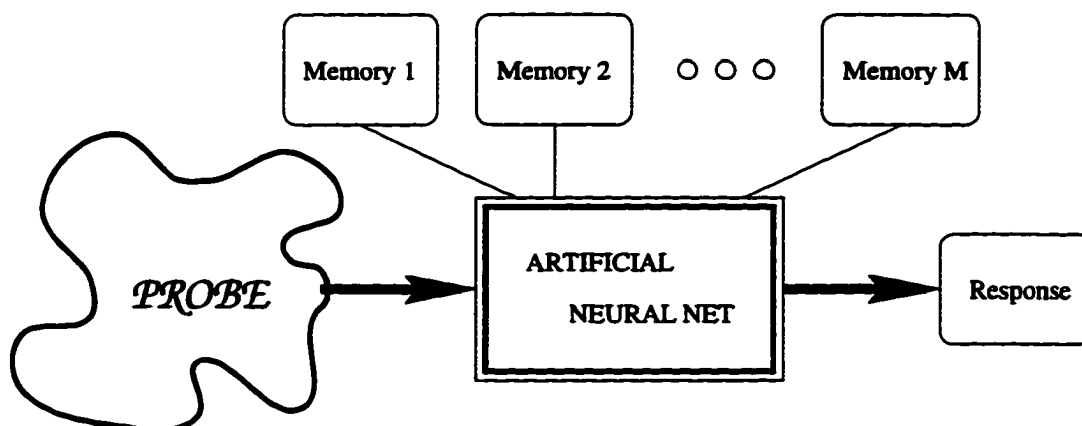


Figure 2.1: Typical Neural Processing Task

it does not distinguish between two or more of the learned memories, the result is reached with uncertainty.

Definition 2.1: An ambiguous probe is defined as one that correlates equally well with two or more learned memories.

In such a case, the response may be one of the equally best matched memories, arbitrarily selected by the CAM retrieval process, or it may be a linear combination of the memories best matched by the probe. The latter of these occurs whenever the learning process has spuriously created a stable state of the linear combination. Not all learning schemes will produce spurious memories.

With either outcome, the response will be interpreted as being completely reliable unless a measure of the uncertainty with which it was reached is somehow attached to the response. How should uncertainty be expressed? One of the best existing approaches involves adding onto each memory a *tag* of M bits that identifies the response as being a specifically learned memory, a linear combination of memories or the complement of a memory. (Complements of stable points are sometimes also stable.) Each bit of the tag is associated with exactly one of the learned memories.

If a stable final state is reached with more than one active bit in the tag, this represents an uncertain result.

Two or more active tag bits (active = 1, inactive = 0) do not express which of these identified memories more closely match the probe. They merely show that the match is sufficient to cause the tag to be active. But tag bits with a graded response, of say the range from 0 to 1, will supply this information.

These schemes still do not convey the uncertainty of individual neurons. To do this, each neuron of the outcome would have to produce a graded output. But a stable final state with a graded response could itself be a memory. Such a scheme would not utilize its potential storage capacity and it is doubtful that the brain employs such methods.

2.2 THEORY FORMULATION

We present a theory that describes the structure and behavior of the cerebral cortex. Our theory, in regard to cortical behavior, has three parts: (i) The low intensity chaotic background present throughout the cerebral cortex is treated as the base condition from which all other activity emerges; (ii) Isolated bubbles of activity that appear against the background exhibit lower fractal dimension as a result of having less interaction with the surrounding cortex; and finally, (iii) fragments of *limited activation* confine the spread of activity from involving entire distributed representations. This last part is seen as being needed to prevent the complexity of a hierarchical memory, for example, from adding complexity to the neurodynamic response. It also provides a natural means of producing economic representations that are important to such cognitive tasks as feature extraction.

Our theory, in regard to structure, divides the cortex into four organizational levels: (i) Local cortical circuits (microcolumns), (ii) Columns, (iii) Regional circuits, and (iv) Global circuits. Each of these are discussed in more detail in Section 2.3. For now, we concentrate on the above three aspects of cortical behavior.

2.2.1 CHAOTIC BASE CONDITION

We begin with an approximation of cortical neurodynamics. Let $\Psi_{u,v}$ be a time-varying surface function defined parametrically over the entire cerebral cortex, such that the point (u, v) on the parametric surface \mathcal{S} corresponds to the point (x, y, z) on the cerebral cortex by the transformation $\langle x(u, v), y(u, v), z(u, v) \rangle$. The independent variables u, v are discrete; $u_{i+1} = u_i + \Delta u$ and $v_{i+1} = v_i + \Delta v$ define the spatial resolution assumed by the model. The variable t represents time, which is continuous. The transformation is needed to preserve spatial relationships among points on the cortex and the resulting interconnection structure. Spatial relations determine the kinds of interconnections, and to some degree their strengths as well as temporal delays and periods of integration.

For every point (u, v) defined above, we ascribe a vector of time-varying functions representing a neuron assembly contained within the small area $\Delta u \Delta v$. Let the vector

$$Y_{u,v} = (y_{u,v,1}, y_{u,v,2}, \dots, y_{u,v,n_{uv}}) \quad (2.4)$$

represent the set of neuron output values of the neuron assembly, where n_{uv} is the size of the vector (the number of neurons in the assembly at the coordinate (u, v)). We next define a system of equations to be k_{th} order partials taken with respect to t , as shown below, where the vector functions \mathcal{G} and \mathcal{H} map the elements of Y onto

itself through the cortical interconnection structure and $\mathcal{I}(t)$ is the input applied to the system.

$$A_k \frac{d^{(k)}}{dt^k} Y_{u,v} + A_{k-1} \frac{d^{(k-1)}}{dt^{k-1}} Y_{u,v} + \dots + A_1 \frac{d}{dt} Y_{u,v} + A_0 Y_{u,v} = \mathcal{G}(Y) + \mathcal{H}(Y) + \mathcal{I}(t) \quad (2.5)$$

The time constants $A_k \dots A_0$ are assumed to be uniform for all cortical neurons represented by this model. (A_0 represents the natural frequency of all cortical neurons, A_1 their decay rate, etc.) The term A_k is assumed to be unity after factoring it from the equation, and in most cases, it is necessary to include terms only up to $k = 2$. The terms of \mathcal{G} may include nonlinear operators such as threshold or saturation functions as well as time delay and integration. This function is described in detail in Chapter 3. The function \mathcal{H} is used to express lateral interaction among neurons of relatively close proximity. This function models the lateral receptive field of most cortical neurons and is often referred to as the *Mexican hat* function because of its shape [23]. It may be approximated as the *sinc* function, defined for one dimension as $\text{sinc}(x) = \frac{\sin(\pi x)}{\pi x}$. Another way to model this function is to use a variation of the Bessel function. The Kaiser function, defined as the Bessel function of the first kind divided by the modified Bessel function of the first kind, $\frac{J_0}{I_0}$, is used in a model we developed in Chapter 3 that demonstrates generation of the base condition. It also is used in our investigation of *self-partitioning* through lateral interaction that appears in Chapter 4.

The surface function Ψ is related to Y as the instantaneous mean of its vector components.

$$\Psi_{u,v} = \frac{1}{n_{uv}} \sum_{i=1}^{n_{uv}} y_{u,v,i} \quad (2.6)$$

This is similar to the electromagnetic potentials, such as the excitatory post-synaptic potential (EPSP) that are measured using micro-electrode recording methods.

2.2.2 STABILITY BUBBLES

A major feature of this theory is the way in which uncertainty is depicted in the phase-space portraits of chaotic neurodynamics. In this depiction, isolated fragments of simple periodic motion emerge from out of a chaotic background. We define a *stability bubble* as an isolated area in \mathcal{S} over which Ψ yields a stable time series. Any point in \mathcal{S} not covered by a stable bubble is assumed to yield a chaotic time series.

The periodic activity of a bubble, being of a lower fractal dimension than the background is considered to be less uncertain and therefore conveys the fact that information has been received. The view is that information must be supplied to the system to drive a bifurcation into low dimensional behavior, observation of a simple periodic waveform conveys this same amount of information. Another analogy one may use is that of receiving an unlikely symbol sent from a code book of symbols used for communication, where the background represents the code book.

The clusters are isolated from surrounding neurons by the lateral function \mathcal{H} and appear as bubbles of stable periodic activity against an otherwise chaotic background. The larger a bubble, the more hierarchical links there are leading into and out of it. Hierarchical links are generally longer path connections than those that

occur laterally. Most are made by pyramidal cells that have long axons. Long neural pathways create a delay and integration of the activity traveling down these axons. Delay and integration are both nonlinear operators that add to the complexity of the response. A small, well isolated bubble is most likely to bifurcate into periodic activity.

2.2.3 CONFINED ACTIVATION

It is necessary for this theory to limit the spread of activation from involving large regions of the cortex at any one time. This is in fact physiologically plausible since any synchronization that might occur across large distances of the cortex does so only transiently, except in the case of epileptic behavior, which is considered abnormal.

Our theory allows complex memory structures, even hierarchical arrangements, in spite of this requirement. As new stability bubbles form, others must return to the background state to keep a balance in the dynamical system.

Suppose a topological ordering is established at each of several levels of a distributed hierarchical memory structure. A level is physically represented by a two-dimensional spatial array of neurons composing a connected region of the two-dimensional surface of the cerebral cortex. Topological order is based upon the relative spatial position, within the cortex, of individual neurons, or groups of neurons, and a regular lateral feedback interconnection function as well as asymmetric hierarchical connections. Examples of these structures are detailed in Chapter 5. Clusters of neurons, their size and spatial position determine topographical patterns that may be learned by training the hierarchical links.

Principles of pattern completion methods allow distributed representations to be expressed by only a fraction of the full memory. From work we have done on the pattern completion problem, it is shown that the order elements are updated is sufficient to identify full distributed representations [54]. A demonstration of improved pattern completion performance obtained through updating rules that we developed can be seen in Chapter 5.

2.3 CORTICAL ARCHITECTURE

The structure of any circuit determines much of the character of its function. It is reasonable to consider the organization of the brain before characterizing its neurodynamics. The view taken in this dissertation on the functional organization of the brain is that it is composed of a hierarchy of levels. There are believed to be many functional levels that work together in a very well coordinated manner.

A simple list of the brain's various organs include the cerebrum, cerebellum, brain-stem, etc. At this level of organization, the largest of these is also the most recognizable part of the brain, the cerebrum. Its overall mass is divided into two hemispheres. Each has a number of visible divisions (large folds in its surface) forming what are called lobes. Any cross section cut perpendicular to the surface reveals even more structure. Two kinds of material are immediately seen. *White matter* is the name given the material that fills up the central volume of the cerebrum. *Grey matter* surrounds it much like bark covers a tree. The name, cortex, means bark.

Toward the lower end of this hierarchy, brain functions deal with information in its rawest form. Much of the initial processing is performed by brain structures such as the retinal neural network in the eyes, the olfactory system responsible for

a sense of smell and the aural process that deals with hearing. These are among the most studied regions of the brain because of the ability researchers have to directly influence them by stimulating their respective sensory receptors.

2.3.1 FORMULATION OF THE INTERCONNECTION STRUCTURE

In this section we elaborate on the function \mathcal{G} responsible for hierarchical interaction in our theory. We begin with the surface function $\Psi_{u,v}$ that we defined in Chapter 2, and extend our discussion downward through the vertical dimension of the cerebral cortex. A variety of local cortical circuitry lies just beneath the surface at every point (u, v) . If an area of size Δu by Δv is completely cut off from the rest of the brain, we assume it will oscillate in a stable periodic fashion.

Definition 2.2: We define a *cortical microcolumn* as a small vertical structure capable of resonating at some natural frequency.

The name of this structure and its inspiration are due Mountcastle [32] who first speculated on its existence. It is adapted here with the addition that it act as a resonating circuit of some stable frequency. Its stability may be disturbed by interaction with activity from elsewhere in the brain, through the hierarchical function G . The microcolumn is considered by us to be the smallest functional unit of the brain above the individual neuron.

A structure somewhat larger than the microcolumn is the column. The boundaries of columns are fixed during the development of the brain, which begins before birth. A zone of inhibited neurons surrounds each column demarcating its extent and isolating it from the activity of neighboring columns. Isolation is important for two reasons: (i) it establishes a partition of the cortex by dividing it into distinct

functional groups, and (ii) it prevents the activation at one location from spreading throughout the entire cortex, as occur in epileptic seizures.

An average is computed over a column-wide region of the cortex by the broad dendritic span of a nonspecific pyramidal neuron. Frequency sensitive inter-neurons, depicted as circles in Figure 2.2, were theorized by Crick and Koch [4] to be involved in an oscillatory basis of the attention process. These interneurons in our theory re-

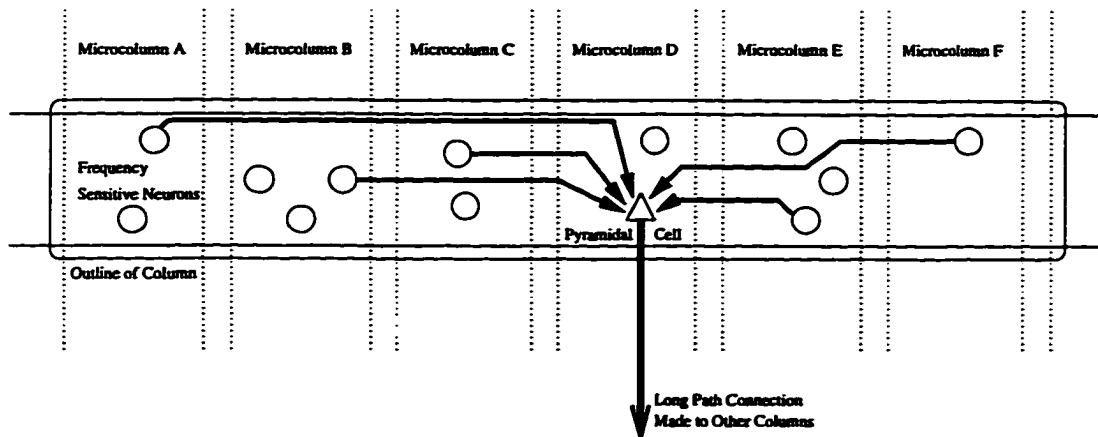


Figure 2.2: Frequency Sensitive Connection

pond when a microcolumn is permitted to resonate at its natural frequency without disturbance from other sources.

The output of pyramidal cells such as these have long axonal processes that reach out to distant regions of the cortex as well as other structures, such as the thalamus, that are not even found in the cortex. These long neural pathways introduce delays as well as temporal integration due to the propagation time down the axon path.

From this organization principle we speculate on the existence of transiently reconfigurable large scale cortical circuits such as depicted in Figure 2.3. In this figure five columns are shown with a certain type of local circuit illustrated within each. Input is applied to columns I and II only in this particular example which

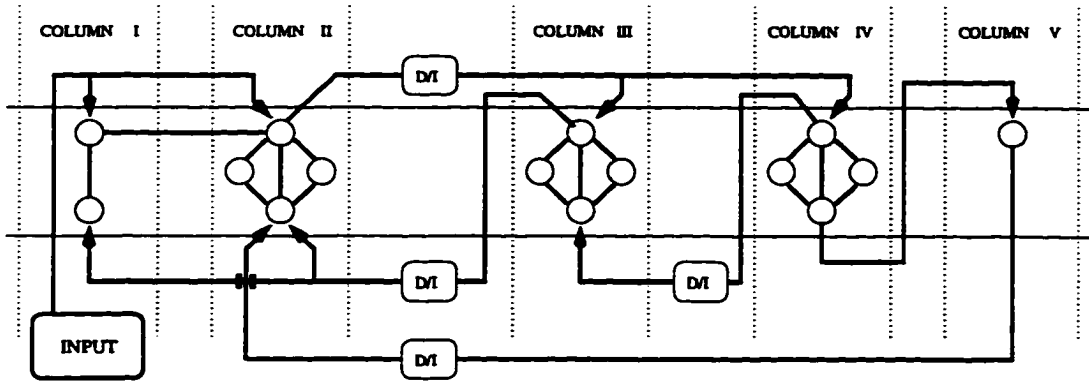


Figure 2.3: Large Scale Cortical Circuit

is modeled after Freeman's representation of the olfactory system [9]. Delay and integration occur along paths labeled "D/I" due to the relatively longer transmission time and stored energy in these connections compared to close connections. Stable activity that appears in a given column will tend to spread along these longer paths to other columns due to the frequency sensitive connections within the columns. The system of equations describing the dynamics of this system grows in complexity as this happens, introducing more of the nonlinear terms of delay and integration. The result is that the system begins to destabilize as more and more recurrent long-path connections are added. Eventually, stability breaks down and activity returns to the base condition. This process establishes the transient nature of large cortical circuits.

The formulations we present permit organization in a distributed hierarchical structure. One approach is to adopt the scheme of nested structures proposed by Sutton [48]. Figure 2.4 illustrates the basic concept of a nested structure. Large shapes, representing clusters, are shown to be interconnected at the same hierarchical level. A similar arrangement is seen within each of these, indicating its recursive

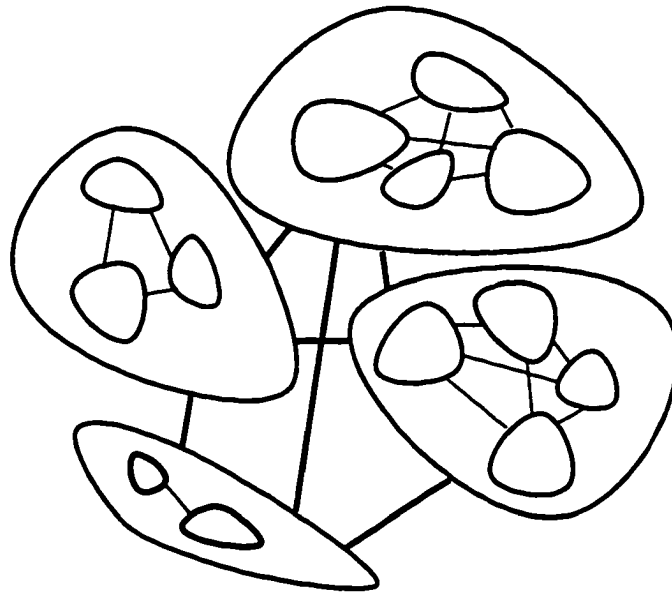


Figure 2.4: The Nested Structure

form. The smaller shapes (also interconnected) are at a level below that of the larger ones. Taken together, they represent a single cluster at the higher level. This may be repeated for several levels and in this sense the organization is recursive.

At the lowest level, the elements of a cluster ultimately represent individual neurons which may themselves be considered as level zero clusters. A first level cluster is the smallest grouping of individual neurons and is represented in our model by the microcolumns proposed by Mountcastle [32]. Second level clusters are the stability bubbles of our model that form when stable microcolumns begin to agglomerate. The third level is defined by the boundaries of the standard cortical column which form developmentally during the early stages of growth. Higher levels are established by the long-path connections between neurons of distinct columns.

Connections between clusters at any level are always between individual neurons belonging to the clusters at the level the connection is made. A heterogeneity of

network elements is seen in [48] as the division between elements that only form connections to other elements within the same cluster and those that project to elements in other clusters. First-level elements are linked together into clusters by a subset of projection elements forming a second-level cluster. Other subsets of projection elements link elements in second-level clusters and so forth. In a circuit with r -levels, there are therefore $r - 1$ subsets of mutually exclusive projection elements. Mutual exclusion is assumed for the sake of simplification in Sutton's model, but strictly speaking, any degree of overlap can occur in natural circuits.

This distributed hierarchical model is described by a method that labels clusters and individual neurons. A cluster at nesting level k is identified by the sequence of indices $i_k \dots i_r$, where r is the highest level. A cluster at level zero is considered to be an individual neuron. The index i_r is always 1, and at level 1 there are $N_{i_1 \dots i_r}$ neurons while at level k there are $N_{i_k \dots i_r}$ level $k - 1$ clusters. The reader may refer to Sutton's work [48, 49] for further details.

This method may be applied toward describing the connectivity of our formulation as stated. But it is important to point out that Sutton's model does not express differences in neuron function beyond that of its connection pattern. We are adapting his model to allow clusters that exist due to dynamic patterns of stable neural activity.

2.3.2 LOCAL CORTICAL CIRCUITS

Recent attempts to model oscillatory systems in the brain involve neural circuits governed by a complex system of nonlinear differential equations. Let us closely examine the model of olfactory neurodynamic behavior proposed by Freeman [9].

The remainder of this section is taken from Freeman [9]. The dynamics of a local collection of non-interactive neurons in parallel is modeled by what is called a $K0$ subset. This is the basic module from which the Freeman olfactory system model is constructed. The neurons represented by a $K0$ subset may be either all excitatory $K0_e$, or inhibitory $K0_i$, and each simultaneously performs four serial operations: (i) nonlinear conversion of afferent axonal impulses to dendritic currents; (ii) linear spatiotemporal integration; (iii) nonlinear conversion of summed dendritic current to a pulse density; and (iv) linear axonal delay, temporal dispersion, translation and spatial divergence. A static sigmoidal function with bilateral saturation converts an internal waveform into a suitable pulse function. In feedback loops, saturation restricts this conversion to its linear range. Each $K0$ subset is described by a single ordinary differential equation, cascaded with the static sigmoid function. Thus the $K0$ subset is split into two parts, a linear time-dependent operator $F(t)$ and a nonlinear time-invariant operator $G(v)$. The linear part is defined as:

$$abF(v_n) = \ddot{v}_n + (a + b)\dot{v}_n + av_n, \quad (2.7)$$

where

v_n is the voltage at time t of the n_{th} $K0$ subset element,
 \dot{v}_n is the first derivative of v_n with respect to t , dv_n/dt ,
 $\ddot{v}_n = d^2v_n/dt^2$,
 $a=220/s$ and $b=720/s$ are fixed rate constants found
 experimentally for all $K0$ subsets that determine
 the carrier frequency of the KII set.

The KII set is constructed out of two KI subsets which are likewise formed by two $K0$ subsets. The nonlinear part is expressed below in terms of the input variable v and the output variable p :

$$p = u_0(Q + 1), \tag{2.8}$$

where

$$Q = \begin{cases} Q_m \{1 - e^{[-(e^v - 1)/Q_m]}\} & v > -u_0 \\ -1 & v \leq -u_0 \end{cases}$$

$$u_0 = -\ln [1 - Q_m \ln(1 + 1/Q_m)]$$

$Q_m = 0.5$ is the asymptotic maximum of the sigmoid curve.

The modification $u'_0 = u_0 d_1 e^{(-d_2 u_0)}$ where $d_1 = 1.64$ and $d_2 = 0.53$ permits the equation to be stable over all values of Q_m .

The formation of KI subsets is illustrated in Figure 2.5. The KI_e subset is

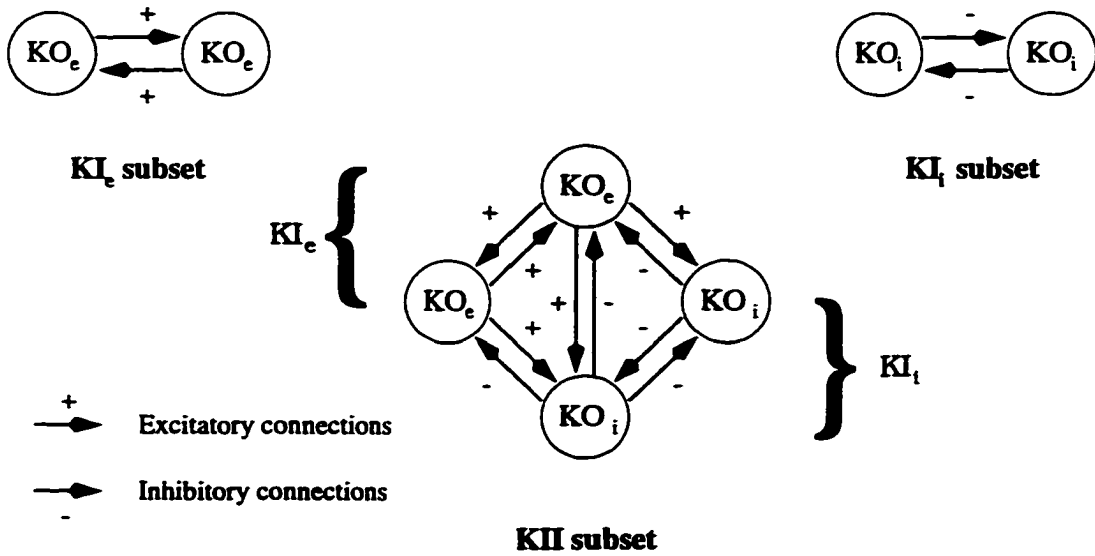


Figure 2.5: KI and KII Subsets

formed by mutually excitatory connections between two KO_e subsets. Likewise the KI_i subset uses mutually inhibitory connections between two KO_i subsets and two KI subsets are combined to form a KII set as also shown in Figure 2.5.

The braces identify the KI_e and KI_i subsets and the excitatory and inhibitory connections between them are labeled. The equations for the full KII set with N subsets are:

$$\begin{aligned} F(v_{e1j}) &= k_{ee}p_{e2j} - k_{ie}(p_{i1j} + p_{i2j}) + \sum_{k \neq j}^N k_{ee}p_{e1k} + I_j \\ F(v_{e2j}) &= k_{ee}p_{e1j} - k_{ie}p_{i1j} \\ F(v_{i2j}) &= k_{ei}p_{e1j} - k_{ii}p_{i1j} \\ F(v_{i1j}) &= k_{ei}(p_{e1j} + p_{e2j}) - k_{ii}p_{i2j} + k_{ii} \sum_{k \neq j}^N p_{i1jk} \end{aligned}$$

where

I_j is the input to the j th KII subset,
 k_{ij} is the gain coefficient, such that $v_j = k_{ij}p_i$,
 $(0.2 < k_{ij} < 2.0)$,
 $k_{ee}, k_{ei}, k_{ie}, k_{ii}$ are four types of internal connections,

and simulation is over all the other KII subsets.

There are three main parts of the central olfactory system: the olfactory bulb (OB), the anterior olfactory nucleus (AON), and the prepyriform cortex (PC). Each of these are modeled individually by a single KII subset. When coupled together with both excitatory and inhibitory feedback loops that include delays and integration, then the $KIII$ set is formed. Simulations run on the $KIII$ set reproduce the chaotic *electro-encephalogram* (EEG) patterns associated with the complete olfactory system. These patterns include the normal low-level background activity, high-level relatively coherent “bursts” of oscillation that accompany reception of input, and a degenerate state associated with epileptic seizure.

2.4 THE FUNCTION OF THE CEREBRAL CORTEX

To better understand the cerebral cortex, its structure and function, it is necessary to consider what tasks are understood to be performed by the cortex and what

is known of its physical structure that give it those particular properties. The discussion in this study of cortical function is limited to the cognitive process of *selective attention*, the hierarchical organization of memory, and processes related to the *dynamic binding* problem.

The natural organization of cortex interconnections forms perhaps one of the most complex structures known. The organization is examined here with an emphasis on its recursive construction and heterogeneous neuron types.

Biological circuits are composed of a heterogeneity of neuron types as opposed to the uniform circuit elements employed by most models. Different neuron types in biological circuits determine the kinds of interconnections between neurons. For example, some types influence only those neurons that are near-by while others, especially pyramidal cells, have a greater range. Furthermore, the number of connections formed by a particular neuron depends on the neuron type.

At first glance, the brain reveals that it is divided into two halves and that each half contains several distinct lobes. The brain seems to be built compartmentally to handle various tasks with specialized equipment for each. Indeed neuropsychological studies have long identified correlations of the activity of specific cortical regions with certain motor and cognitive tasks or sensory input [1, 12, 26, 27, 35, 38, 40, 41, 50].

2.4.1 SELECTIVE ATTENTION

In spite of the great variety of connections in the cortex, we believe that at any moment only a fraction carry signals that require processing. The brain must ignore

most of its own activity, much the same as it does with perceptual data. According to our cortical theory, the brain's attentional mechanisms are presumed to act internally as well as upon data from external stimuli. That is to say, that activity occurring in the various regions of the brain are selectively attended to, or ignored, by the activity in other regions.

The cognitive process of attention is subjectively familiar to us all, even though the mechanism behind it is not fully understood. It is integrally tied into what the brain does yet no consensus of an understanding exists among those who study it. What is known is that the attention process filters sensory data for useful information because not all data is informative. The work of the attention process is then to identify what is useful, ignore what is not, and do this at a rate that keeps up with the input stream. The process creates a grouping of input data into attended, which receives more processing, and unattended, which does not.

Attention as a neuropsychological phenomenon can be expressed in many forms including focused, selective, divided and sustained [3]. For the purposes of this discussion attention shall be considered a task of information processing that can be thought of in terms of a filter extracting salient information from raw input data. The criteria for what is salient may change over long periods of time. Therefore the filter is an adaptive one.

2.4.2 DYNAMIC BINDING

The transient synchronization of chaotic EEG patterns observable in the neocortex [18, 50] lasts usually on the order of a few hundred milliseconds, making it a likely candidate for the underlying mechanism of very short term conscious memory [5].

The rapid and efficient formation of transient interactions on a systems level is viewed as a necessary aspect of cognitive function. Such interaction provides a means for the formation of composite objects by grouping distinct features of a complex unit into an associated whole. Called the *dynamic binding problem*, it has been a familiar topic for symbolic rule-based systems but has only recently been addressed among neural network and connectionist researchers [2, 14, 15, 18, 27]. Observations of synchronized neural oscillations in separate cortical regions of the brain [2, 26, 33] have now inspired new approaches to this problem as well.

Synchronized neurodynamics are typically observed as the correlated time-series of electrochemical or electromagnetic activity. Electromagnetic field potentials are averages of neuron activity within the local vicinity of a measuring instrument. Typically, whenever measurements of brain activity are made, it is the dynamics of these field potentials, not the individual neurons, that are recorded. The monitoring of individual neuron firings (action potentials) is much more difficult. When responding to stimuli, cortical neurons tend to oscillate in rhythmical patterns synchronized to peaks in the local field potential waveform. Conversely, neurons firing at uncorrelated times tend to flatten the local field potential waveform. This interplay

between individual action potentials and average field potentials is fundamentally important to the kind of processing done by the cortex. Interaction is governed by characteristics of the connection structure such as the number, type and strength of connections. For example mutually associative links in a fully connected local group of neurons would promote strongly correlated firing times among these neurons. Many details of the interconnection structure in the cortex are known and yet many are not. Synchronization has also been observed among neurons located in different regions of the cortex.

2.4.3 HIERARCHICAL MEMORY

The problem of the hierarchical organization of memory has been approached from many directions and different hierarchical arrangements exist. A common arrangement organizes a sequence of clustered elements in layers. Each successively performs a coarse graining of the previous through the symmetric fully interconnected structure between adjacent layers. This arrangement however does not capture the variety of high-level associations possible with a distributed hierarchical arrangement which some researchers [32, 48, 49] believe is revealed by the structure of the cortex.

Enough evidence suggests that the cortex, which may be functionally divided into various regions, may be further divided into structures known as cortical columns. These columns, so named because of an apparent vertical connectivity pattern, are believed to be still further subdivided into microcolumns. These observations

therefore seem to imply that a thoroughly nested structure exists within the cortex. This was in fact the conclusion reached by Mountcastle [32], as well as the motivation for a distributed hierarchical model [48].

The nested structure observed in biological circuits is a recursion of subcircuits each containing many types of neurons. The similarity among subcircuits gives a kind of regularity to the overall nested structure, with clusters of subcircuits at the first level coming together to form subcircuits at the second level that in turn cluster together forming third-level subcircuits and so forth. The significance of this arrangement is the distributed manner in which the brain on a whole is organized; an arrangement through which even remotely separated regions may interact.

Consider now the reaction of such a structure to an input stimulus. First-level subcircuits, organized into parallel columns, are associated with physiological responses produced by various stimuli. Successive higher levels integrate these responses and modify the boundary relations among clusters of first-level as well as some higher level subcircuits. The result is that responses at the first level are associated together, hierarchically, into a global distributed response.

According to the model put forth by Sutton [48], elements in first-level subcircuits are fully interconnected in an *apparently disordered* manner similar to Hopfield-style neural networks. A small number of memory states are therefore associated with each of these subcircuits that represent the physiological responses. The fact that there are only a few memory states per subcircuit is not a limitation since the

storage capacity is not emphasized. Instead it is the hierarchical response of the overall system that provides the necessary richness of its behavior.

2.5 SUMMARY

A theory of cortical neural processing was presented in this chapter along with a formulation that serves as a framework for modeling the cortex according to our theory. Three parts were identified in this theory. They are a *chaotic basis*, *stability bubbles* and *confined activation*. Also neuroscience issues related to the cognitive function of the cerebral cortex was discussed. These include *selective attention*, *the dynamic binding problem* and the structure of a *hierarchal memory*.

CHAPTER 3

CHAOTIC NEURODYNAMIC NETWORKS

Most immediately noticed about the activity of the brain is its oscillation. The brain is in constant flux as every neuron in the body oscillates in ever changing ways. In fact a neuron must at all times oscillate to survive. Incredibly, very little has been done to understand the computational advantages of oscillatory dynamics. Since early on, research in artificial neural networks has avoided, for the most part, this natural feature of the brain. The goal of most traditional neural network models is a static “*final*” system state; a concept entirely alien to biological computers. Only recently do oscillations appear in neural network models. Therefore, no real framework exists, as yet, for how to systematically approach this complex problem. Our view is one of the new views now emerging for how oscillatory neurodynamics are useful. Periodic oscillatory neurodynamics appear in many of the new artificial neural network models that seek to be more physiologically realistic [1, 5, 15, 37, 47, 48]. But few of the new models treat chaotic neurodynamics as a desirable feature. One that does is Freeman’s model of olfaction (odor perception) [8, 9]. Our theory differs from Freeman’s view of the role played by chaotic neurodynamics in cortical processing. Specifically, we assert that chaotic activity represents uncertainty in the outcome of tasks performed by the cerebral cortex because of its unstable nature, where *chaotic instability* refers to the tendency to depart from simple periodic motion.

3.1 CORTICAL BEHAVIOR MODELING

Our approach is to investigate oscillatory dynamics in cellular automata made in the form of a two-dimensional array of processing elements interacting according to a regular connection structure. The model is meant to represent the laminar structure of the cerebral cortex and is adapted from Freeman's model of the olfactory system [9]. Each neuron is modeled as a second order differential equation of the form

$$\frac{d^2}{dt^2}y_{u,v} + \frac{d}{dt}y_{u,v} + y_{u,v} = \sum_{\mathcal{R}} \mathcal{H}(Y) + I_{u,v}(t), \quad (3.1)$$

where Y is an array of elements $y_{u,v}$, $0 < u < n$, $0 < v < n$, and n is the size of the array; \mathcal{R} is the *receptive field* of the element $y_{u,v}$ defined by some radius of points surrounding the point (u, v) ; \mathcal{H} is a lateral interaction function; and $I(t)$ is an input function.

The goal is to develop a model that adequately represents the behavior of the cerebral cortex. To do this we begin with a description that characterizes cortical behavior and acknowledges the usefulness of chaotic neurodynamics.

3.1.1 CHARACTERIZATION OF BEHAVIOR

The activity described by our theory of cortical neural processing is bimodal in regard to the kinds of oscillations that neurons are said to exhibit. Neurons or groups of neurons working together in a local cortical circuit must be capable of both kinds of behavior described by our theory. They must have a base condition (without stimulation) of a low intensity waveform that is highly chaotic. Then as input is applied, a strong periodic, or at least quasi-periodic, signal quickly appears.

Such rapid transitions are known as bifurcations. Note that the term *input* is used here in a general sense. It may refer to stimulation due to sensory receptors, such as the visual, auditory and olfactory systems, or it may simply mean a signal that originates elsewhere in the cortex.

The mechanism of pericolumnar inhibition, as proposed by Mountcastle [32], establishes dynamic regions within the laminar cortical structure. By dynamic regions, what is meant is that these regions form due to the immediate input signal and is not the result of learned or innate structure. This raises the issue of whether input, causing the dynamic isolation of a region, in turn causes its activity to bifurcate; or is it that input causes a bifurcation that later creates isolation. A third possibility is that isolation and bifurcation are both directly produced by received input.

3.1.2 THE COMPUTATIONAL ROLE OF CHAOS

An interpretation for chaotic oscillatory behavior in physiologically realistic systems is to be found in the literature and is the source of the material in this subsection [7, 8, 9]. A vase shaped diagram was developed by Freeman [47] as an attempt to represent the state space bifurcation characteristic of his model of the olfactory process. It illustrates the action of odor perception during the normal respiratory behavior of rabbits [9]. A spectrum of distinct behavioral modes begins at the lowest possible level, a condition while only under *deep anesthesia*. Then comes *sleep* and *waking rest*, where the amplitude is low but considerably more complex than before. Later are *exhalation* and *inhalation*, the two states of *motivation*. Finally, the most excited state of all is *seizure*. The ability to model seizures is very important in its

own right, independent of what cognitive modeling insight it may bring, because it takes medical researchers that much closer to understanding and perhaps controlling the debilitating disease of epilepsy.

An important feature to bring out of the bifurcation diagram is the number of limit cycles present at the inhalation level. This differs from the waking rest level in which only one central limit cycle can be found. The limit cycles, or spatially patterned attractors, classify respective stimulus odors that animals are trained to respond to.

From this description there come four suggested functions performed by chaotic activity in biological neural systems. (i) It provides rapid and unbiased access to all the collection of latent attractors. Any attractor may be selected, without warning, by environmental factors. The process “turns-off” the low-dimensional *noise* at the moment of bifurcation to a patterned attractor, and is “turned-on” again on reverse bifurcation as the patterned attractor vanishes. (ii) The chaotic attractor provides for global and continuous spatio-temporally unstructured neural activity. This is vital for the survival of neurons, in periods of low demand, which perish without proper conditioning to prevent atrophy of the tissue. (iii) A special pattern provides response to the contextual component of the environment. In this way any new odor stimulus, not already a member of the latent attractors, interferes with the contextual response leading to failure of convergence to any of the learned patterned attractors. The resulting chaotic activity also differs from the contextual response, signaling that what has been encountered is an unidentified stimulus. The power of this process is that classification of unknown odor stimuli can occur as rapidly as the classification of any known odor, without requiring an exhaustive search through

an ensemble of classified patterns. (iv) A function that deals with learning. Chaos allows the system to escape from its established repertoire of responses in order to add a new response to a novel stimulus under reinforcement. The process is analogous to the Hebbian learning rule. Chaotic activity evoked by a novel odor provides unstructured activity that can drive the formation of a new nerve cell assembly by strengthening synapses between neurons of highly correlated activity.

3.2 SIMULATED LAMINAR STRUCTURE

We develop a model in this section that is less complex than the structure described previously. The purpose is initially to simulate the base condition of our proposed cortical processor without requiring a discouraging amount of computing overhead. Then we examine responses to a number of different stimuli. Only lateral interaction is taken into account by our simplified model.

We begin by setting up an n by n array of processing elements (neurons). The output of each is numerically calculated from a 2^{nd} order differential equation having a similar form to that of the model by Freeman [9]. Our important modification is a coupling between neurons that reflects the lateral interaction of the cortex as seen in the right hand side of the expression:

$$\frac{d^2 y_{u,v}}{dt^2} + A \frac{dy_{u,v}}{dt} + B y_{u,v} = k_1 \sum_{\mathcal{R}} \mathcal{H}(y_{u+i,v+j}) + k_2 I_{u,v}(t), \quad (3.2)$$

where $(y_{u,v} : u = 1, \dots, n; v = 1, \dots, n)$ are the neurons of the array and \mathcal{R} is the receptive field surrounding neuron (u, v) defined below.

Definition 3.2 : For some radius r , the *receptive field* \mathcal{R} defines the set of points $(u + i, v + i)$ by their Euclidean distance to the point (u, v) .

The receptive field is defined in our model as:

$$\mathcal{R} = \{(u + i, v + j) : (u + i + n)_{mod_n}^2 + (v + j + n)_{mod_n}^2 \leq r^2\}. \quad (3.3)$$

The radius r and the function \mathcal{H} are considered to be uniform throughout the array. Also, to eliminate edge effects, neurons near the outer limits of the array wrap around to points on the opposite edge using the modular operator mod_n . A and B are constants found experimentally that represent the natural frequency and damping coefficients, respectively. The constant gains k_1 and k_2 are also determined experimentally. The function $I_{u,v}(t)$ is an input signal applied to the neuron at coordinate (u, v) . The fourth order Runge-Kutta method of integration is used to evaluate this system of simultaneous equations. The advantage of having only one differential equation per coordinate (u, v) is to reduce the complexity of our model.

3.2.1 LATERAL INTERACTION FUNCTION

Most neurons in the cerebral cortex interact with neighboring neurons through a nonlinear spatial function. The range of this interaction may extend as far as several centimeters in some cases but the majority of the influence covers a much smaller area. Specific neuron types determine the characteristics of the interaction function and most follow the same general form which may be approximated as a single gain function common to every neuron in a two dimensional array of neurons. The form of the interaction function used in our simplified model may be seen in Figure 3.1.

It is generated by taking the Kaiser function (the Bessel function of the first kind divided by the Modified Bessel function of the first kind, J_0/I_0) and scaling it along lateral dimensions. Units in the figure are in microns. Only the area covered

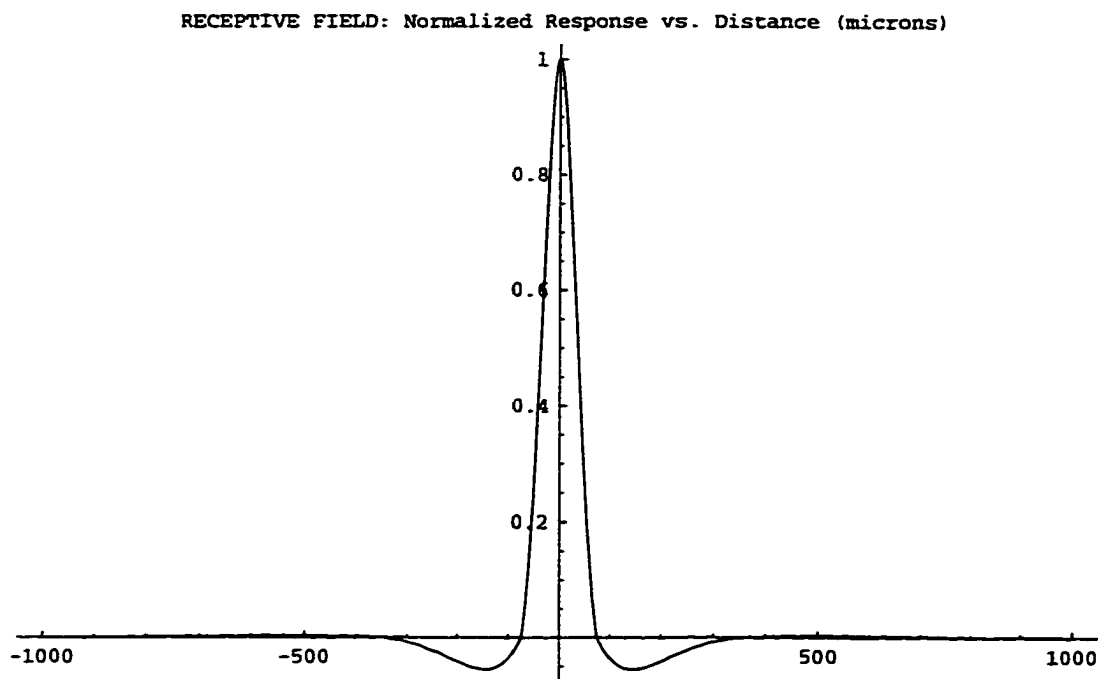


Figure 3.1: Lateral Interaction Function

by radius r (microns) was used in the implementation of the function. This is accomplished with the two dimensional gain matrix depicted in Figure 3.2.

The point (0,0) of this matrix represents the coordinates of the neuron using this gain to compute its output. To hasten the simulation of this structure, our model implemented this matrix as a look-up table which avoided unnecessary calculation.

It can be seen from this figure that spatial resolution below that shown would have difficulty in representing the central peak of the interaction function while keeping the relative scale in the lateral dimension of its various features. It was for these reasons that the array was chosen to be 8 by 8, where $n = 8$. At this scale, however, edge effects become considerable. To avoid this and yet keep the number of neurons in the model few, the modular operator was used in defining the receptive field.

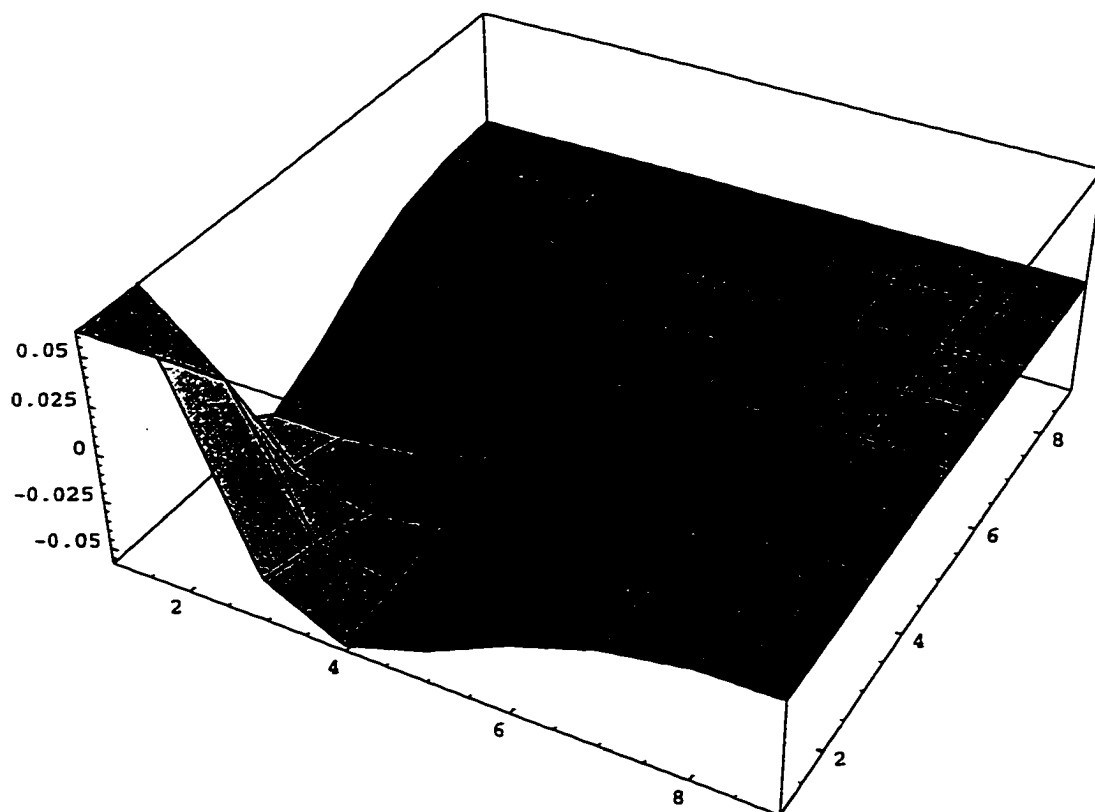


Figure 3.2: Gain Matrix(Upper Right Quadrant)

3.2.2 SIMULATION OF CHAOTIC BASE CONDITION

To observe the base response of our model, a simulation was run without applying an input stimulus. We constructed an 8 by 8 array and initialized each neuron according to a pseudorandom number generator to create the start state. Parameters were set at $A = 0$, $B = 50$, $k_1 = 40$ and $k_2 = 0$ and the system was integrated for 4000 steps of size $dt = 0.01$.

To characterize this behavior and to get an idea if it is, in fact, non-periodic, we plot the phase diagram of any two neuron responses; one against the other. Figure 3.3 is just such a phase diagram, showing the base response of $y_{3,6}$ against that of $y_{4,1}$. The plot appears to be very disorderly and certainly non-repeating over

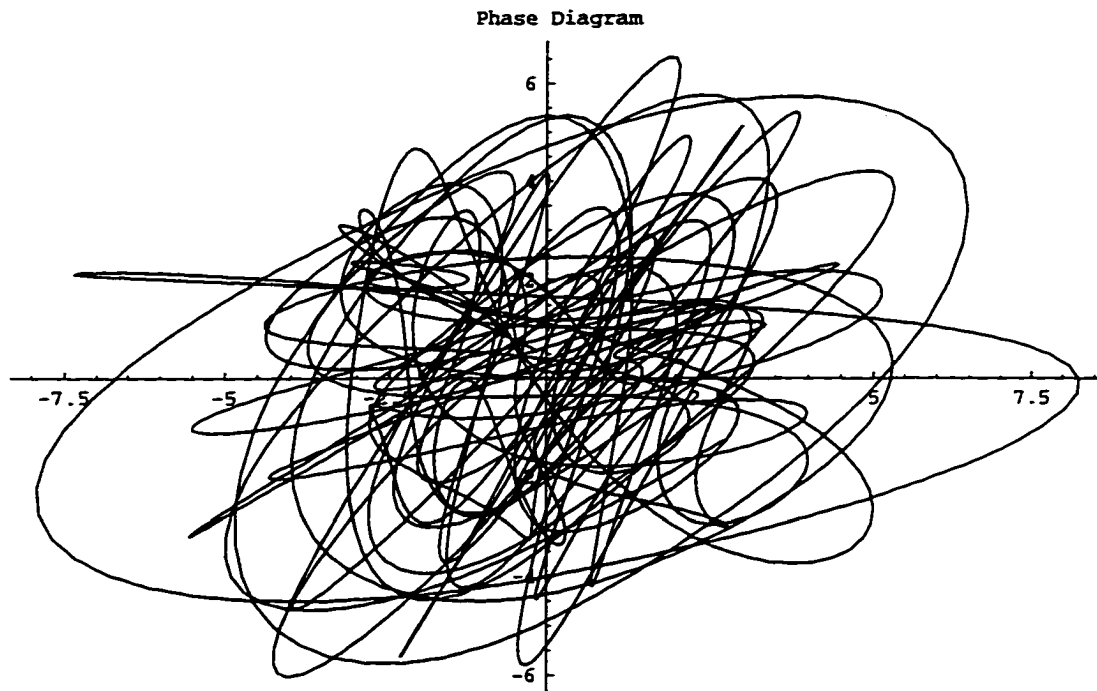


Figure 3.3: Base Response ($y_{4,1}$ vs $y_{3,5}$) : $t=0,40$

the interval of the simulation. To help determine if any long-term stabilization is occurring, another graph (Figure 3.4) is shown for only the first 2000 data points of the previous graph.

When compared, these two graphs show that the path traced out on the phase diagram continues to have both low and high amplitude orbits, showing no indication of settling. A more conclusive determination of chaotic behavior can be had through other more computationally intensive analysis techniques such as calculation of the Lyapunov exponents of the system. In this case, over 64^2 simultaneous equations must be solved.

3.2.3 RESPONSE TO STIMULI

When a sinusoidal input is applied to one or more sites within our simulated cortical array, an area of stronger response appears in the immediate vicinity of the applied

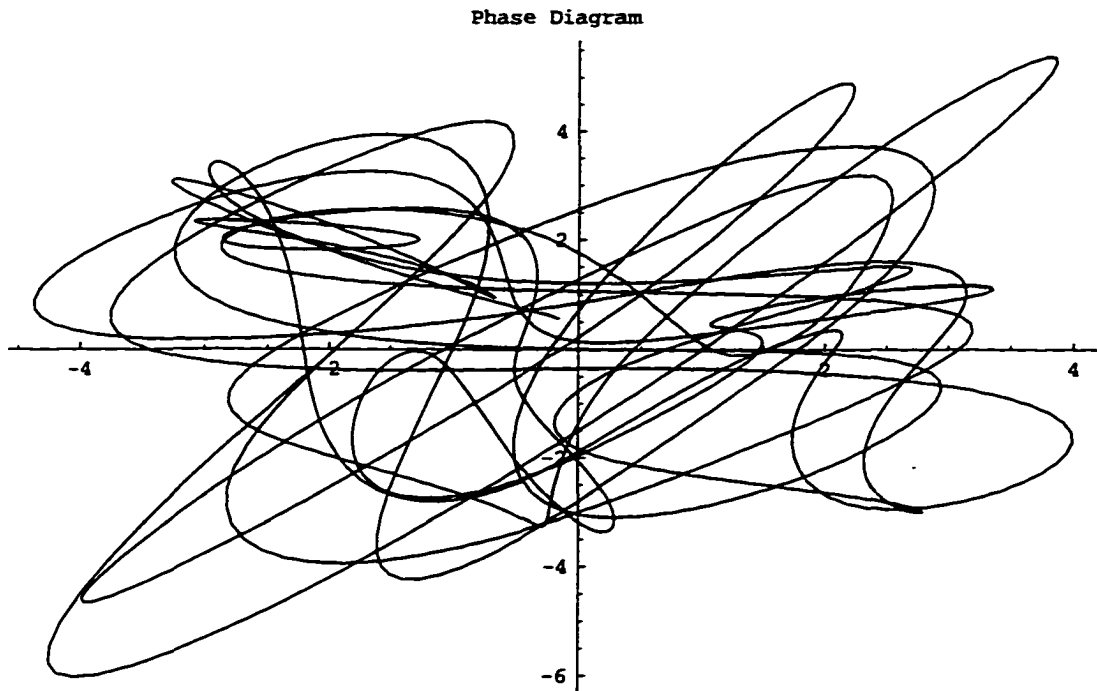


Figure 3.4: Base Response ($y_{4,1}$ vs $y_{3,5}$) : $t=0,20$

input. This is similar to the stability bubbles predicted by our theory. What's more, the response appears to be much more stable than the surrounding activity. A series of experiments were done. Sinusoidal waveforms of the same frequency and phase were first applied to three pairs of locations in the array. Distances of one (adjacent locations), three and five separated the pairs of applied inputs. Also, frequency and phase shifts between the two inputs were considered. From all the variations tried, the results of four are shown in Appendix A in Figures A.1, A.2, A.3 and A.4. In this example, input is applied to two adjacent locations in Figure A.1. The same frequency of $\pi/25$ is applied to both and the phase angle between the inputs is zero.

The top of the figures depict the time series response of each simulated neuron in an 8 by 8 array. Fourier transforms were calculated for each using fast Fourier transforms, and are depicted below the time series response. The base condition is

certainly quasi-periodic. This is seen in the high number of spikes in their Fourier response. However, the Fourier response of the neurons to which input is applied is not as complex. Significant high-frequency response is almost non-existent. Neurons nearby the locations where input is applied are also affected, due to the lateral interaction function. Note that only one bubble is generated in spite of the fact that two inputs are applied. What would have been two separate bubbles merged into the one shown.

Two frequencies are applied at a distance of 3 locations in Figures A.2, A.3 and A.4. The frequency of one input is changed, $\pi/22$, in Figure A.2. The other input frequency remains at $\pi/25$. In Figure A.3, the frequencies are the same, but there is a phase angle of $\pi/4$ between them. The phase is increased to $\pi/2$ for the experiment depicted in Figure A.4.

3.3 SUMMARY

The behavior of the cerebral cortex was characterized as an interplay of chaotic and stable neurodynamics. Issues relating to the way in which chaotic neurodynamics is employed by the brain were discussed. A simulation of the lateral interaction function was shown to produce the chaotic base condition predicted by our theory. The application of stable, periodic oscillation to our model created bubbles of stable activity. However, these bubbles were not entirely isolated from the surrounding cellular array. The low-intensity reaction to the applied input, experienced by neurons lying beyond the boundaries of stable bubbles, is viewed as a kind of pre-conscious processing.

CHAPTER 4

SELF PARTITIONING CORTICAL STRUCTURES

In this chapter we study the automatic formation of clusters by the agglomeration of neurons and how this serves to create partitions in the cortex. We also suggest a new application for this process relative to our theory. We are interested in the ability of the cerebral cortex to automatically divide available computing resources (the set \mathcal{S}) into two nonempty disjoint subsets (s_1, s_2) whose union is \mathcal{S} . These resources correspond to microcolumns, but may also generalize to other structures.

Cortical neural structures may be viewed as being formed by two modes: (i) the developmental mode, where the characteristic columns emerge through self-partitioning; and (ii) the dynamic mode, where the mature structures are used for various cognitive tasks. Here we show how the Mexican hat function (an example of lateral interaction) operating on random initial states, leads to self-partitioning of neural activity which by some other biological process is converted into isolated physical substructures.

Transient partitions (dynamic mode) are considered as well as more permanent ones (developmental mode). The division of resources made by a transient partition is done on the basis of neurodynamic activity (stability). This process forms, within columns, the stability bubbles of our theory. More permanent partitions form the columns themselves by grouping together clusters of microcolumns according to similarities in neurodynamics that establish topological mappings within a hierarchical

structure. Transient cluster formation and column formation are distinct processes, but the mechanism they share is the focus of this chapter.

The formation of clusters due to the Mexican hat function as described by Kohonen is already well established [23]. Mexican hat functions of successively smaller spatial frequency are used to create a mapping of specific input patterns onto individual neurons that yield the strongest response to that pattern. The result is a topological ordering of high dimensional data onto a lower dimensional array or vector.

Our investigation of self partitioning through lateral interaction is not concerned with mappings made to individual neurons. Instead the aim is to partition computing resources in a hierarchical manner that is well adapted to the kinds of data represented by input patterns encountered. This is an important concern for the simulation of intelligence as it is believed that biological systems continually reorganize their conscious structure in a complementary relationship with the environment [21]. The development of ocular dominance columns in the striate cortex reported by LeVay, Wiesel and Hubel [25] documents a process in which characteristics of the input environment shape the developmental process that partitions computing resources of the striate cortex.

The structural organization of the cerebral cortex outlined by Mountcastle [32] implies that the size and shape of a column are likely to determine how many connections to other columns are expected. Therefore, we are interested in knowing what kinds of spatial clustering patterns are formed when various input are clustered together by agglomeration, and what parameters of the lateral interaction function influence this.

Clusters that become columns develop an isolation from one another in regard to lateral interactions. One way this is done is by weakening lateral connections between neurons crossing any border surrounding a cluster. This is a slow developmental process that occurs during the formation and growth of the cortex. Another method is to set up a zone of inhibited neurons that serve as a wall across which lateral influences cannot pass. This technique can be done rapidly without slow synaptic changes and is, therefore, suggested as a means for transient partitioning.

Definition 4.1 We define an *agglomerated cluster of microcolumns* as a set \mathcal{C} such that each member $\mu_{u_i, v_i} \in \mathcal{C}$ is adjacent to another microcolumn of the same set, or the set contains only one member.

Definition 4.2 An agglomerated cluster is said to be *functionally isolated* if members of it are not influenced by, or exert an influence upon, members of another cluster.

An agglomerated cluster is more specific than the clusters referred to by Sutton [48, 49] in his *nested structures* model. Note that individual neurons are considered clusters by his model and he has no restriction similar to Definition 4.1. For the sake of simplification, lateral interactions are the focus and Definition 4.2 ignores hierarchical connections.

4.1 CORTICAL CLUSTER FORMATION

The method for which this isolation is accomplished is based on Mountcastle's process of pericolumnar inhibition [32] that establishes the boundaries of active columns and isolates them from the surrounding cortex. Activity traveling vertically (perpendicular to the surface) excite neurons along its path. Around the periphery of

this path, neurons are inhibited. This creates an active and isolated microcolumn of neurons in an otherwise highly interconnected and highly interacting structure.

Pericolumnar inhibition creates lateral interaction similar to that created by the nonlinear receptive field of many cortical neurons. Accordingly, we simulate both mechanisms with a single general model of lateral interaction across a two dimensional cellular array.

The model we build is a two dimensional structure. Therefore vertical columns (microcolumns), as such, are not physically represented. Instead, groups of neurons massed together closely on a flat surface depict the extent of a vertical column (microcolumn) in the cortex. In reduced form, two neighborhoods of cells are defined. Those that lie within a radius, r_1 , of a central point are referred to as the immediate neighborhood. The *distant neighborhood*, on the other hand, refers to cells lying beyond r_1 but within the radius $r_2 > r_1$. Every cell of this structure is connected to every neighboring cell surrounding it from both of these neighborhoods. The distinction deals with the lateral interaction function. The immediate neighborhood is generally excitatory, while the distant neighborhood is inhibitory. The extent of the structure is considered finite, but connections to cells on the edges wrap around to neurons on opposite edges of the cellular array.

A graph of the excitation versus lateral distance resembles the receptive field surrounding most cortical neurons but on a smaller scale. The plot shown in Figure 4.1 shows a function similar to the scaled Kaiser function used in Chapter 3. This function is repeated so our results may be applicable to the simulated laminar structure as well as developmental column formation. For pericolumnar inhibition the horizontal dimension is assumed to be smaller than the receptive field model.

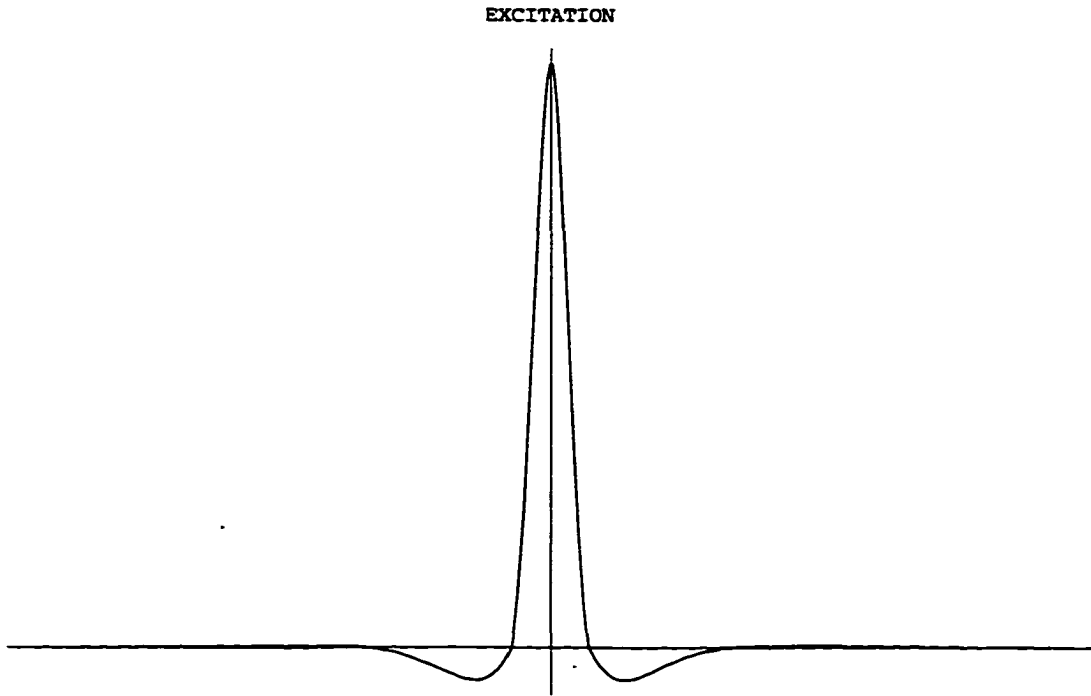


Figure 4.1: Pericolumnar Inhibition

Considered as an excitation (output) or as a receptive field (input), the lateral influences of this function are similar. No distinction is made between the two for the simulations done in this chapter, so that the results may be scaled and applied to either process.

The model we use in this chapter consists of a 41 by 41 square array of binary elements with the value $x_{u,v} = +1$ ($x_{u,v} = -1$) representing membership in the subset s_1 (s_2). Cluster formation is an iterative process that follows the equation:

$$x_{u,v}(t+1) = \text{SIGN}\left[\sum_{\mathcal{R}} \mathcal{H}(x_{u+i,v+j}(t))\right], \quad (4.1)$$

where $SIGN$ is a nonlinear operator defined as:

$$SIGN[k] = \begin{cases} +1 & \text{if } k \geq \text{threshold} \\ -1 & \text{otherwise} \end{cases}, \quad (4.2)$$

and \mathcal{H} is the lateral interaction function. The receptive field, \mathcal{R} is the region over which \mathcal{H} operates and is defined as in Equation 3.3 of Chapter 3. Three neighborhoods are identified as the alternating excitatory and inhibitory regions for which r in Equation 3.3 take the following values: (i) $r < r_1$, excitatory; (ii) $r_1 < r < r_2$, inhibitory; and (iii) $r_2 < r < r_3$, excitatory. The parameter *threshold* in Equation 4.2 is experimentally determined.

Consider the example in Figure 4.2. A sequence of iterations are depicted, where

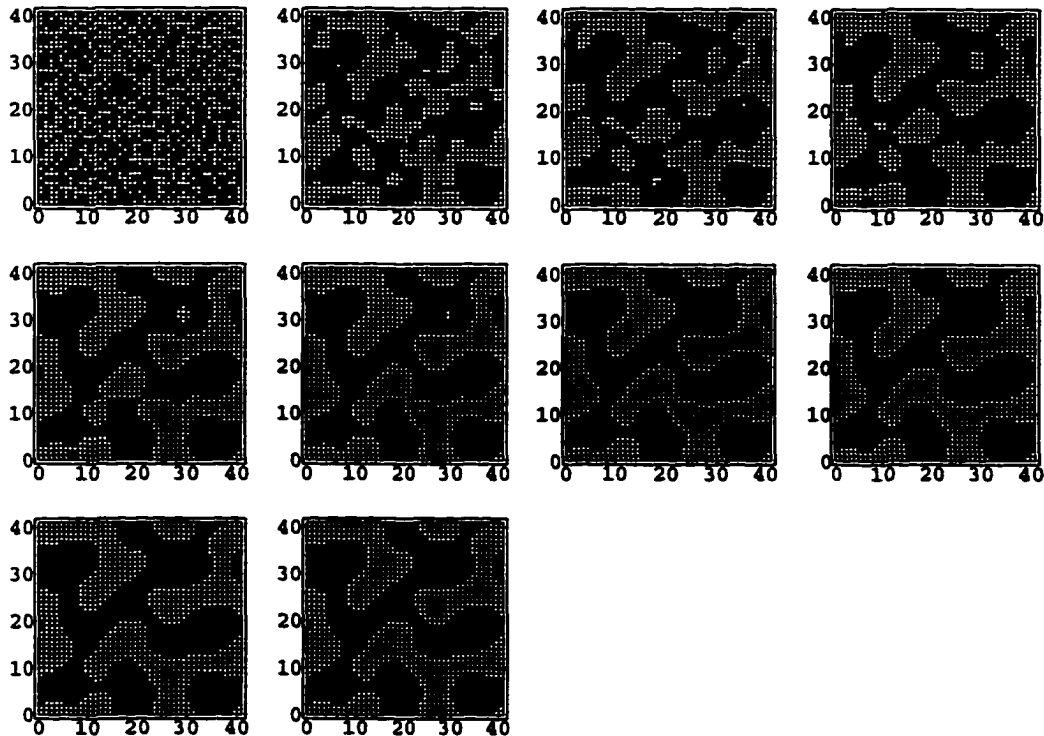


Figure 4.2: Cluster Formation A

the entire set of neurons is updated in parallel between each step. We assume it takes unit time to update a frame based on the values of its predecessor, and assign $t = 0$ to the initial state. The state at time $t = 1$ is to the right and the system is stable at time $t = 9$. As simulated in this chapter, cluster formation begins by initializing the entire array with values chosen from the set $\{-1,+1\}$. The array is initialized in this example using a pseudo-random number generator to make the choices, with an even probability between them.

The final state shows an elaborate pattern of activity displayed across the array. The array elements with output values of $+1$ (depicted in white) have agglomerated into a region that sprawls out in all directions. The remaining elements (depicted in black) have output values of -1 . In spite of the interesting shape, only one cluster was produced. Our model wraps the lateral interaction function around the edges of our array to prevent edge effects, so clusters should also be interpreted as wrapping around in the same way.

Although both sets s_1 and s_2 existed initially, their membership has changed. The boundary between the two sets in the final state is much smaller. That is to say, the number of adjacent element pairs with opposite output values has decreased.

Partitioning in this way has two physiological effects. The first is that a smaller boundary simplifies the job of isolating clusters. The second has more to do with the area than with the circumference of these clusters. A region of some specific area covers a number of array elements. The average of the output values of elements in this region is typically close to zero for any large enough area taken anywhere in the array at time $t = 0$. But at time $t = 9$, when the clusters have formed, the average is highly dependent on the area and location of the region.

Another example, cluster formation B, is shown in Figures 4.3 and 4.4. The

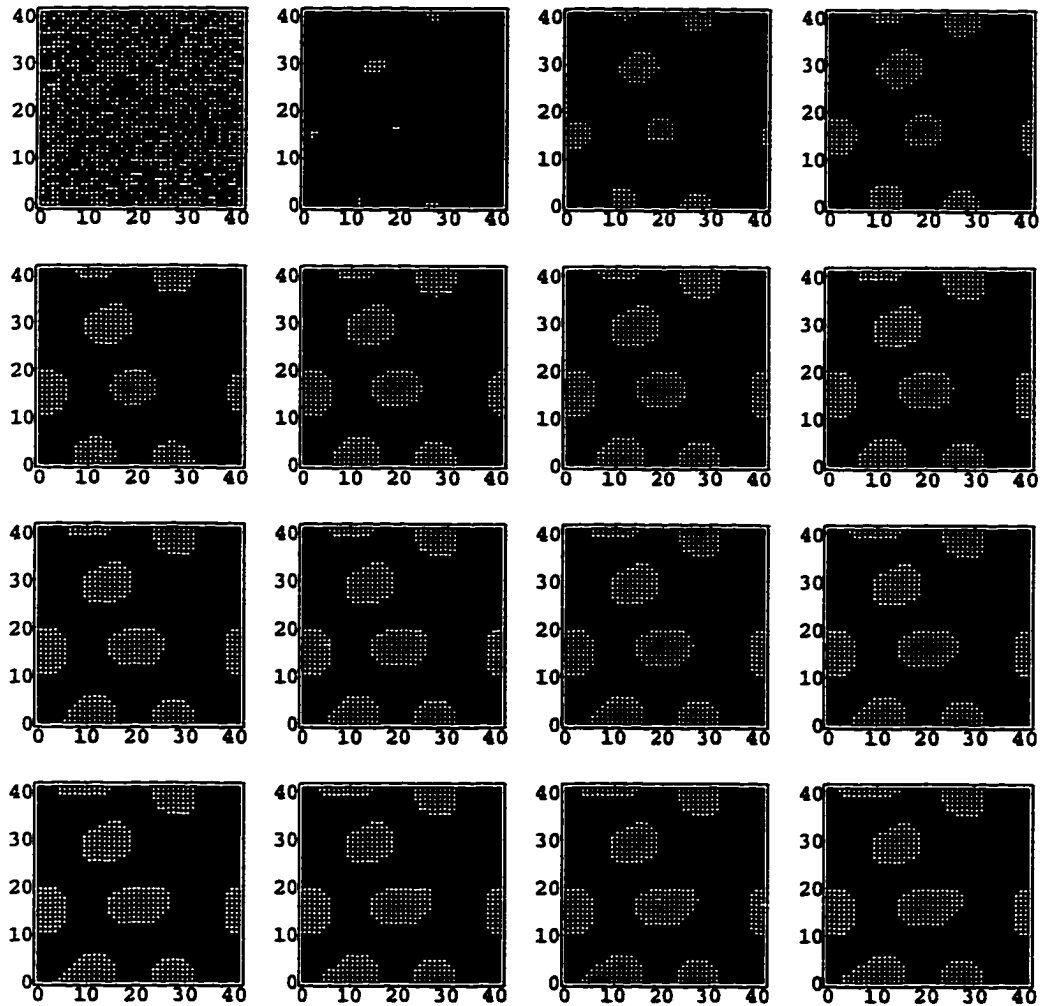


Figure 4.3: Cluster Formation B : Part 1

only difference from the previous example is in the form of the lateral interaction function. The lateral interaction function was reduced in size compared to that used in the previous example. The new simulation does not fully stabilize until time $t = 30$, even though most of the pattern of clusters had formed in the first few iterations. A total of 5 clusters were created.

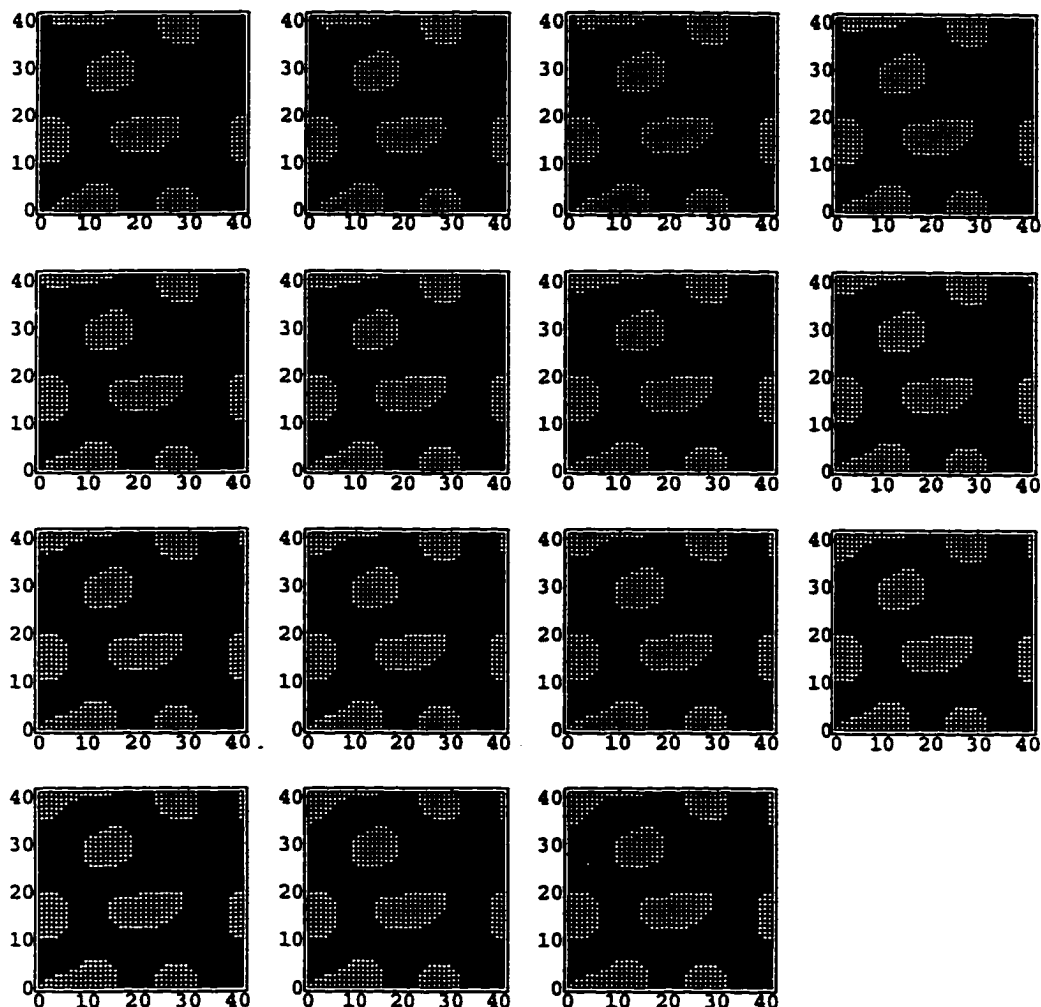


Figure 4.4: Cluster Formation B : Part 2

4.1.1 THRESHOLD VARIATION STUDY

Next we wish to explore the influence of varying threshold values. Figure 4.5 shows 5 simulations run for each of 5 threshold values. Again, the initial state is randomly chosen with each run. The rows of the figure depict, from the top, threshold values of $\{-2, -1, 0, 1, 2\}$. Immediately, it is seen that positive threshold and the reduced lateral function create similar cluster patterns. The percent of the array that was

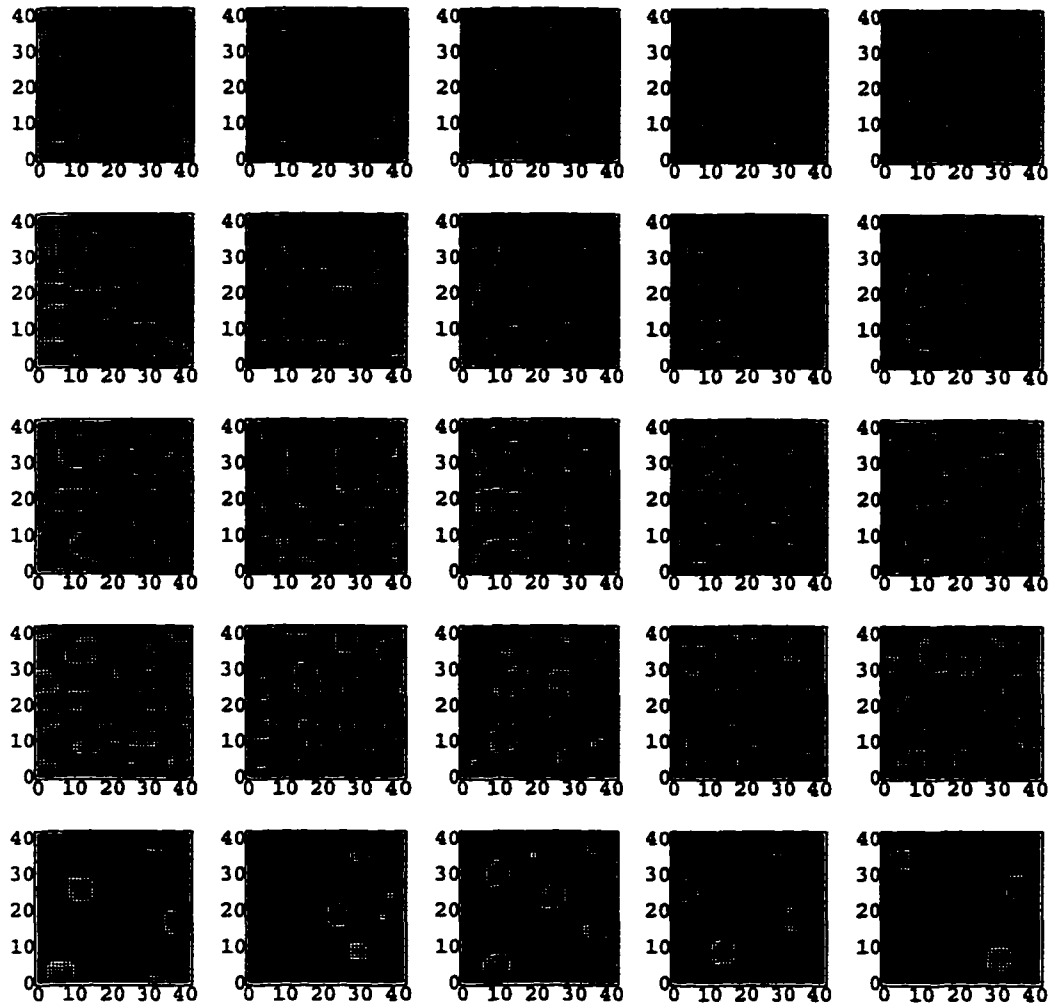


Figure 4.5: Threshold Variation Study

active in the final state for all 25 runs depicted in Figure 4.5 is plotted in Figure 4.6. A linear relationship is seen between the percent active and the threshold. Threshold values of 3 and above produce no active array elements, values of -3 and below produce no inactive elements. The number of clusters formed is also of interest. Figure 4.7 shows a plot of the number of clusters found in the final state for all 25 runs. Negative numbers represent clusters of elements with output values of -1 .

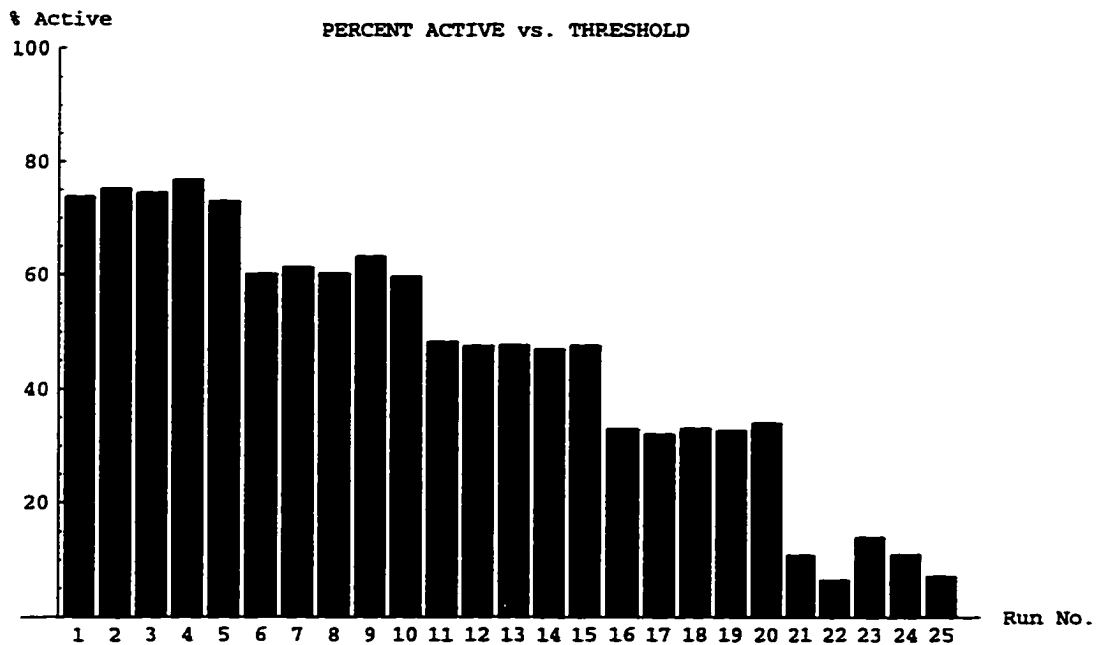


Figure 4.6: Active Percent of Array

4.1.2 FUNCTION VARIATION STUDY

We now wish to examine the influence of the form of the lateral interaction function by comparing simulations with a simplified variation of it. The basic form of the interaction function, described in the previous section, generally has three parts. A central excitatory region is the first part. This is surrounded by the second part, an inhibitory region. Pericolumnar inhibition has only these two parts. But the lateral receptive field surrounds these two with a third part, a very shallow (low intensity) excitatory region. These regions are marked by the radius to which each extends. In our first set of simulations, all three parts of the basic form are used. The results of this set are shown in the sequence given by Figures B.1, B.2, B.3, B.4, B.5, B.6, B.7 and B.8 in Appendix B.

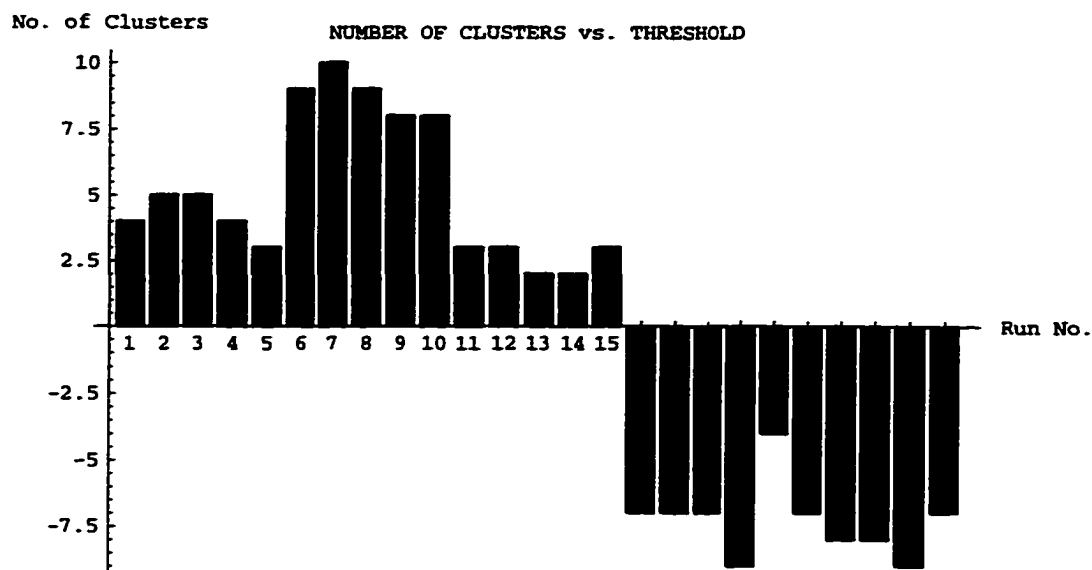


Figure 4.7: Number of Stable Clusters

The second set of runs we report are shown in Figures C.1, C.2, C.3, C.4, C.5, C.6, C.7 and C.8 in Appendix C.. These final states have spatial patterns that are very similar to those produced by the complete function with a threshold of +2. To obtain some idea of the variety of clusters that can be formed, we ran a series of simulations, varying the initial state with each case. The results summarized in Appendix B and Appendix C are based on random initial states. The response to patterned initialization (Walsh patterns) are also investigated. These results are in Appendix D.

4.2 DISORDERED BOOLEAN CIRCUITS

One of the attractive features of connectionist structures in general is their adaptability. For instance *in situ* training of a neural network, by which changes are made to connection weights during operation, has many applications from controls to pattern classification and signal processing. But with each type of structure there

is a somewhat different behavior. This implies an obvious limitation in adaptability. In other words, a feedforward structure cannot adapt into a recurrent structure no matter what assignment of weights is made to the connections available because it has a less general interconnection structure. What would make a structure more adaptable is of course some means of altering its connectivity *in situ*. Dynamic reconfigurability refers to this ability.

The remainder of this section is from Kauffman [22]. Consider the example of a recurrent synchronous network depicted in Figure 4.8. In the first of the three

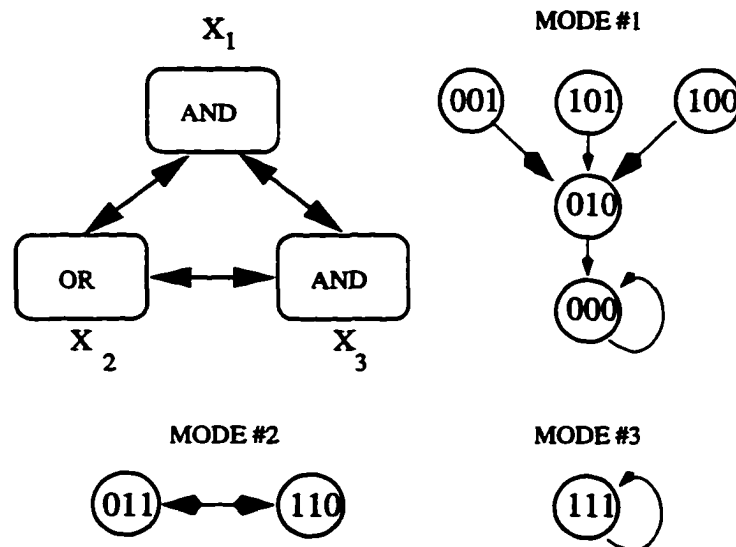


Figure 4.8: Recurrent Synchronous Network

modes of behavior the system reaches the stable point $x_1x_2x_3 = 000$. The system is said to be stable because once this point in state space is reached no more changes occur to any of the elements. Another way to describe this is to say that x_1 , x_2 and x_3 are frozen to the output value zero and that therefore these elements represent frozen components of the system. The second mode of behavior represents a limit cycle whereupon once entered the system repeats a sequence of states. Although

the system repeats a sequence of states, close inspection reveals that x_2 is in fact frozen and only x_1 and x_3 continue to change.

This behavior occurs in large boolean logic networks whereby the network state space is effectively divided into functionally discrete regions. The process begins with a small number of frozen components that quickly spread, or percolate to many other network elements. When a region of the network that is not frozen is completely surrounded by components that are frozen, this region is referred to as an island because it is functionally isolated from the rest of the system.

Two mechanisms responsible for percolation are forcing structures and internal homogeneity clusters. In both cases, percolation would not occur if the network were updated asynchronously. The principle behind forcing structures is the class of boolean functions termed canalizing, which refers to the property whereby the outcome of a function is completely determined by a single input regardless of other input values. Logical functions such as AND and OR are examples, whereas XOR is not canalizing. A function is canalizing only if that the element has at least one input having at least one value, 1 or 0, which guarantees that the element assumes a specific value, 1 or 0. To illustrate how forcing structures are formed, an example is worked out involving six OR gates arranged as shown in Figure 4.9. Note that this structure contains feedback loops.

The 1 state in any element will guarantee, or force, its descendent OR gates to be in the 1 state as well. Then, in turn, these gates will force all those elements which they regulate, and so forth. In the loop, the 1 value cycles around. When the loop has filled up the entire loop remains in a fixed state and cannot be perturbed by outside influence. What is more, all elements descending from the fixed loop will

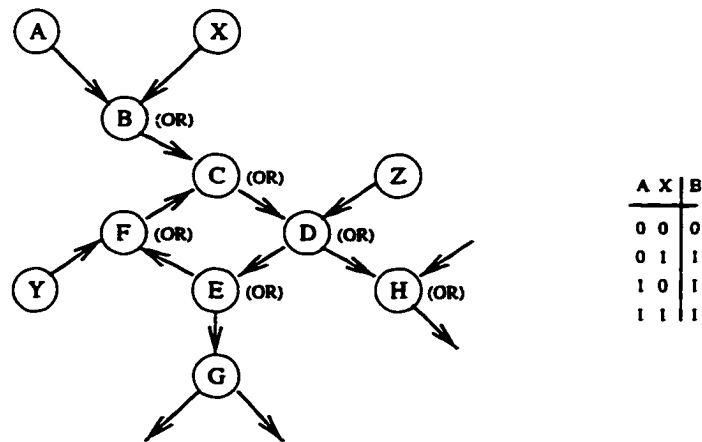


Figure 4.9: Forcing Structure of OR Gates

also be fixed at the 1 state. Thus a single fixed element can in this way percolate across several elements until a wall of constancy is established through which no signal may pass. Of course, these structures need not be limited to those made purely of OR gates. As shown in Figure 4.10, a variety of gates are involved.

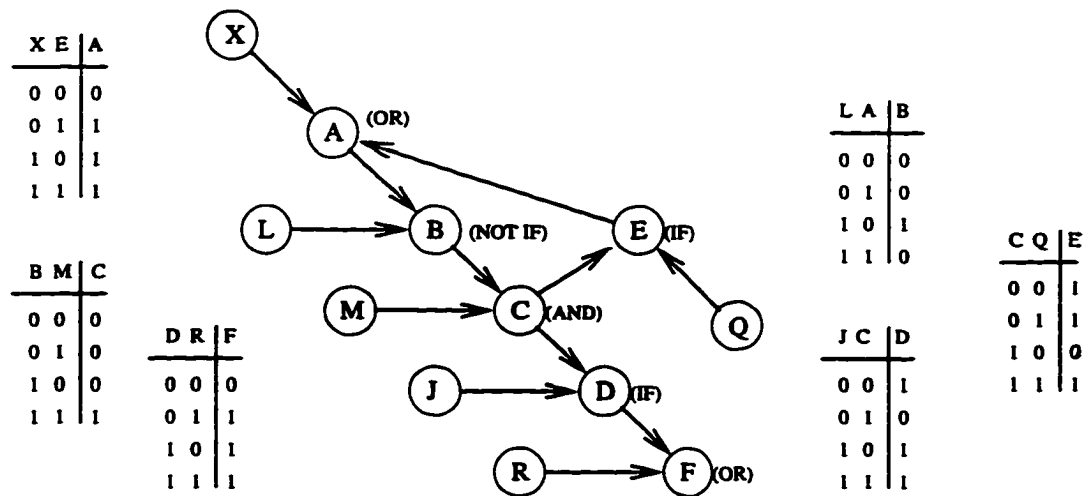


Figure 4.10: Another Forcing Structure

The defining principle is still at work, namely that at each point in the structure an element is in a state, 1 or 0, that can force a descendent element to a specific state, 1 or 0, regardless of its other inputs.

A forcing connection is defined as a connection between two regulated elements each governed by canalizing functions, the first of these supplying an input value to the second which guarantees the activity of the second element. The second element may also be indirectly governed by a canalizing boolean function via $K = 1$ input connections. If two elements regulated by canalizing functions are connected, one as input for the other, then the probability that this connection is in fact a forcing connection is exactly 0.5. This typically leads to large forcing structures of frozen elements. The threshold above which frozen structures form is called the percolation threshold. This threshold occurs when the ratio of forcing connections to elements is unity. For example, the $K = 2$ network has $2N$ connections (N is the number of elements), half of which, on average, may be forcing connections, assuming that all of the elements have been assigned canalizing functions. In such a network the ratio of expected forcing connections to elements is $N/N = 1$ which is high enough for forcing structures to form.

Internal homogeneity of a boolean function is defined in terms of P , the fraction of the 2^K input patterns (where K is the number of inputs), which produce a 1 response by the element.

Specifically the deviation of P above 0.5 is the internal homogeneity. Figure 4.11 corresponds to a network of binary elements connected together in a two-dimensional square lattice. The number at each site gives the periodicity of the site on the state attractor. A 1 represents an element frozen in either the active 1, or inactive 0, state. Clearly a frozen web of elements has formed and isolated islands of connected elements are free to oscillate but are functionally cut off from other islands. A web

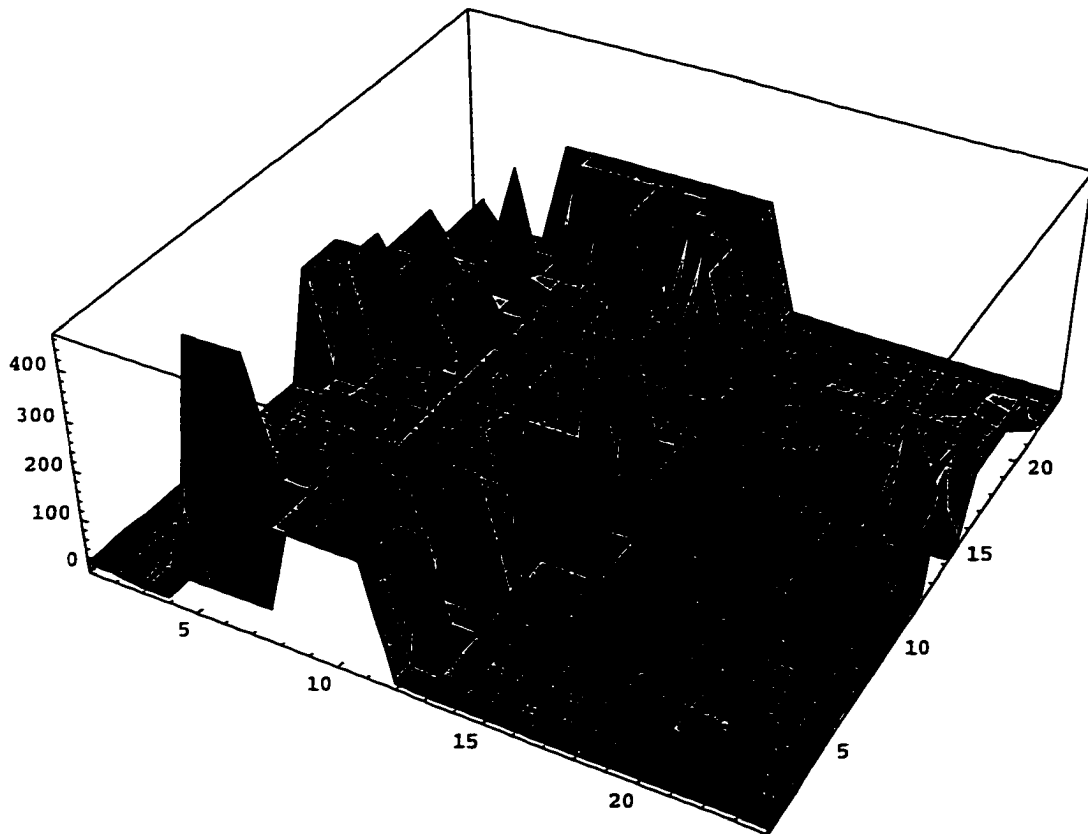


Figure 4.11: Boolean Network with Frozen Elements

will form in any such network if $P > 0.5$ is above a critical percentage P_c . This represents a kind of *phase transition* in behavior.

4.3 A DEVELOPMENTAL MODEL OF THE STRIATE CORTEX

The brain of a living creature continues to grow after birth, in the early stages of life. Studying the postnatal development of the brain during this period is a useful way to learn more about how the brain organizes its own structure and if there are any environmental influences on the process.

One such study by LeVay, Wiesel and Hubel [25] investigated the plasticity of ocular dominance columns in the striate cortex. Three figures in [25] show a series

of images of healthy macaque monkeys at (A) one week, (B) three weeks and (C) six weeks of age. In this section we present a model that mimics this developmental process. These images are autoradiographic photos and the reader may wish to examine and compare them to those generated by our model.

An ocular dominance column is a cortical structure, approximately cylindrical in shape, with its long axis running vertically through the cortex, perpendicular to its surface. Neurons in the striate cortex are connected to input from both right and left eyes. Columns in the striate cortex of a healthy adult are connected predominately to one eye or the other, and are therefore ocular dominate.

The autoradiographic images made by LeVay, Wiesel and Hubel were created with a radioactive die (marker) attached to a neurotransmitter used by the neurons in the eyes making connections to the striate cortex. One eye was injected with the marker and the other was not. Striate cortex neurons connected to the marked eye glow in these images.

Initially, these connections are made randomly throughout the entire region, and no clear columnar structure is apparent. The beginnings of cortical columns are barely discernible at one week. What happens as the striate cortex develops, is that connections are reformed from each of the two eyes, eventually grouping them together into columns.

In our investigation of cortical self partitioning, we simulated the process of ocular dominance column formation in the striate cortex. We set up a 100 by 100 array of binary processing elements. The output values of each element, $x_{u,v}$, represents a connection from one of the two eyes. For example, let the value +1 (-1) represent a connection from the right (left) eye.

The behavior of our model is governed by the equations:

$$x_{u,v}^*(t+1) = SIGN\left[\sum_{\mathcal{R}} \mathcal{H}(x_{u+i,v+j}^*(t))\right] \quad (4.3)$$

$$y_{u,v} = \sum_{\mathcal{R}} \mathcal{H}(x_{u+i,v+j}^*(t_{final})), \quad (4.4)$$

where *SIGN* is a nonlinear transfer function defined as in Equation 4.3 and \mathcal{R} is the region of lateral interaction (receptive field or pericolumnar inhibition) defined uniformly as in Equation 3.3 of Chapter 3. The lateral interaction function we use may be seen in Figure 4.12 and is of the same scaled Kaiser function form as described earlier. Three values are associated with each coordinate (u, v) in the array; $x_{u,v}$, $x_{u,v}^*$ and $y_{u,v}$.

The array is initialized with a pseudo-random number generator, as is done in our other simulations already discussed in this chapter. These initial values are copied to the variables $x_{u,v}^*$, which are then iteratively updated according to Equation 4.3 until it stabilizes at a time defined as $t = t_{final}$. From these new values of $x_{u,v}^*$, the values $y_{u,v}$ are computed as shown in Equation 4.4. It should be noted that values of $y_{u,v}$ may also be computed without $x_{u,v}^*$ first becoming stable. An example of the field (surface) resulting from this is shown in Figure 4.13. The rest of the process consists of re-assigning the connections (values of $x_{u,v}$): (i) pick a point (u, v) , with equal probability, from the set of points in the array; (ii) assign the new value by the following probability distribution:

$$x_{u,v} = \begin{cases} +1 & \text{probability} = \frac{y_{u,v} - \min}{\max - \min} \\ -1 & \text{probability} = \frac{\max - y_{u,v}}{\max - \min} \end{cases}, \quad (4.5)$$

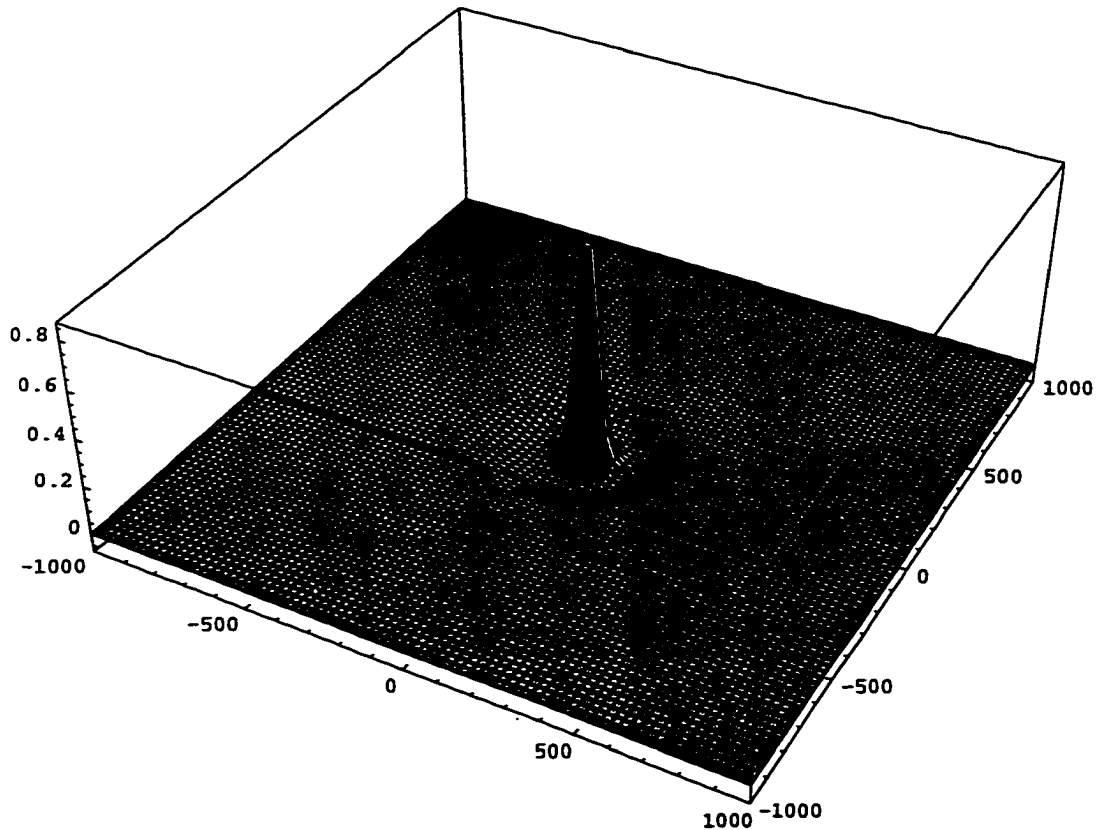


Figure 4.12: Lateral Function for Ocular Dominance Model

where max = maximum value of $y_{u,v}$ in array, min = minimum value of $y_{u,v}$ in array and t_{final} = time when $x_{u,v}^*$ stabilizes.

The initial state is shown in the upper left-hand frame of Figure 4.14. Elements are then reassigned according to our approach and progress is charted in this and the next figure. Neurons were reassigned probabilistically using the values $y_{u,v}$. Large positive values gave the greatest probability of a neuron being reassigned to the right eye (+1). Large negative values made it more likely that a reassignment be made to the left eye (-1). Values near zero were the least likely to be reassigned. The lower right-hand frame of Figure 4.15 shows the state of the array when the simulation ended, after 5000 reassignments were made.

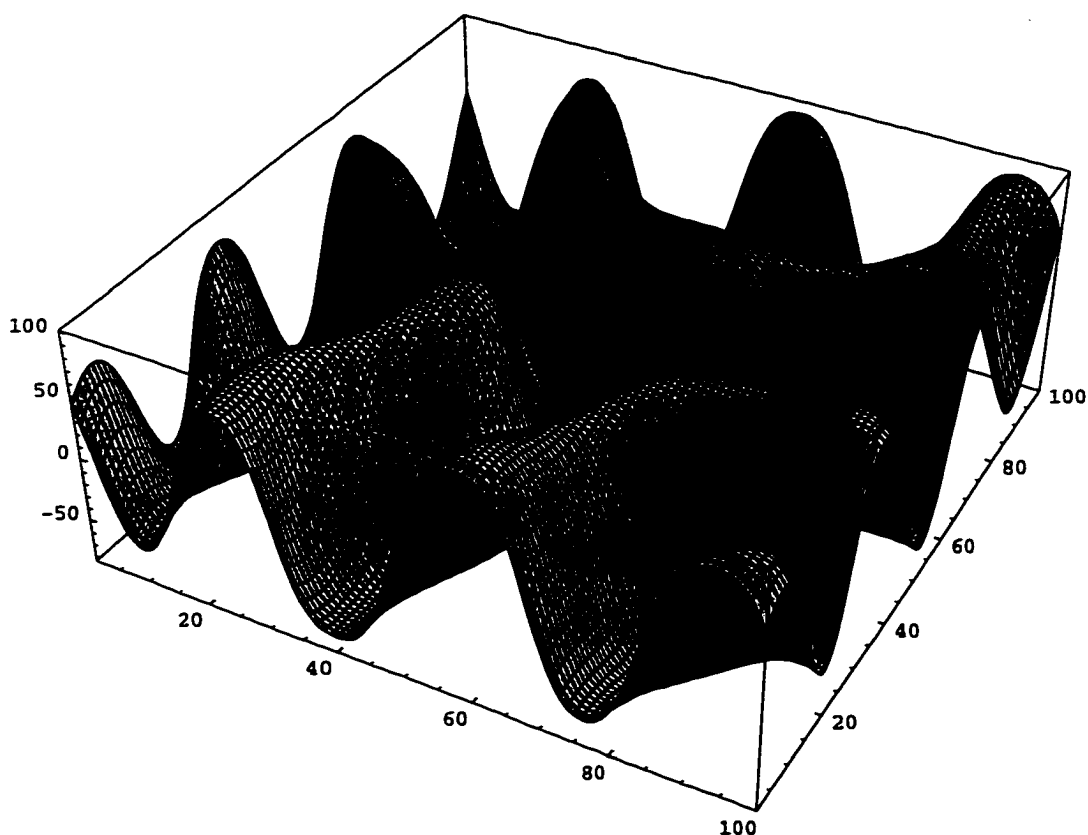


Figure 4.13: Ocular Dominance Surface

When the simulation was stopped, the boundaries between the two columns were still not completely defined. (Compare this with the results of LeVay, Wiesel and Hubel [25] reviewed earlier in this chapter.) Continuing the reassignment eventually produces clear boundaries.

4.4 SUMMARY

The aim of this chapter has been to better characterize the lateral interaction function of our theory, but an understanding of this process also leads to knowledge of how the brain makes adaptive classifications and performs concurrent processing.

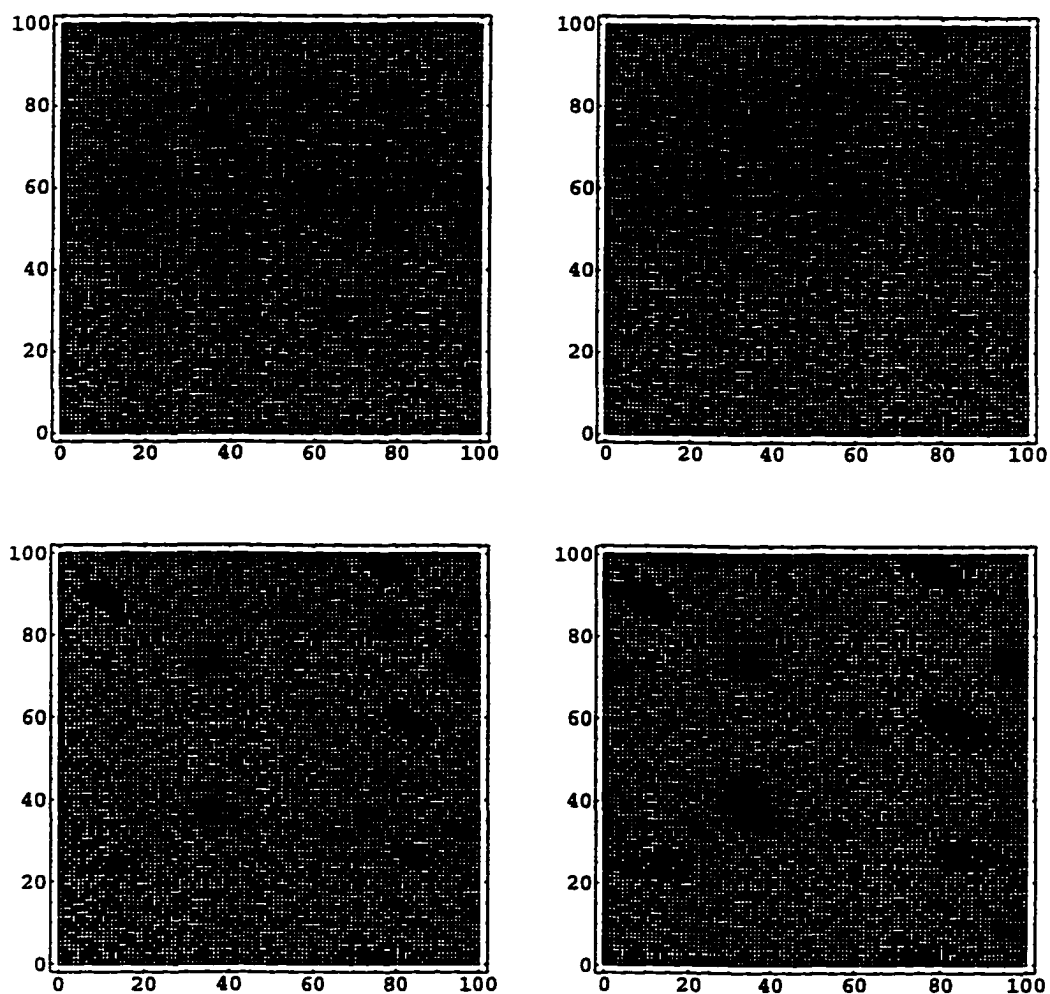


Figure 4.14: Simulated Column Formation : Part 1

An important potential role for oscillations in connectionist structures may be to partition computing resources for concurrent processing. Partitioning requires that all direct and indirect interaction between specific groups of processing elements (neurons) be broken. Without a mechanism for partitioning, some connectionist structures can only perform one task at a time; that task being the overall function of the neural network. In a fully interconnected structure such as the Hopfield neural network [17], every neuron in the network directly influences all the others.

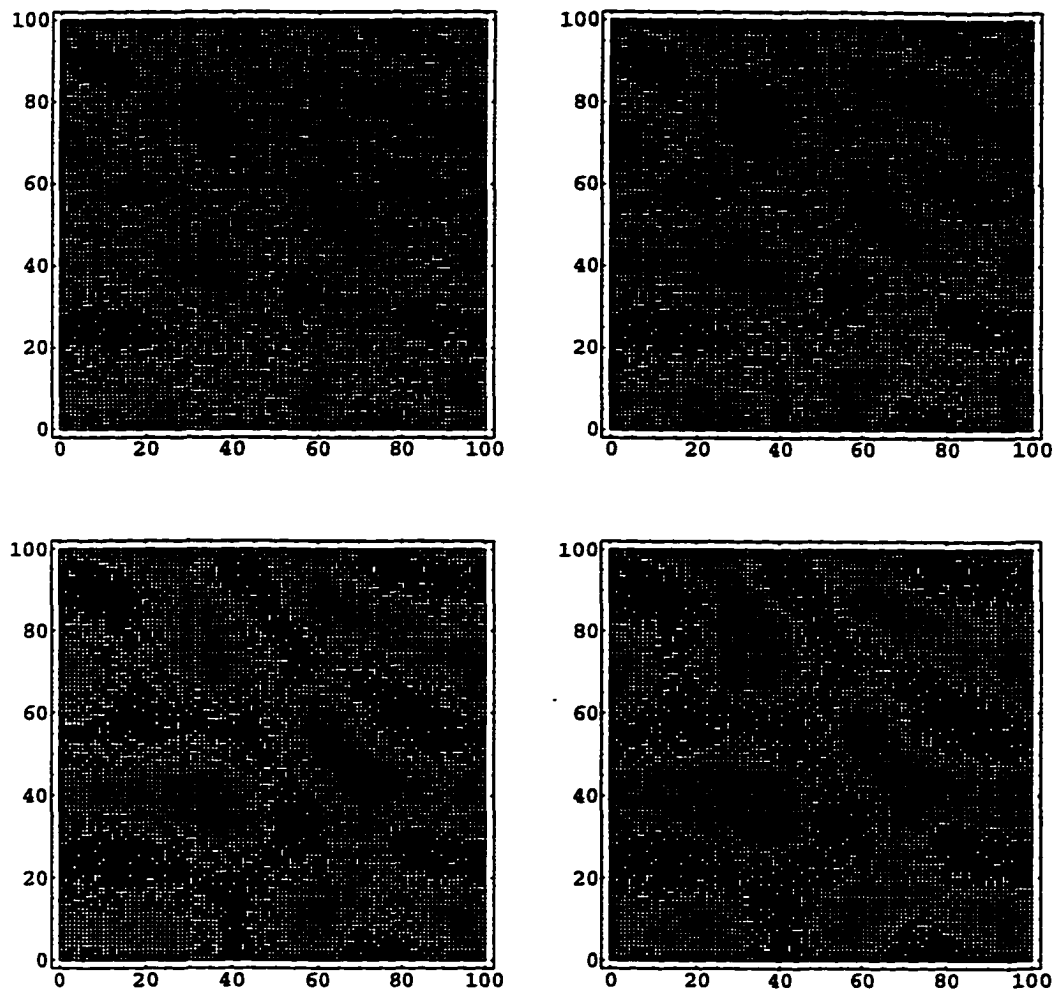


Figure 4.15: Simulated Column Formation : Part 2

As a result, a connectionist structure of this type, say functioning as a *content addressable memory*, can only retrieve one memory at a time in spite of the massive parallelism employed. But in another type of structure, *Boolean logic circuits*, frozen (not oscillating) network elements have been shown to functionally isolate active (oscillating) groups of elements from one another [22]. Such isolation may enable a network to operate more efficiently in some cases by dividing its resources among separate parallel tasks.

Synchronous discrete networks are structures that simultaneously compute output values for network elements over a sequence of finite time intervals. By contrast, the asynchronous operation of discrete networks does not select more than one element at a time when computing output values. Asynchrony may be a good approximation of the kinds of interactions that occur across great distances in the brain. But brain behavior at close quarters is probably better modeled synchronously. Discrete networks are studied in this chapter to simplify model implementation. This does not cause any loss of generality.

As shown by Kauffman [22] through a previously proposed cellular automaton, functional isolation is a common occurrence when construction is properly constrained. *Random boolean circuits* created within the automaton produce groups of cells that oscillate, separated by cells that are fixed in their output values. But the isolated functions of these groups is simply to cycle through a series of output values. Moreover the patterns of functional isolation and the functions performed are intimately tied together. When changes are made to the structure it effects the function, and vice-versa. This makes it a less suitable mechanism for column formation. As it turns out, greater biological plausibility, specifically, *pericolumnar inhibition*, may provide the basis from which a better approach can be found.

CHAPTER 5

CONFINED ACTIVATION

Our previous chapters have shown how useful activity emerges from out of background chaotic activity and how the spread of useful activity is limited by destabilizing long-path connections. We view such confined activation as being fragments of stored memories and investigate if they may serve as economic forms of completed memory patterns. We propose that the chaotic background may provide information of the ensemble of network memories needed to identify an economic form. In this chapter we examine how fragments of stored memories can spread in the network to become whole.

The aim of pattern completion is to reconstruct a learned memory from its partial representation. For example, an incomplete representation in a visual image can be of an object which is somewhat obscured by another object or of one that extends beyond the observer's view. The completion process reconstructs, from memory, the missing parts of an object's learned appearance.

The *feature based retrieval* (FBR) method, for the asynchronous update of fully connected recurrent structures, was developed by the author [53] to improve pattern completion performance. It is presented here in a new generalized form which can now be implemented in locally connected as well as fully connected structures. This form is shown to be closer to the interconnection structure of the cortex. In it, classifications are made on local data as part of the overall process of pattern completion. Let us now consider the origins of FBR.

5.1 TRADITIONAL PATTERN COMPLETION

The Hopfield neural network is a fully connected asynchronous structure, capable of acting as a *content addressable memory* (CAM). That is to say, it may implement storage of memory items for which context is used to access each item. As will be shown, a CAM may perform pattern completion, provided missing data is initialized to an appropriate value. The Hopfield model may be expressed in terms of the following state transition equation:

$$\vec{X}_{t+1} = \mathcal{F}(T\vec{X}_t), \quad (5.1)$$

where \vec{X}_t is the system state at time t and the matrix T may be created by a learning algorithm such as Delta Learning:

$$\delta T_{i,j} = \sum_p c[x_j^p(x_i^p - \hat{x}_j)], \quad (5.2)$$

where, x_i^p is the desired value of the i_{th} element of pattern p , \hat{x}_j is the evaluated output of the i_{th} element and c is an incremental constant.

The appearance of the Hopfield model of neural processing in the early 1980s ended almost a decade of what seemed to be slow progress in the connectionist field at the time. The basic structure of the Hopfield model is recurrent in form, Figure 5.1. It is composed of binary threshold logic gates, is constructed with symmetric connections and is updated asynchronously by selecting, at random, individual neurons whose outputs are updated one at a time. With the exception of having no self-feedback, the interconnection structure is fully connected. By constructing

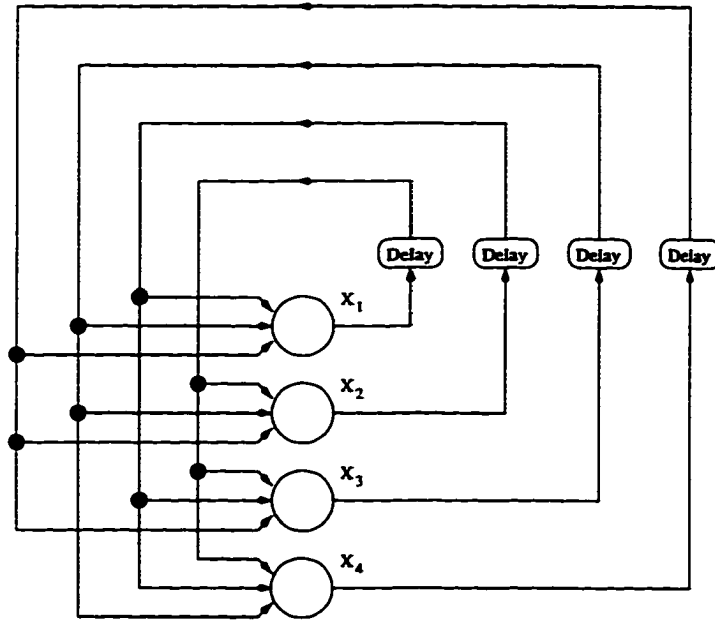


Figure 5.1: The Hopfield Model

his model in this way, Hopfield established an isomorphism with statistical physics models of molecular behavior known as spin glasses [17].

The vector $\{x_1 x_2 x_3 x_4\}$ corresponds to the outputs of the four processing elements as labeled in Figure 5.1. This vector indicates the instantaneous state of the system. The unit delays provide for the evaluation of the system state at discrete time intervals. Hopfield's popularization of the concept of dynamic stability in connectionist structures as a means of storing information is significant in that it permits an implementation of CAM.

Content addressability makes learned memories accessible by content rather than by some abstract and unrelated label or address identifier. Memory access begins by initializing the elements of the network with a vector, which is essentially a corrupted version of one of the learned memories. The network is then allowed to proceed to

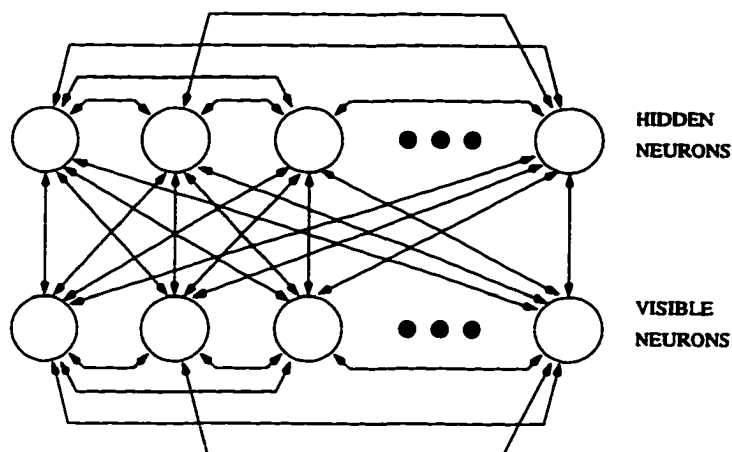


Figure 5.2: The Boltzmann Machine

a stable point where the resulting vector should correspond to the memory most matching the initial vector.

Pattern completion is very similar to the CAM retrieval problem. It is only slightly different in that just a fragment of a learned memory is provided and the complete memory must somehow be restored. A model that appeared soon after Hopfield's was able to achieve pattern completion (Figure 5.2). Called the Boltzmann machine, because it was influenced by ideas that had been put forth earlier by Boltzmann, it is in fact very similar to the Hopfield model but differs from it in the following important ways:

- The Boltzmann machine includes hidden neurons in its structure.
- The neurons of the Boltzmann machine are probabilistic while Hopfield neurons are deterministic.
- The Boltzmann machine is trained using a probabilistic supervised learning scheme.

Pattern completion by the Boltzmann machine is accomplished by applying a subset of a learned memory to the input layer, the elements of the input layer not receiving

input from the subset are initialized to zero and the system is then allowed to settle into a stable state. Key to the operation of the Boltzmann machine was the second, hidden layer of neurons used to store higher order associations.

The hidden layer in this model is not actually required for pattern completion to be performed. It does, however, permit functions that are not linearly separable. Shortcomings of these models include their rigid architecture and the fact that they tend to get stuck in local minima. This is seen most dramatically in the use of the Hopfield model for the solution of optimization problems. The spurious presence of stable states not corresponding to any of the learned memories may also cause an erroneous result. But even without spurious states, incomplete fragments can often lead to a memory that is not the one it most resembles. This difficulty in particular motivated such schemes for pattern completion as the *generator* method and *feature based retrieval*.

Consider the following example in which a fully connected recurrent network, having 100 binary neurons and being of the Hopfield type construction, is used to store memory patterns as stable system states. Let the vector $\vec{X} = x_1x_2\dots x_{100}$ represent the state of this system. For convenience, the 100-bit vector shall be represented as a 10 by 10 array of colored squares, each depicting the value of a single neuron. In Figure 5.3, a fragment of three bits is supplied and the network is allowed to proceed to a stable state.

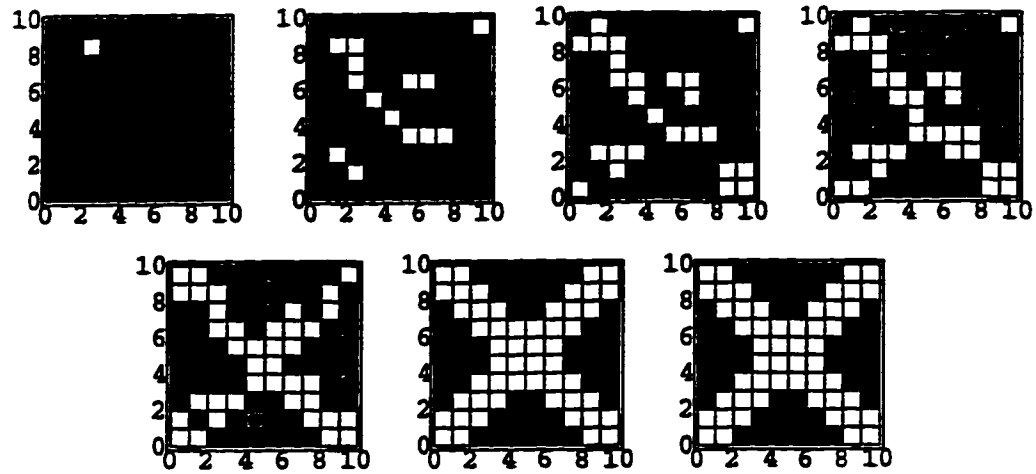


Figure 5.3: Hopfield Pattern Completion

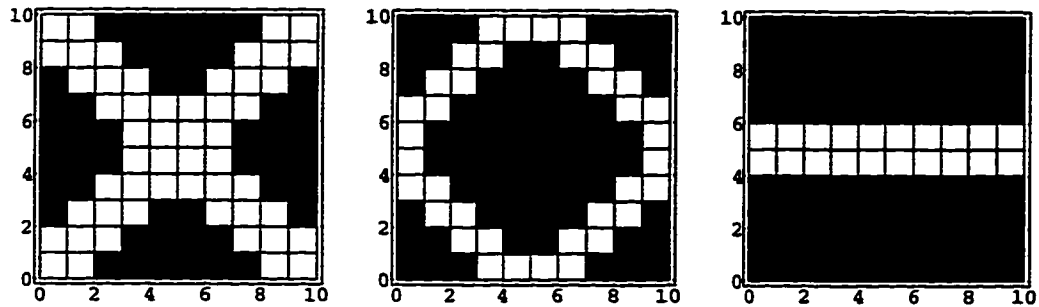


Figure 5.4: Training Set

Seven time frames (at times $t = 0, 20, 40, 60, 80, 100, 120$) are shown from the completion process. Note that the last two frames are the same, indicating stability has been reached. In each frame, a dark square represents an output value of $x = -1$ and a light square the value $x = +1$. Grey squares represent the initial quiescent state of $x = 0$ given to neurons that correspond to missing data.

In this example, the final stable state reached is one of a set of three patterns that were used to train the connection weight matrix according to Delta Learning (Equation 5.2). These patterns are shown in Figure 5.4.

As noted, these are not expected to be the only stable states of the system. In fact, as anticipated, the complements of these patterns were found to be stable as were a number of their linear combinations. An exhaustive search over all 2^{100} states was not performed due to computational limitations. In a later example, a smaller network that can be searched for all stable states is used to determine the influence of probe ambiguity.

The experiment depicted in Figure 5.3 actually shows an incorrect result, due to the difficulties inherent to this approach. That is to say that the final state, although stable, is not the one most closely matched by the original probe fragment. This can be seen by closely examining the active elements in the first frame. These values match the corresponding values of the second pattern of Figure 5.4 better than the other patterns, their complements or any of their linear combinations. The probe was chosen for this particular property. Since the second pattern should have been reconstructed, but was not, the outcome is considered to be in error. In all of 1000 runs of the completion of this probe, approximately 17% were in error. For this reason, alternative methods were developed.

5.2 INFORMATION DRIVEN DYNAMICS

In this chapter it is argued that extended periods of uncertainty should be studied in models of neural systems with oscillatory dynamics from the standpoints that its arbitrary elimination is not always advantageous and that its persistence may be biologically plausible. Rhythmic oscillations are such a common feature of the

electrophysiology of all living creatures, it seems somewhat shortsighted to ignore their rich dynamics in models that only average the activity. Visual and olfactory system research have discovered a number of things about the oscillatory nature of the brain including possible functional uses for the chaotic neurodynamics observed. A link between chaotic dynamics and uncertainty provides motivation for a new information theoretic approach to oscillatory dynamics. Toward this end, a simple feedback model is developed that sustains uncertainty through a collective process based on information content. Rules for selecting the order network elements are activated and quieted sometimes create transient fragments of oscillatory activity that wander through an otherwise quiet system.

5.2.1 THE PRESERVATION OF UNCERTAINTY

The collective properties of traditional neural systems create an undue emphasis of dynamics that arbitrarily seek stability and certainty. While delaying a decision may not be desirable in some instances, it is useful in others. For example, in processing phrases and sentences of natural languages it is sometimes better to delay decisions about the meanings of words because the most likely meaning may change when a later word is read. By waiting for more information at a later time, the computational complexity of unnecessary backtracking can be avoided. In such cases, uncertainty should be preserved and decisions that determine the outcome should be avoided or at least delayed.

Biological neural systems with chaotic oscillatory dynamics can be said to be in a state of uncertainty because more than one learned pattern of activity is reachable from the current activity. This is the role chaos plays in an interpretation popularized by W. J. Freeman in his model of the olfactory system [7] for which a chaotic background serves as an unbiased starting point in the classification of input stimuli. Such a system is well suited to handle new information, being able to rapidly classify novel and learned stimuli and perform selective attention.

Observations of chaotic oscillations of electromagnetic activity in the brain [7, 8] testify to a natural preservation of uncertainty and give further motivation for the persistence of chaotic behavior in artificial neural systems. If uncertainty were not preserved in the brain, then any chaotic oscillation would quickly die off. Freeman reports that the act of recognizing a conditioned stimulus causes a bifurcation of the activity from a chaotic background state to an identifiable pattern in the electrical activity of the olfactory bulb [7, 46, 47]. During exhalation, activity returns to the chaotic background state and persists for the entire period of exhalation [7]. A growing interest in the role that chaotic oscillation plays in neural systems is seen in a number of recent models of brain function and even recent speculations about consciousness [4, 5, 8, 10, 15, 18, 27] that favor chaotic activity over point attractors because of their biological plausibility.

For these reasons the collective properties of traditional connectionist networks, those that arbitrarily remove uncertainty in an effort to obtain stability, seem to

be inappropriate. When traditional networks are faced with more than one stable state that may be reached from a given initial state, a saddle point in state space, the choice made is arbitrary and the result is random. What is sought here is a system that does not automatically make these kinds of decisions. The result is an oscillatory wandering among uncertain states until new input is supplied or the system is driven toward stability by other means. Although more than one stable state may be reached from a saddle point, others may not. Therefore an uncertain state conveys information. Care must be taken when updating the neurons of the system if the information they convey collectively is not to be destroyed by the network dynamics. This suggests that information theoretic concerns should form the basis of a new collectively regulated network dynamic. The uncertainty of outcome created by ambiguous input permits a variety of potential final states that are stable in the neural system and have specific probabilities of being reached. Entropy, a measure of uncertainty and therefore information, can be said to be related to a chaotic system by the number of unstable orbits that make up its phase portrait. The bifurcation from a chaotic attractor into a point attractor or a stable periodic oscillation is somewhat analogous to the stability-seeking behavior of traditional feedback models which are drawn toward a final stable point in state space. The major difference is that a definite action, either a change in a system parameter or the introduction of new input, must be made in order to force the bifurcation to occur.

In what follows it is shown that the persistence of chaotic behavior can also be represented analogously by something similar to a traditional feedback model, provided it is modified to preserve entropy. For simplicity an adaptation of the Hopfield model [17] will be used in this discussion of the operating principles of the proposed model. The Hopfield model here is composed of discrete valued elements that are updated asynchronously and randomly. The focus here is on the rules that govern network behavior that are based on estimations of system state entropy.

Information content in neural systems is a quantity that is not readily observable nor can it be directly calculated from a description of network connection strengths and network activity because a detailed knowledge of the entire set of attractors, among other things, is required. What follows is based on a direct application of the theory of communication developed by Shannon [45]. A neural system in state i shall be said to have produced the symbol k when there is unit probability of reaching attractor k from state i provided all state changes result from evaluating neuron transfer functions individually (asynchronous update). In this system, states are taken as *messages* and the set of all attractors comprise the *code book* of possible meanings. For each possible state i , there is a set of probabilities $p_i(k)$ of producing the various possible symbols. There is, therefore, an entropy H_i of the system for each state i which serves as a measure of the information the state conveys. The reason why we use the term entropy is because we average the information over all reachable states from the given fragment.

It is important to realize that sustaining a given value of uncertainty does not mean that the potential outcomes will keep their original probabilities. This is a separate problem because a distribution of probabilities can yield an uncertainty equal to that of another even though the respective outcomes have different probabilities. What is desirable is that the same information, not just the same amount of information, be preserved. Therefore, not only a similar distribution is needed but it is important that the very same one be maintained. Simulated annealing and other methods that make small random changes to neuron output values may also bring about delay in stabilization. But these methods do not attempt to preserve the distribution. Their goal is to reach a global optimum, which is quite different from the one taken up in this model.

A state change that significantly alters the likelihood of an outcome alters the very thing that the state represents. Such change can and should be allowed with the application of input, but avoided otherwise. Of course, the easiest way to avoid this is to prevent state changes of any kind as long as there is an uncertainty greater than zero. Unfortunately, a network of this sort performs no useful function beyond the mere accumulation of input until such time as sufficient information permits the network to proceed and reach a determined stable point. On the other hand, if care is taken in choosing the kinds of state changes that are allowed, a limited amount of network dynamics might be possible without significantly influencing the probability distribution.

5.2.2 QUIET NEURONS

To preserve any level of uncertainty other than zero, state changes that alter the entropy of the system must be met with changes that restore it. But almost all movement in state space from any point to another will change the distribution of probable outcomes. From this fact it seems that little can be done to restore the original distribution except to return the system to its initial state. There is in fact something that can be done involving quiet neurons that will provide greater freedom to the network dynamics.

A quiet neuron considered as a communication channel should carry zero information about the condition of its inputs. To do this the output must not bias the other neurons toward any particular state and it must be a value that is not arrived at through the operation of its transfer function. A quiet value can, for example, be the average of all the output values of a discrete transfer function provided the average itself is not one of them. All other values of the transfer function are considered active values.

On the other hand, a continuous transfer function as illustrated in Figure 5.5 includes its average in the range of output values. If this average represents a naturally occurring stable neuron condition, then it is not suitable as a quiet value because it can be learned by the network. But if the neuron ordinarily passes through the average only briefly as it approaches a stable saturation state, as shown in the figure,

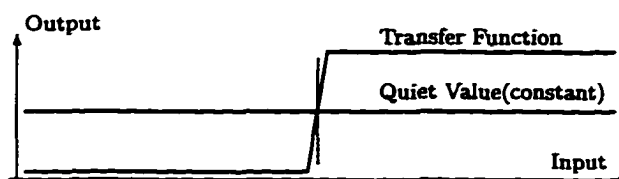


Figure 5.5: Continuous Transfer Function

then it can be used to represent a valid quiet value when assigned to the neuron instead of having its transfer function evaluated.

The modified model is based on a discrete transfer function that performs a binary operation on the weighted sum of its inputs. This means that assigning the average creates a quiet neuron having an output it would not have had the transfer function been evaluated to update the neuron. Although the system has a larger state space that fact alone does nothing to increase the storage capacity of the network. A network with n neurons has 3^n states when quieting is used though $\frac{3^n - 2^n}{3^n}$ of them are potentially unstable. This is because evaluating a quiet neuron will always change the network state thus making all state vectors with quiet elements unstable. The modified network behaves as if it were in fact a smaller network than it is physically because all evaluations operate on only the active network and none will yield a quiet value. It is as though all connection to the quiet neurons are cut off from the point of view of any present evaluation. With a number of weights essentially removed from the connection matrix the neuron response and,

therefore, the network behavior can be very different. This represents a form of dynamic reconfigurability based on network activity rather than synaptic plasticity.

5.2.3 ENERGY AS AN ESTIMATE OF ENTROPY

An entropy surface can be cast over the points of state space just as an energy surface can. In fact the entropy surface is determined using the energy surface though it is not a simple functional relationship. The procedure begins by exhausting all possible monotonic non-increasing paths along the energy surface from state i and counting the number of times each of the final states k is reached. The number of paths to state k divided by the total for all k is the probability $p_i(k)$ that state k is reached from the initial state i . The product of this probability and its logarithm when summed over all values of k gives H_i , the entropy of state i

$$H_i = - \sum_k p_i(k) \log p_i(k). \quad (5.3)$$

Repeating this procedure for all states produces the complete entropy surface. Clearly this is a monumental task, using $O(n2^n)$ time, for large or even moderate size networks. Precalculating these values for use by each neuron complicates the distributed processing requirements of connectionism. But, more significantly, every time any interconnection weight is changed the entire entropy surface must be recalculated. The overhead demanded would be so great that this approach is simply not practical. Since entropy is a labor-intensive measurement, it is desirable to relate it to a more readily available value such as energy. The system energy

E_i is not directly known by individual neurons but it may be decomposed into the contributions from each neuron $E_{i,j}$ which are available at each neuron. For the purposes here the following is an adequate form of the energy function, where $w_{j,k}$ is an element of the connection weight matrix and the terms $x_j(i)$ and $x_k(i)$ are the j and k neurons of the state i

$$E_i = \sum_j E_{i,j} = -\frac{1}{2} \sum_{j,k} w_{j,k} x_k(i) x_j(i). \quad (5.4)$$

In the physical sense energy which describes the thermal temperature of a system is directly related to entropy. This is not true as defined in the neural sense. It is important therefore to determine exactly what can be said of a correspondence, if any. To begin, one already knows that a nonzero value of entropy attributed to a state implies that a number of possible outcomes may be reached from that state whereas an uncertainty of zero means only a single possible outcome exists. Consequently an uncertain state is also an unstable one and a stable state has zero uncertainty. Given the correspondence of stability with energy minima, this implies some relationship with entropy. Beyond this nothing can really be said of a consistent relationship. The zero entropy at a global energy minimum is the same for all energy minima and a global energy maximum is not necessarily a global entropy maximum. The latter is easily seen for cases where all monotonic nonincreasing paths from the point of highest energy lead to relatively few unevenly distributed energy minima. If there also exists another point from which many more energy

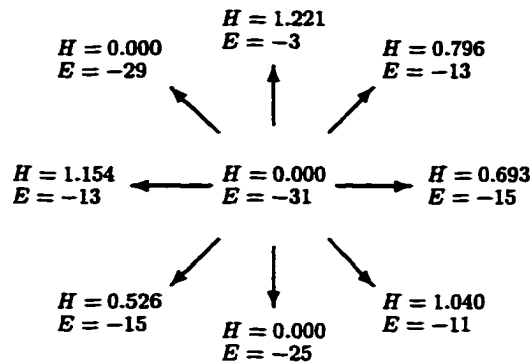


Figure 5.6: Energy and Entropy

minima may be reached with nearly equal probability, then this point has more entropy.

Calculated values of entropy and energy are given in Figure 5.6 for all adjacent points surrounding a central one in a very small network that has only eight neurons. It is clear the central point is a stable state since the energy is higher in all directions. Entropy on the other hand is higher in all of the adjacent states but two. Elevated entropy indicates that there are paths from these adjacent states leading toward stable points other than the one shown. Still other regions of the topology show state changes between adjacent points where the two gradients are opposed to one another, that is to say that a rise in entropy is sometimes seen along with a drop in energy and vice versa.

5.2.4 COLLECTIVE AND INDIVIDUAL UNCERTAINTIES

Since having a detailed knowledge of the entire entropy surface to compute the probabilities $p_i(k)$ is not practical one must look at how small changes in the *message*

affect the information it conveys. This is done through an approximate decomposition of H_i . An individual uncertainty h_j is associated with the output of the j th individual network element. The average \bar{h} computed over the number of active network elements η will serve to approximate H_i

$$\bar{h} = \frac{1}{\eta} \sum_j h_j. \quad (5.5)$$

Just as system energy is the sum of many individual energy contributions, neuron uncertainties can form an approximate decomposition of the collective uncertainty. For simplicity, consider a network element that evaluates a threshold function on the weighted sum of its inputs. The proximity to a threshold may be considered to be related to the uncertainty of that element's output. For example $h_j = y_j^2$, where y_j is the weighted sum of element j . In biological systems h_j may be related in some way to somatic membrane potential. A new output value from element j changes the uncertainties of every element that receives it. Controlling the amount of change by selecting which element should be updated regulates the information content of the system state.

The n -dimensional binary vector $x_1(i)x_2(i) \dots x_j(i) \dots x_n(i)$ describes the i th state and the following transfer function for the j th neuron is used to evaluate every neuron

$$x_j(i) = \mathcal{F} \left(\sum_k w_{j,k} x_k(i_0) \right). \quad (5.6)$$

The coefficient $w_{j,k}$ is a connection weight and i_0 is simply the state before state i and before updating the j th neuron. The function $\mathcal{F}(q)$ evaluates to $+1$ if $q \geq 0$ and to -1 otherwise. Since $x_j \in \{-1, +1\}$ is the range for all elements, $x_j = 0$ serves to represent an inactive neuron condition. The following two rules are used for regulating entropy and are based on the expression $h_j(i_0) = [\sum_k w_{j,k} x_k(i_0)]^2$ for individual uncertainty.

Rule 1: A quiet element is eligible for activation when its uncertainty $h_j(i_0)$ is greater than $\bar{h}(i_0)$, the average uncertainty of the system:

$$h_j(i_0) > c_1 \bar{h}(i_0). \quad (5.7)$$

Rule 2: An active element is returned to the quiet state only if the following inequality holds:

$$h_j(i_0) < c_2 \bar{h}(i_0). \quad (5.8)$$

The control parameters c_1 and c_2 are positive real numbers that regulate the decrease and increase of entropy, respectively. Suitable values of $c_1 = 0.75$ and $c_2 = 2.25$ were found experimentally for use with the networks described below. These eligibility rules only delay the eventual removal of uncertainty and in some cases entropy is seen to fluctuate considerably before dropping off completely. The size of the active set may also change as the network is updated but this is fine since the eligibility rules do not ensure that there is always an eligible neuron.

5.3 THE IDD MODEL

The information driven dynamics model (IDD) makes network state changes by sometimes activating neurons and sometimes quieting them in a way that preserves uncertainties concerning which final state is reached or indeed if one is ever reached. A fully connected feedback structure is used for the simulations analyzed in this chapter because feedforward architectures will not support the long state-change sequences described. Fully connected structures are preferred over ones with lower connectivity in order to maximize redundancies within the learned patterns. If the IDD model is incorporated into a larger system, the overall structure does not need to be fully connected to support the kinds of activity reported in this chapter. As long as enough redundancy exists to permit a variety of fragments to represent any learned pattern then the activity characterizing the IDD model can be supported.

Let $\vec{x}(t_0) = x_1(t_0)x_2(t_0) \dots x_n(t_0)$ represent the state at time t_0 of a network having n neurons. The network is updated to the next state $\vec{x}(t) = x_1(t)x_2(t) \dots x_n(t)$ in one of two ways. An active neuron, $x_i(t_0) \neq 0$, may be quieted by the operation, $x_i(t) = 0$, and a quiet neuron, $x_i(t_0) = 0$, may be activated. The activation of neuron i is done in the same way as it is for the traditional Hopfield-style neural network:

$$x_i(t) = \mathcal{F}\left(\sum_j w_{ij}x_j(t_0)\right), \quad (5.9)$$

where w_{ij} is the connection weight from neuron j to neuron i and \mathcal{F} is a function taken to be the same for all neurons. For simplicity, and without loss of generality, zero bias will be assumed for all neurons and \mathcal{F} shall be the sign function.

From the above activation function we derive an estimate of the system entropy. The value $\bar{h}(t_0)$ represents this estimated value at time t_0 . It is taken to be the mean of the square of the sum performed by the activation function. The contribution by each neuron to $\bar{h}(t_0)$ is accordingly given by $h_i(t_0)$ as defined below:

$$h_i(t_0) = \left[\sum_j w_{ij} x_j(t_0) \right]^2. \quad (5.10)$$

The IDD model is distinguished from the traditional Hopfield model mainly by the way it maintains and uses two neuron sets. The first of these, set A, is a subset of the set of all quiet neurons and represents those chosen as eligible to be activated. Set B contains the active neurons that may be quieted. An algorithm constructs these sets and updates the outputs of neurons from them accordingly. Once a state change is made the sets themselves are updated and the process repeats. The basic form of the algorithm (Figure 5.7) has two rules for establishing sets A and B that use the estimates of individual and system uncertainties described above. The algorithm was implemented in several different forms to evaluate the merits of certain modifications.

Notice that when sets A and B are both the empty set, the system is in a stable equilibrium condition. If set B is empty and set A contains only those neurons such

IDD Algorithm : Basic Format

Step 1 Construct set A such that $x_i(t_0) \in A$ if $x_i(t_0) = 0$ and

$$h_i(t_0) > c_1 \bar{h}(t_0) \quad (5.11)$$

Step 2 Construct set B such that $x_i(t_0) \in B$ if $x_i(t_0) \neq 0$ and

$$h_i(t_0) < c_2 \bar{h}(t_0) \quad (5.12)$$

Step 3 Select and activate a neuron from set A

Step 4 Select and quiet a neuron from set B

Step 5 Assign $\bar{x}(t)$ to $\bar{x}(t_0)$ and return to Step 1,

where
$$h_i(t_0) = [\sum_j w_{ij} x_j(t_0)]^2$$

$$\bar{h}(t_0) = \frac{1}{\eta} \sum_i h_i(t_0)$$

$$\eta = \text{number of active elements at time } t_0$$

$$c_1, c_2 \text{ are constants}$$

Figure 5.7: Basic format of the IDD algorithm

that $x_i(t) = x_i(t_0)$ for all i then the network is also stable. These are the only conditions that permit stability. While keeping in mind that stability is not always the desired end result, it may be interesting to see when stability will occur. In the traditional Hopfield-style network, stability is ensured for asynchronous updated networks. This can be seen from an argument using the following energy function:

$$E(t) = -\frac{1}{2} \sum_{i,j} w_{ij} x_j(t). \quad (5.13)$$

Using the IDD algorithm, an increase in $\bar{h}(t_0)$ will tend to cause set A to grow smaller while set B will grow larger. As more neurons become quiet, set B will see fewer active neurons from which to choose eligible neurons, while set A will have more of a selection. This implies that as $\bar{h}(t_0)$ increases an equilibrium will be reached.

In fact, as will be seen, this is borne out in the experimental results. It is important, however, to realize that an equilibrium in the sizes of sets A and B does not mean the system dynamics are in equilibrium (i.e., the activity of the neurons has reached a stable state condition). If neither sets A or B are empty, the network will continue to select neurons to activate and quiet regardless of whether the sizes of these sets are changing.

Suppose, on the other hand, that the fragment is one that decreases the value of the function $\bar{h}(t_0)$. In this situation, set A increases in size while set B decreases. The expected result is that the fragment will grow. This was observed for the following condition. If the initial fragment was close in Hamming distance to only one learned

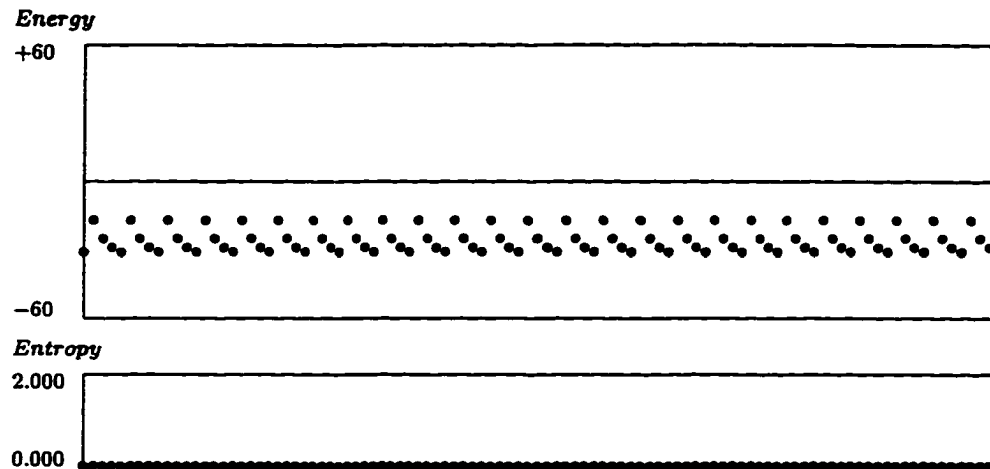


Figure 5.8: Small Network Example

pattern, while relatively farther from all the others, then the fragment grew. This is expected since it corresponds to a fragment that bears stronger similarity to only one out of the possible learned patterns. In other words the uncertainty is low.

5.3.1 SMALL NETWORK EXAMPLES

Small networks of $n < 10$ neurons were studied because of the time needed to calculate entropy. Connection weights were chosen with a random function and assigned to a matrix that was made to be symmetric and have a zero diagonal. The following examples are from a network of $n = 8$ neurons that had 10 stable points found through an exhaustive search of all 2^8 states.

Whenever the network was initialized to a state that had zero uncertainty, the entropy remained at zero. In some cases, but not all, this did not prevent the energy from oscillating as seen in Figure 5.8. The initial state here is in fact a stable

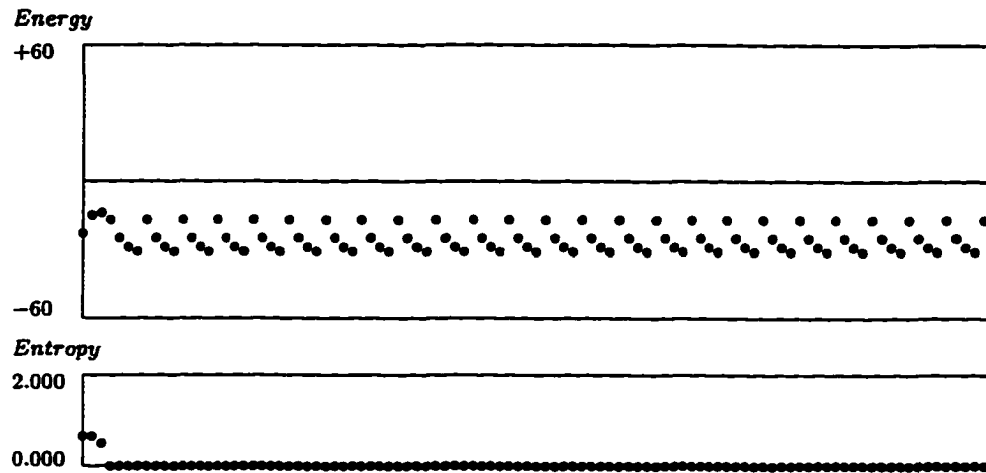


Figure 5.9: Oscillating Energy

state under normal circumstances but because of the eligibility to quiet at least one neuron the system does not remain static.

A small initial entropy tends to drop off very rapidly as shown in Figure 5.9 where again the energy is seen to continue to oscillate after the entropy has reached zero. It can be seen that some stable points are no longer stable because of the eligibility to quiet neurons. More important than stability is that the network reaches a condition of zero uncertainty and remains there. If each previously stable point is considered a stored memory item, then the modified model will retain all of these items on the basis of zero entropy assuming reasonable values for the control parameters are used.

Figures 5.10 and 5.11 show cases where a stable point is actually reached as indicated by their final steady values of energy. These figures also show the comparative times needed to stabilize as related to the initial entropy. The general

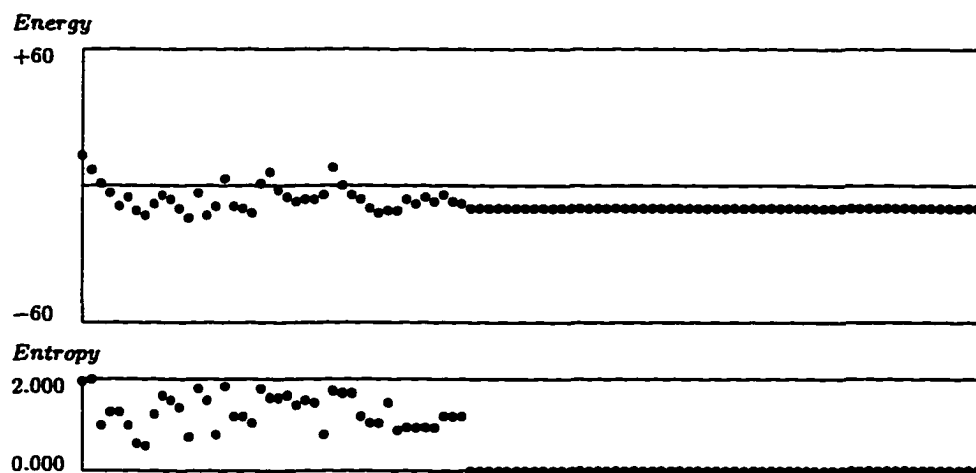


Figure 5.10: Initial Entropy: Long Decay

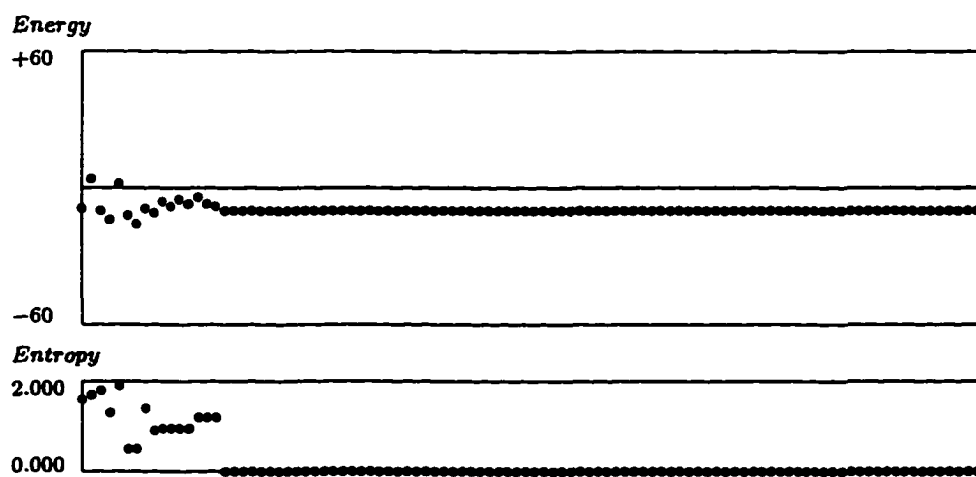


Figure 5.11: Initial Entropy: Rapid Decay

trend observed is that the delay is longer when the uncertainty of the initial state is high. But this is only a trend and not a direct relationship because the actual delay varies with the specific update order followed. Since the eligibility rules only restrict but do not completely determine the update order, there will be some variation between runs.

In any neural system, especially those with inactivity, update order plays a major role in determining the outcome of the system. This is easily shown experimentally with a network that has been arbitrarily trained. While exhaustively permuting the order of the indices j , evaluate the elements x_j of a vector that begins in the completely inactive state. The dependence of the outcome is seen by comparing the results of each different update order. In some cases update order alone can determine which final state is reached. Update order was determined competitively in [20] by delaying the evaluation of each neuron a period proportional to the proximity to threshold of y_j , the weighted sum of the j_{th} neuron. Only quiet neurons were updated so that fragments grew until complete vectors were formed. A similar competition might be used to establish update order among the eligible active and eligible quiet neurons of the modified model. In this case an interval should be assigned each neuron defining the minimum time before an active (inactive) neuron may be quieted (activated). This permits those eligible neurons not absolutely closest to threshold to occasionally win the competition but only after those closer have been updated. This also modifies the direct competitive selection process by

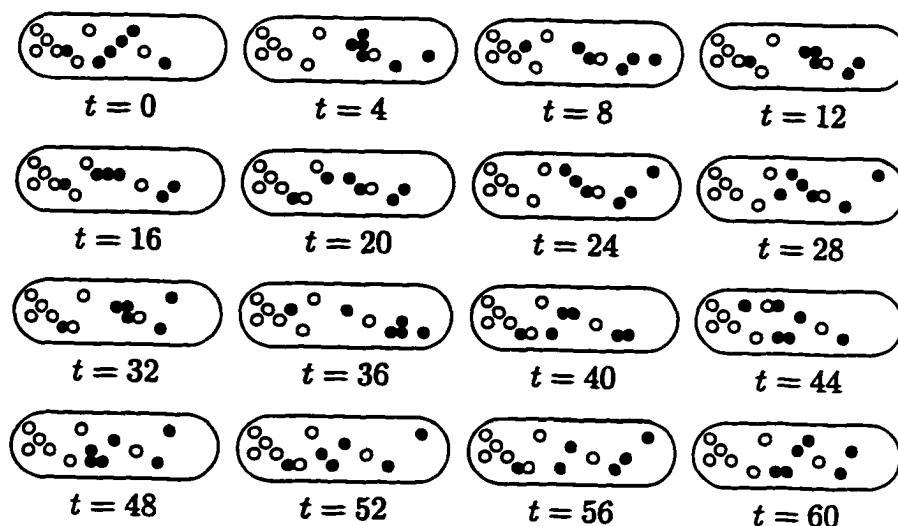


Figure 5.12: Retrieval Dynamics

imposing the update order of the elements most recently affected. Thus the selection is based not only on the instantaneous state but also the update order leading to that state. This is important because it enables smaller fragments to convey more information.

5.3.2 LARGER SIMULATIONS

In what follows networks of 64 neurons were used. A low number of patterns were stored (usually three) and were constructed to have a large average Hamming distance and high level of redundancy. An example of one run of this model on such a network is illustrated in Figure 5.12. A total of 60 time steps are shown as 16 frames at intervals of 4 steps. Each frame represents the output values of the active neurons at a specific time in this process. An active value of +1 (-1) is depicted as a closed circle (open circle). Any inactive neuron, with the output value 0, appears as a blank space. The 64 neurons of this simulation are represented in 4 rows of

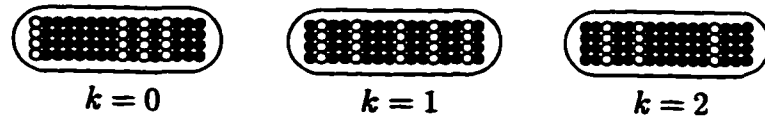


Figure 5.13: Memory Set

16. Note that the active neurons with the output value -1 at time $t = 0$ remained so throughout the simulation. Several neurons that were inactive initially also remained inactive throughout this period, as well. However a number of neurons seem to alternate between the inactive and active $+1$ values.

In this particular simulation, only three patterns were used as the memory that had trained the network. As with the small network example, Hebb's rule was adequate to store the three rather redundant patterns of 64 bits shown in Figure 5.13. These patterns are labeled $k = 0$, $k = 1$ and $k = 2$. Redundancy was desired in this example to provide a very likely case for multiple fragments to represent the same information. The initial fragment in Figure 5.12 was deliberately selected to be equally distant to as many of the stable memory set states of Figure 5.13. The resulting wandering among similar network states demonstrates the expected behavior of IDD when the ambiguity (uncertainty) of the probe is high.

5.4 FEATURE BASED RETRIEVAL

The progression of a recurrent network structure from an initial to a final stable state is an iterated process. This fact, together with the highly redundant nature in which information is stored in a fully connected network, permits the reconstruction of memories without use of a hidden layer [19, 20, 53, 54]. This redundancy is seen in that from the 2^n states of a network having n elements only $0.143 * n$ randomly chosen memories can be reliably stored by the usual means. Pattern completion by way of *feature based retrieval* and its predecessor, the *generator* method, both utilize this fact.

The *generator* method of pattern completion is a straightforward way of avoiding retrieval error of the kind not caused by spurious states. The subset of a memory, that comprises the active elements used to initiate the reconstruction process, is called a generator [20, 53]. These elements are clamped (or fixed at their initial values) while all other elements are initialized to a quiescent state and then evaluated sequentially following some fixed order. The quiescent (or quiet) state is taken to be the output value zero while all active states are either -1 or $+1$. This is similar to Boltzmann. Each newly activated element is in turn clamped as the process develops until all quiet elements have been activated.

All memories can be correctly reconstructed in this way with perfect reliability, provided the generator is not corrupted and is sufficiently large. Minimum generator lengths for accurate recall are found experimentally by beginning with a complete

memory, then by working backward in the reverse order that evaluations are done, the generator is shortened one element in length with each iteration. The new, shorter candidate generator is tested by evaluating the quiet neurons as before. The smallest generator to successfully reconstruct its respective memory represents the minimum required length, which usually varies between memories. This variation may occasionally demand generator lengths approaching the number of elements in the network for success.

Improving upon this was the motive behind developing *feature based retrieval* [53, 54]. In this approach, update order is not fixed but is a function of the network state as the state is advanced. As before, initially active elements are clamped. But now, once all quiet elements are activated, clamped elements are then allowed to be updated in the same order they were originally evaluated. When the network state is stable, the process ends.

The FBR model performs so well in fact, that update order alone, without any initial fragment, can sometimes completely specify a memory with perfect reliability. This is to say that a network, starting with all of its elements quiet, can be made to reconstruct any desired memory simply by specifying which quiet element to evaluate first.

It should be noted that, by the previous model, generators of zero length can be obtained experimentally if, instead of a fixed update order, a search is made for a suitable update order for each memory item. Such a search, in the worse case,

might have to be done over all $n!$ possible update orders. But to find the correct zero length probe of a desired memory using FBR one need only search through at most n neurons for the appropriate one to start with.

The underlying power of both methods derives from the fact that the decision of which element to update on each iteration of the network state carries with it information that is otherwise lost with a random update scheme. In the first method the order is blindly predestined. But what gives FBR greater capability is that it uses available information, as it develops, to make each successive choice.

The precise amount of information is estimated by considering the number of elements available when a choice is made that, once evaluated, will yield an output value different from its current value. All quiet elements will yield an active value ($-1, +1$) once evaluated, while generally, only some active elements may change.

A system that clamps the output of each evaluated neuron per iteration effectively reduces the incremental information gained with each subsequent choice. The theoretical amount of information needed to distinguish $O(n)$ memories is $\log(n)$ bits. The information supplied by choosing which of the n quiet elements to evaluate first is n bits. The information given by clamping the first element to a preset value is 2^n bits. Clamping two elements yields $4^{\binom{n}{2}}$ bits of information and for k clamped elements it is $2^{k\binom{n}{k}}$ bits, which approaches 2^n as k approaches n . Of course n clamped elements represents a stable state by virtue of the fact that all n elements have been fixed.

An example of the performance of FBR is seen in the tables listed in Appendix E. The FBR approach was cast in terms of a cellular automaton in which a training set of 3 patterns were stored using Hebbian learning. An exhaustive search of all system states found 14 to be stable. Six probes were constructed so that each would uniquely identify each of the three training set patterns and each of their complements. Table E.1 shows the percent of the active neurons in the probe that correspond to the values they have in each of the 14 stable states. From this table, we see that our six probes uniquely identify the stable patterns 4, 14, 9, 11, 1 and 6, respectively.

Random selection was first used to determine update order as a basis for comparison. The percent of the final stable state reached that correlates with each of the 14 stable patterns is listed in Table E.2 for each of the six probes used to initialize the array. We see that probes 2 and 5 failed to reconstruct the patterns best matched initially. Probe 2 lead to pattern 13 instead of 14, and probe 5 produced pattern 2 when it should have yielded pattern 1. In both cases, the initial probe percent correlations were 75 percent, which was the next nearest to 100 percent.

Finally, in Table E.3 we show the results of using FBR to determine the update order. In every case, the probe reconstructed the correct stable pattern. This performance is obtained for any training set and set of probes that are chosen, provided the necessary guidelines are followed.

5.5 SUMMARY

The important work begun in the control of asynchronous update order that was begun with the feature based retrieval model [53] has been expanded in the information driven dynamics model. Rules for quieting as well as activating network elements enable an entirely new form of connectionist dynamics that seek to preserve the information conveyed by a fragment of active elements. This often results in an oscillatory wandering of the active fragment among similarly uncertain states. The notion that uncertainty should be preserved instead of arbitrarily removed, as occurs with random update ordering, is key to the IDD principle. Only when enough information is present in the fragment is the system driven to pattern completion.

The issue of network states having a reconfigurable influence on the function performed was raised in the discussion about the boolean circuit model in Chapter 4 [22]. This has some similarity with IDD in the sense that network states influence the propagation of information in the structure. The quiet elements do not enter into the function computed by a neuron when it is activated. Perhaps this is a distributed form of functional isolation. We believe that the IDD model provides a better understanding of the oscillatory dynamics of brain processes.

CHAPTER 6

CONCLUSIONS

We have presented an original theory of cortical neural processing that describes aspects of the structure and behavior of the cerebral cortex. We use an interaction function among neighboring neurons that alternates between excitatory and inhibitory regions to explain transient and long-term structures that form around stable oscillatory neural activity. Our theory is unique in its interpretation of the interplay of chaotic and stable oscillatory neurodynamics. We demonstrated that a *chaotic base condition* can exist as the result, and as an expression of, an ensemble of potentially stable behavior patterns. We show experimental evidence for at least one mechanism for generating the base condition. Our theory asserts that stable dynamics form as temporary bubble-like clusters within the fixed boundaries of cortical columns, and we show experimental support for it. With our theory, we outlined a means for cortical columns to interact in a hierarchical manner through frequency sensitive interneurons and non-specific pyramidal neurons working together in such a way so as to limit the spread of stable, high-intensity activity.

Our investigation of pericolumnar inhibition and the lateral receptive field of many cortical neurons produced two major results. We identified a common mechanism for partitioning the cortex dynamically as well as developmentally. And we believe we are the first to convincingly model the postnatal development of ocular dominance columns in the striate cortex.

Our theory is the first to suggest two new purposes for the existence of chaotic neurodynamics: (i) as a natural means of representing the uncertainty in the outcome of performed tasks, such as memory retrieval or classification, and (ii) as an automatic way of producing an economic representation of distributed information. The mechanisms and models we propose are physiologically realistic and are relevant to the goals of many cognitive processes and artificial neural network applications.

6.1 DISCUSSION

The oscillatory nature of the brain can and should be exploited in physiologically realistic models to better understand brain function and to advance the field of artificial neural networks. The many uses of oscillations in the brain already identified in this emerging field include short term memory representations, dynamic binding of separate but related activity and the perceptual benefits of low-intensity chaotic activity.

The Freeman model of olfactory perception accounts for selective attention in terms of global patterns of chaotic activity across the olfactory bulb that emerge from a low level chaotic background [7, 8, 9, 10, 11, 47, 52]. Olfactory perception begins with internally generated low level chaotic oscillation that by virtue of the character of its dynamics has the ability of selecting the class of receptor input that leads to specific global patterns. When such input arrives, the activity grows forcing out alternative lobes of a more complex basal chaotic attractor. The resulting pattern corresponds to a specific stimulus in the class being attended. This process therefore relies on a background chaotic state that will carry the information needed to identify the desired class of global activity.

A similar problem is classification with the related tasks of generalizing and instantiating. As depicted in the olfactory perception model described above, classes are represented transiently through neuron activity. The information content of the background activity determines how selective is the focus of attention and thus the size of the represented class. Not only size but also the constituency of the class of attended input can be changed as rapidly as change can occur in the background activity. Moreover, even as a stimulus that leads to a global pattern response is an instance of the attended input class, the corresponding response is likewise an instance of a class of responses. Following this interpretation, a class in the modified model might be thought of as a set of possible outcomes reachable by an active fragment. Since the fragment also conveys the probabilities of these outcomes, this sort of class has properties similar to a fuzzy set. These classes would have the advantage that they could be quickly formed or destroyed without any permanent changes made to the network. This is quite different from approaches that must modify connection weights to form classes. Such classifications are generalized by widening the corresponding attraction basin. For example making small random changes to the connection weights of a feedforward network constructed using the corner classifier algorithm [20] produces generalized classes around the existing corners.

By extrapolating the problem of perception to the problem of interaction among the various functional regions of the brain, one sees a possible analogy where each region might pay selective attention to the activity of other regions. But associated with the problem of interaction is the well known dilemma that although neural networks are massively parallel devices, they effectively do only one thing at a time. Methods, such as staggered memory retrieval, though giving the illusion of

concurrency, do not actually solve this problem. This is because every element of the network at any moment is actively involved in the same computation whether or not staggering or its equivalent is used. In theory, a representation that involves only a fragment of a complete network interconnection structure leaves portions not used and, therefore, free to be utilized by other processes without interaction.

With the discovery that the stability of a subsystem can be independent of the stability of the rest of the system [36], it is speculated by the author that interaction of neural activity between subsystems of an overall cognitive system may be possible even while some uncertainty exists in the patterns of the activity.

There are a number of useful things that may result from this approach. First of all it has been shown that sets of active neurons can identify specific stable states of full network activity using only a fragment of the network [20, 53, 54]. The fragment size needed is related to the redundancy with which stable states are encoded but may be smaller if information is supplied in the form of a prescribed update order. A fragment may represent a window of attention directed onto the portion of the network that is active. It may also allow the network to operate on a general group of points rather than a single point. In this case the points covered by the quiet neurons are the generalized group. Finally, fragmented activity combined with low network connectivity promises to be an approach for concurrent processing in a reconfigurable network structure that may be hierarchically organized into many levels above that of the individual neuron.

6.2 FUTURE RESEARCH

Our theory is the conclusion of our investigation and the beginning of even brighter possibilities. The models developed, extensively studied and used in this dissertation to illustrate aspects of our theory are what inspired our theory. What is needed now is that they be brought together. A single model, as outlined in Chapter 2, incorporating all of these aspects and suitable for simulation, would be a desirable extension of the work we have begun. The computational requirement of such a simulation is expected to be considerable due to the great number of second order differential equations anticipated to model even a small part of the cerebral cortex. But the requirement is probably not beyond that of a massively parallel, high speed, supercomputer.

Before such a simulation is attempted, one may wish to explore alternative rules, besides the one we suggest, for guiding the mechanism that extracts economic representations from the ensemble information our proposed chaotic base condition provides. Since our rule places a restriction on the make up of the ensemble, it would be better if something more general could be found.

Finally, the best way to continue with our work is to develop new artificial neural network models that incorporate the principles of our theory, directing them toward practical applications. Problems in control theory, signal classification and pattern recognition can serve to test the performance of such models if developed. We firmly believe that the representation of uncertainty as described by our theory and the means for obtaining economic representations that it suggests will establish chaotic neurodynamic modeling as the preferred approach for many applications.

BIBLIOGRAPHY

- [1] Basak, J., C.A. Murthy, S. Chaudhury, and D.D. Majumder, "A Connectionist Model for Category Perception: Theory and Implementation", *IEEE Transactions on Neural Networks*, vol. 4, no. 2, 1993, pp. 257-269.
- [2] Bressier, S.L., R. Coppola, and R. Nakamura, "Episodic multiregional cortical coherence at multiple frequencies during visual task performance", *Nature*, vol. 366, 1993.
- [3] Cohen, R.A. *The Neuropsychology of Attention*, Plenum Press, 1993.
- [4] Crick, F. and Koch, C., "Towards a neurobiological theory of consciousness", *Seminars in the Neurosciences*, vol. 2, 1990, pp. 263-275.
- [5] Crick, F., "The Astonishing Hypothesis: The Scientific Search for the Soul", Charles Scribner's Sons Macmillan Publishing Company, New York, NY, 1994.
- [6] Dreher, B., and S. Robinson, *Neuroanatomy of the Visual Pathways and Their Development*, IN: *Vision and Visual Dysfunction*, J.R. Conly, Dillon, eds., vol. 3, The Macmillan Press, 1991.
- [7] Freeman, W.J., *Chaotic Dynamics in Neural Pattern Recognition*, IN: *From Statistics to Neural Networks*, V. Cherkassky, J.H. Friedman, H. Wechsler, eds., Springer-Verlag, 1994.
- [8] Freeman, W.J., "Perceptual Processing Using Oscillatory Chaotic Dynamics", *Advance Topics in Neuroelectric Signal Analysis*, IEEE Engineering in Medicine and Biology Society 11th Annual International Conference, 1989.
- [9] Freeman, W.J., "Simulation of Chaotic EEG Patterns with a Dynamic Model of the Olfactory System", *Biological Cybernetics*, vol. 56, 1987, pp. 139-150.
- [10] Freeman, W.J., "Why neural networks don't yet fly: inquiry into the neurodynamics of biological intelligence", 2nd Annual International Conference on Neural Networks, San Diego, CA, 1988.
- [11] Freeman, W.J., and G.V. Di Prisco, "Relation of olfactory EEG to behavior: time series analysis", *Behavioral Neuroscience*, vol. 100, no. 5, 1986, pp. 753-763.
- [12] Geusz, M.E., and G.D. Block, "The Retinal Cells Generating the Circadian Small Spikes in the Bulla Optic Nerve", *Journal of Biological Rhythms*, vol. 7, no. 3, 1992, pp. 225-268.

- [13] Gross, G.W., "Internal Dynamics of Randomized Mammalian Neuronal Networks in Culture", Academic Press, 1993.
- [14] Grossberg, S., and A. Grunewald, "Synchronized neural activities: a mechanism for perceptual framing", Tech. Report CAS/CNS-94-014 Boston University, 1994.
- [15] Grunewald, A., and S. Grossberg, "Binding of object representations by synchronized cortical dynamics explains temporal order and spatial pooling data", Tech. Report CAS/CNS-94-015 Boston University, 1994.
- [16] Haykin, S., *Neural Networks: A Comprehensive Foundation*, Macmillan Publishing Company, 1994.
- [17] Hopfield, J.J., "Neural Networks and physical systems with emergent collective computational abilities", *Proceedings of the National Academy of Science of the USA*, vol. 70, 1982, pp. 2554-2558.
- [18] Joliot, M., U. Ribary, and R. Llinas, "Human oscillatory brain activity near 40Hz coexists with cognitive temporal binding", *Proc. Natl. Acad. Sci. USA*, vol. 91, 1994, pp. 11748-11751.
- [19] Kak, S., "Feedback Neural Networks: New characteristics and a generalization", *Circuits, Systems Signal Process*, vol. 12, no. 2, 1993, pp. 263-278.
- [20] Kak, S.C., "New algorithms for training feedforward neural networks", *Pattern Recognition Letters*, vol. 15, 1994, pp. 295-298.
- [21] Kak, S.C., "Speed of Computation and Simulation", *Foundations of Physics*, vol. 26, 1996, pp. 1375-1386.
- [22] Kauffman, S.A., "Requirements for Evolvability in Complex Systems: Orderly Dynamics and Frozen Components", *Complexity, Entropy, and Physics of Information, SFI Studies in the Sciences of Complexity*, Addison-Wesley, 1988, pp. 151-192.
- [23] Kohonen, T., *Self-Organization and Associative Memory*, Springer-Verlag, 1989.
- [24] Kowalski, J.M., G.L. Albert, B.K. Rhoades, and G.W. Gross, "Neuronal networks with spontaneous, correlated bursting activity: theory and simulations", *Neural Networks*, vol. 5, 1992, pp. 805-822.
- [25] LeVay, S., T.N. Wiesel, and D.H. Hubel, "The Postnatal Development of Ocular-Dominance Columns in the Monkey", IN: *The Organization of the Cerebral Cortex*, Schmitt, Worden, Adelman, and Dennis, eds., The MIT Press, 1981.

- [26] Llinas, R.R., and U. Ribary, "Coherent 40-Hz oscillation characterizes dream state in humans", *Proc. Natl. Acad. Sci. USA*, vol. 90, 1993, pp. 2078-2081.
- [27] Llinas, R.R., "The Intrinsic Electrophysiological Properties of Mammalian Neurons: Insights into Central Nervous System Function", *Science*, vol. 242, 1988.
- [28] McCulloch, W.S., and W. Pitts, "A logical calculus of the ideas immanent in nervous activity", *Bulletin of Mathematical Biophysics*, vol. 5, 1943, pp. 115-133.
- [29] Menon, V., W.J.Freeman, B.A. Cutillo, J.E. Desmond, M.F.Ward, S.L.Bressler, K.D. Laxer, N. Barbaro, and A.S. Gevins, "Spatio-temporal correlations in human gamma band electrocortigrams", *Electroencephalography and clinical Neurophysiology*, vol. 98, 1996, pp. 89-102.
- [30] Minsky, M.L., and S.A. Papert, *Perceptrons*, Cambridge, MA, MIT Press, 1969.
- [31] Moon, F.C., *Chaotic Vibrations: An Introduction for Applied Scientists and Engineers*, John Wiley and Sons, 1987.
- [32] Mountcastle, V., *The Mindful Brain*, MIT Press, 1978.
- [33] Niebur, E., C. Koch, and C. Rosin, "An Oscillation-Based Model for the Neuronal Basis of Attention", *Vision Res.*, vol. 33, no. 18, 1993, pp. 2789-2802.
- [34] Okeefe, J., and L. Nadel, *The Hippocampus as a Cognitive Map*, Clarendon Press, Oxford, 1978.
- [35] Optican, L.M., and B.J. Richmond, "Temporal Encoding of Two Dimensional Patterns by Single Units in Primate Inferior Temporal Cortex. III. Information Theoretic Analysis", *Journal of Neurophysiology*, vol. 57, no. 1, 1987, pp. 162-178.
- [36] Pecora, L.M. and Carroll, T.L., "Synchronization in chaotic systems", *Physical Review Letters*, vol.64, no. 8, 1990, pp.821-824.
- [37] Pribram, K., "Brain, mind, and consciousness: the science of neuropsychology", In: A. Bocaz (Ed.), *Proceedings: First Symposium on Cognition, Language and Culture: Crossdisciplinary Dialog in Cognitive Sciences* (pp. 9-38), Santiago, Chile: Unsveridad de Chile.
- [38] Ralph, M.R., and G.D. Block, "Circadian and light-induced conductance changes in putative pacemaker cells of *Bulla gouldiana*", *J. Comp. Physiol. A*, vol. 166, 1990, pp. 589-595.

- [39] Rhodes, B.K., and G.W. Gross, "Potassium and calcium channel dependence of bursting in cultured neuronal networks", *Brain Research*, vol. 643, 1994, pp. 310-318.
- [40] Richmond, B.J., L.M. Optican, M. Podell, and H. Spitzer, "Temporal Encoding of Two Dimensional Patterns by Single Units in Primate Inferior Temporal Cortex. I. Response Characteristics", *Journal of Neurophysiology*, vol. 57, no. 1, 1987, pp. 132-146.
- [41] Richmond, B.J., and L.M. Optican, "Temporal Encoding of Two Dimensional Patterns by Single Units in Primate Inferior Temporal Cortex. II. Quantification of Response Waveform", *Journal of Neurophysiology*, vol. 57, no. 1, 1987, pp. 147-161.
- [42] Rosenblatt, F., "The Perceptron: A probabilistic model for information storage and organization in the brain", *Psychological Review*, vol. 65, 1958, pp. 386-408.
- [43] Saito, T., "Chaos and Fractals from a Forced Artificial Neural Cell", *IEEE Transactions on Neural Networks*, vol. 4, no. 1, 1993.
- [44] Schmitt, Worden, Adelman, and Dennis, eds., *The Organization of the Cerebral Cortex*, The MIT Press, 1981.
- [45] Shannon, C.E. and Weaver, W., *The Mathematical Theory of Communication*, Illini Press, 1949.
- [46] Shimoide, K., and W.J. Freeman, "Dynamic Neural Network Derived from the Olfactory System with Examples of Applications", *IEICE Transactions on Fundamentals of Electronics, Communications and Computer Sciences*, vol. E78-A, no. 7, 1995.
- [47] Skarda, C.A., W.J. Freeman, "How brains make chaos in order to make sense of the world", *Behavioral and Brain Sciences*, vol. 10, 1987, pp. 161-195.
- [48] Sutton, J.P., and L.E.H. Trainor, "Hierarchical model of memory and memory loss", *J.Phys. A: Math. Gen.*, vol. 21, 1988, pp. 4443-4454.
- [49] Sutton, J.P., "Network Hierarchies in Neural Organization, Development and Pathology", Harvard Medical School and Massachusetts Institute of Technology, 1995.
- [50] Tiitinen, H., J. Sinkkonen, K. Reinkainen, K. Alho, J. Lavikainen, and R. Naatanen, "Selective attention enhances the auditory 40-Hz transient response in humans", *Nature*, vol. 364, 1993.

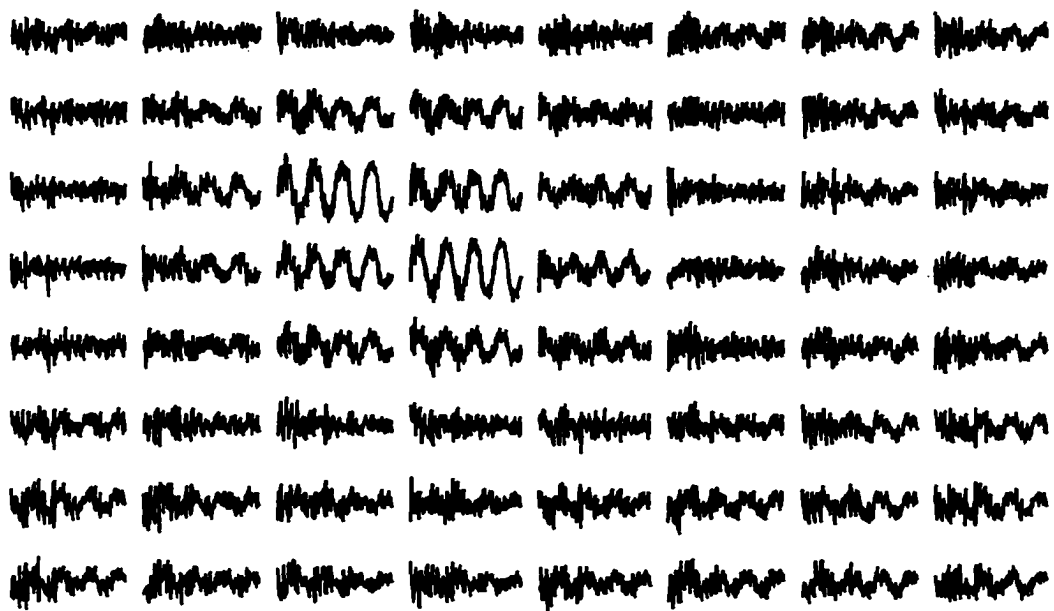
- [51] Traub, R.D., and R. Miles, *Neuronal Networks of the Hippocampus*, Cambridge University Press, 1991.
- [52] Yao, Y., and W.J. Freeman, "Model of biological pattern recognition with spatially chaotic dynamics", *Neural Networks*, vol. 3, 1990, pp. 153-170.
- [53] Young, D.T., *Feature Based Retrieval for Neural Networks*, Master's Thesis, Louisiana State University, 1989.
- [54] Young, D.T., "The regulation of information as a collective property", *Proceedings of the Joint Conference on Information Sciences*, 1994, pp.115-118.

APPENDIX A

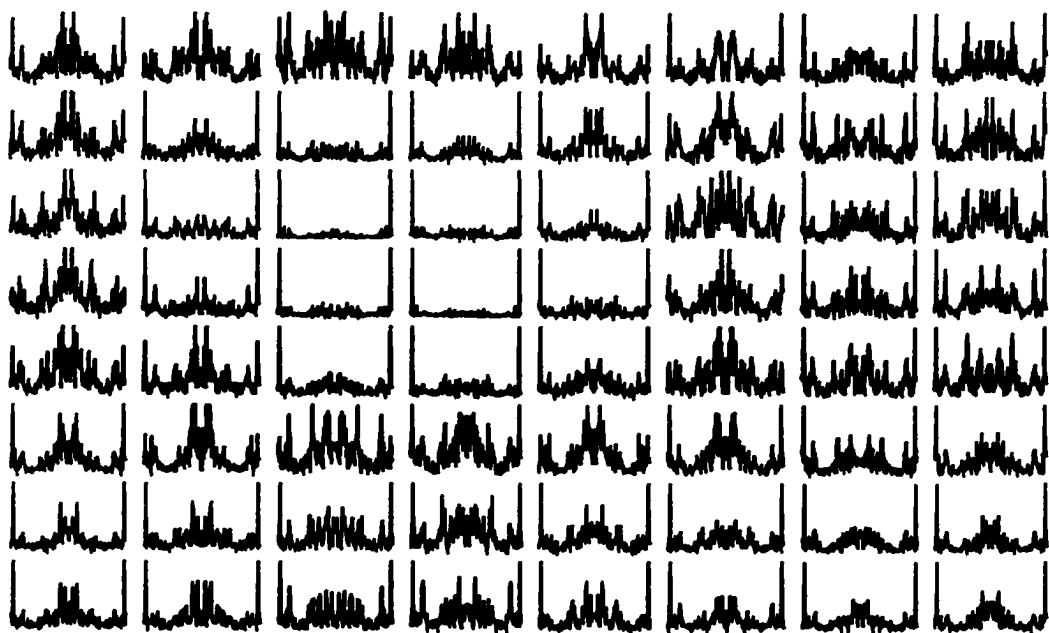
SIMULATIONS OF THE LAMINAR STRUCTURE MODEL

The following four figures illustrate the response of our simulated laminar structure model to sinusoidal input. Each figure shows two 8 by 8 arrays. The top array depicts the time series response and the bottom represents the Fourier response. A discussion of these figures is found in Chapter 3.

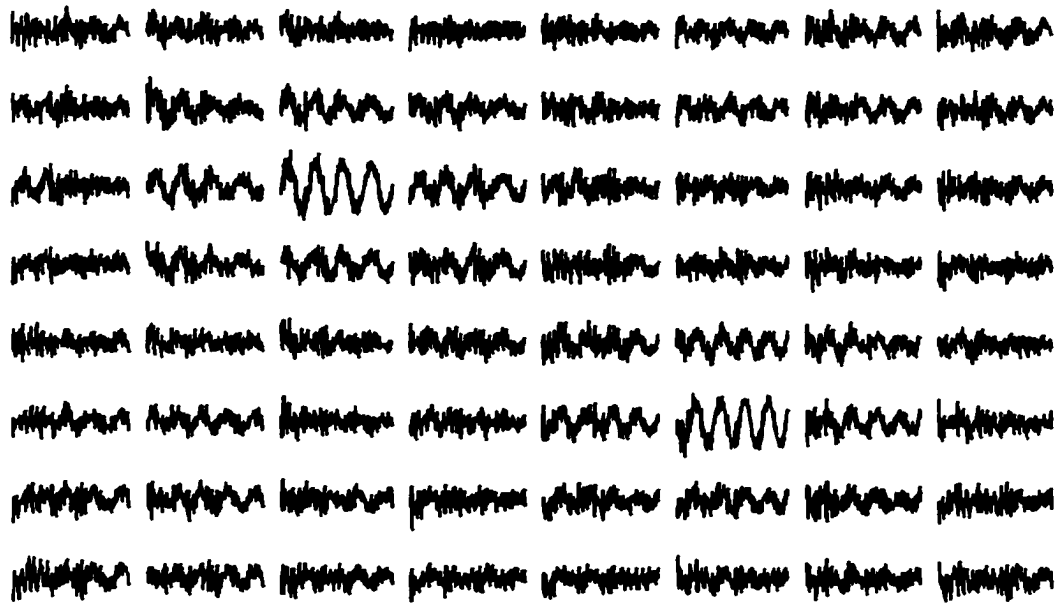
TIME SERIES



FOURIER TRANSFORMS

Figure A.1: $\omega_1 = \omega_2 = \pi/25$, $\phi = 0$, distance = 1

TIME SERIES



FOURIER TRANSFORMS

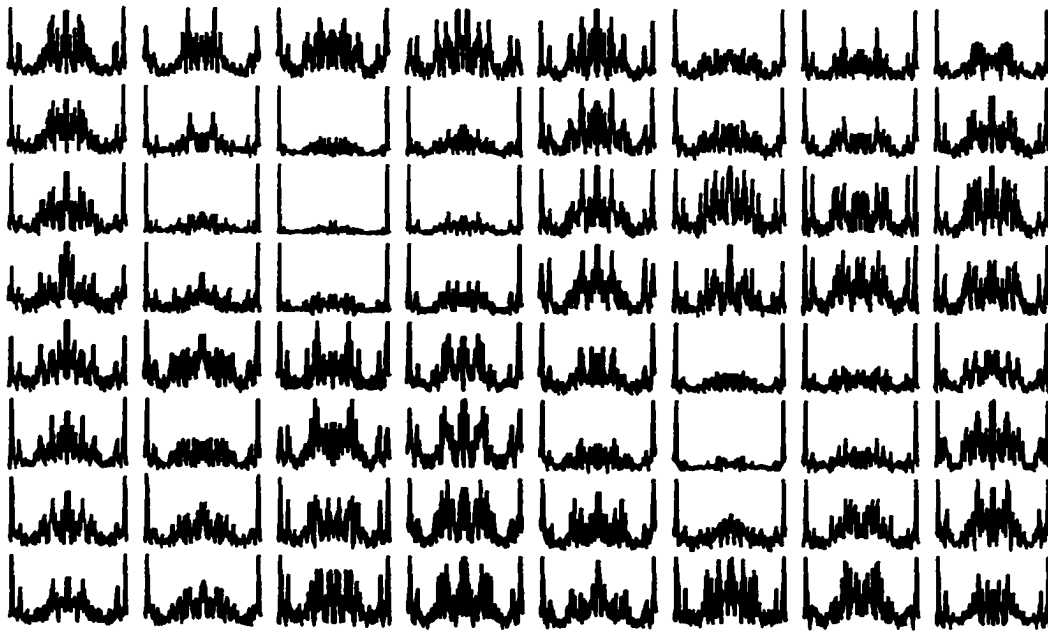
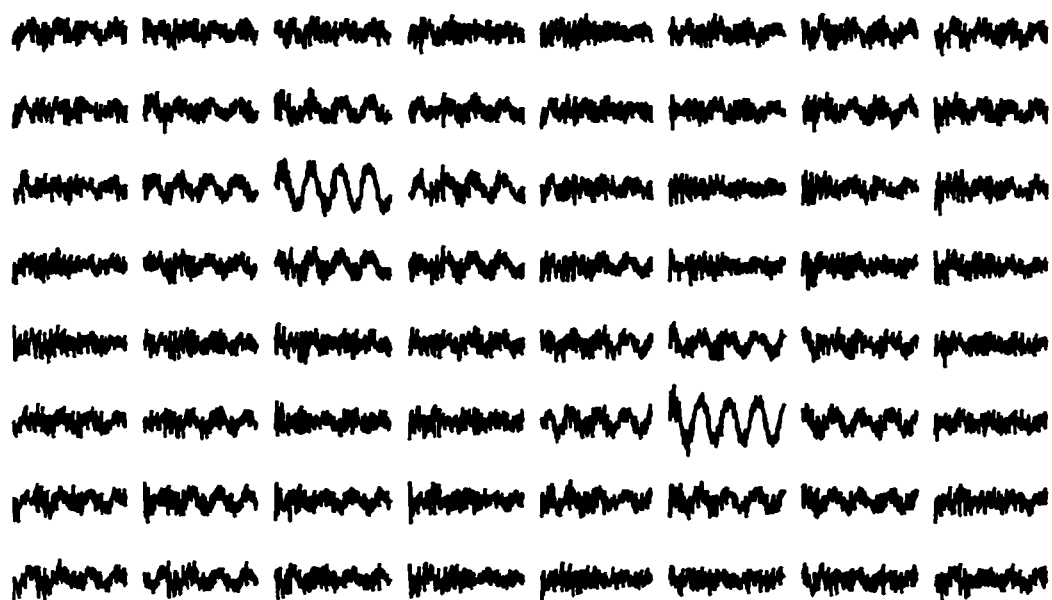


Figure A.2: $\omega_1 = \pi/25$, $\omega_2 = \pi/22$, $\phi = 0$, distance = 3

TIME SERIES



FOURIER TRANSFORMS

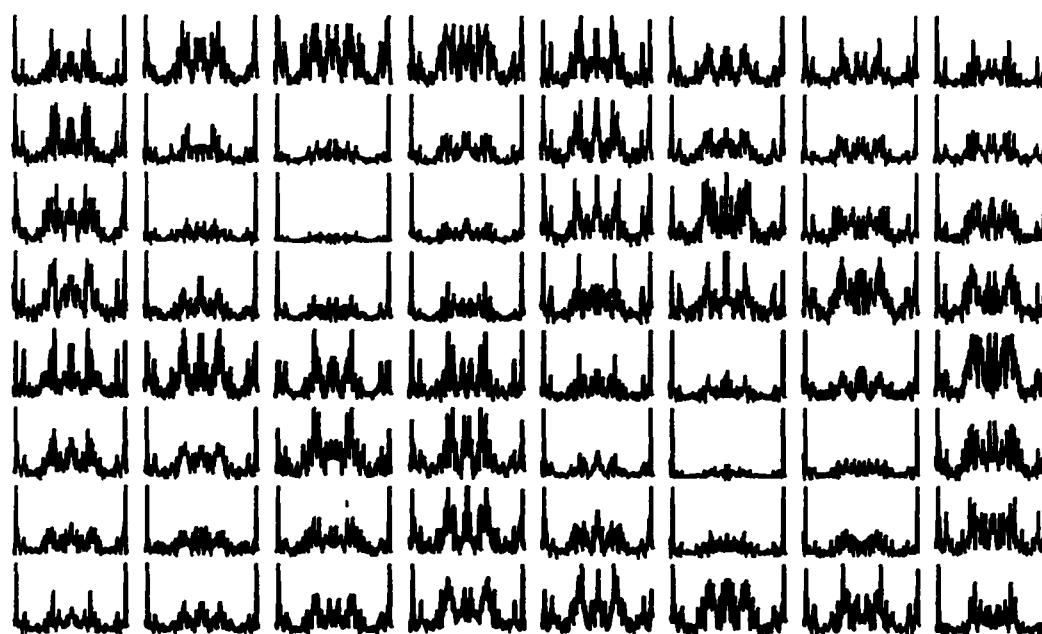
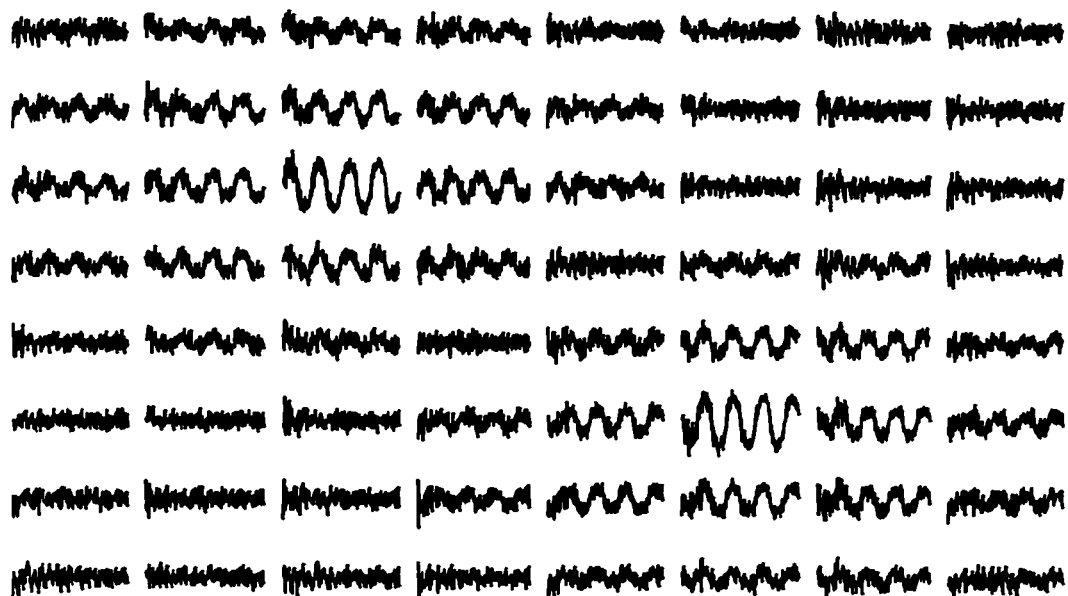


Figure A.3: $\omega_1 = \omega_2 = \pi/25$, $\phi = \pi/4$, distance = 3

TIME SERIES



FOURIER TRANSFORMS

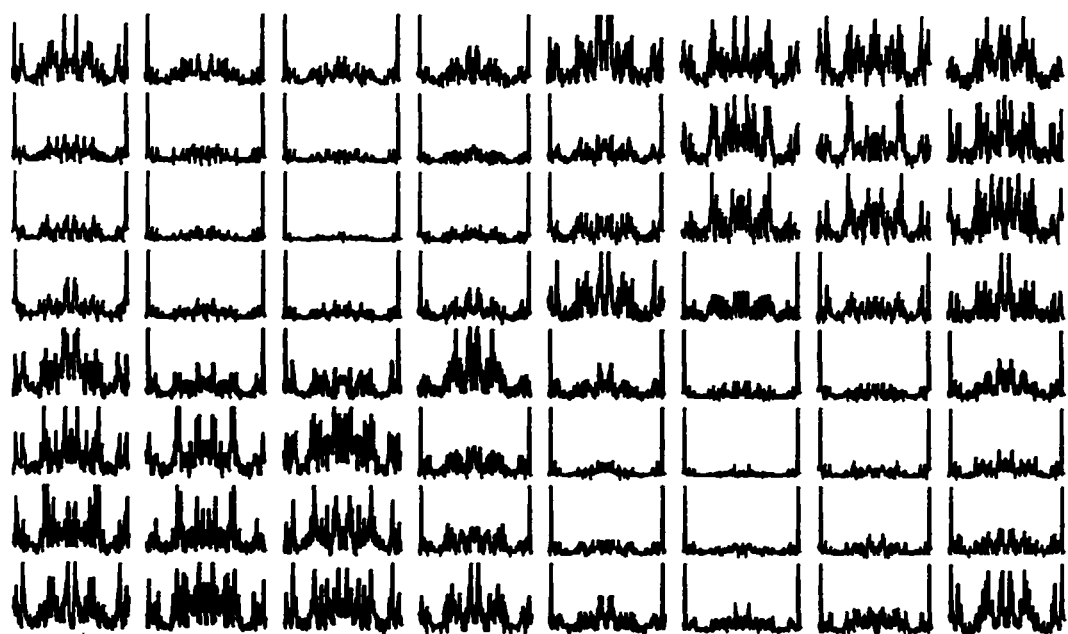


Figure A.4: $\omega_1 = \omega_2 = \pi/25$, $\phi = \pi$, distance = 3

APPENDIX B

FUNCTION VARIATION : COMPLETE

The following eight pages show the steady states reached in a series of simulations of automatic cluster formation. The simulation was run a total of 40 times with a different random initial state for each. The initial and final states of each run are shown flanking a three-dimensional chart. This chart indicates the number of iterations for which each array element was in the active state (+1) during that run.

The complete lateral interaction function (all three parts), described in Chapter 4, was used with $r_1 = 3$, $r_2 = 14$ and $r_3 = 41$. No bias was used and the threshold was set at zero.

The percent of the 41 by 41 array found to be active in the final steady state was on average 46.80 with a minimum of 45 and a maximum of 49. The number of iterations required to reach steady state was on average 14.23 with a minimum of 9 and a maximum of 21.

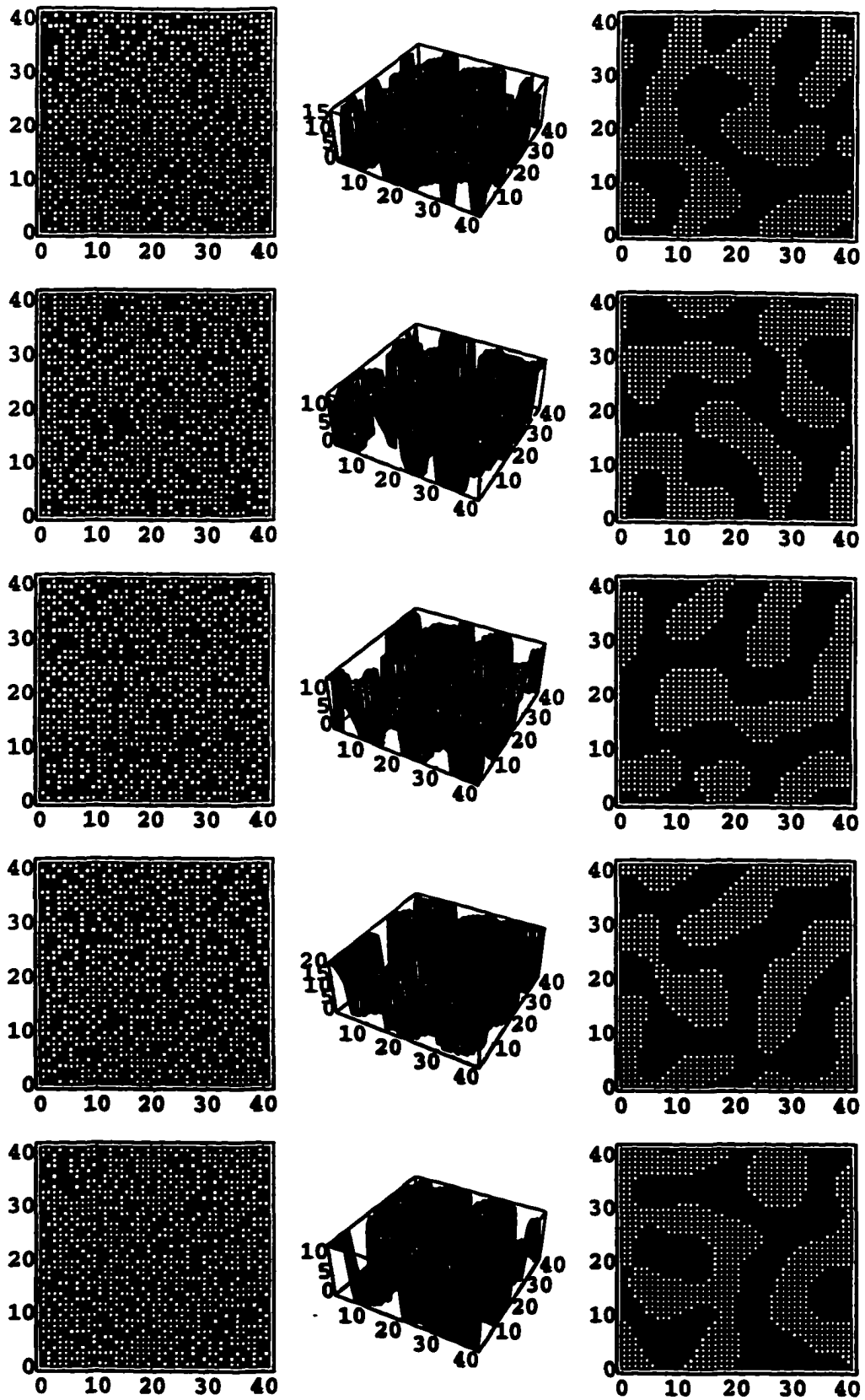


Figure B.1: Complete Function : Set 1

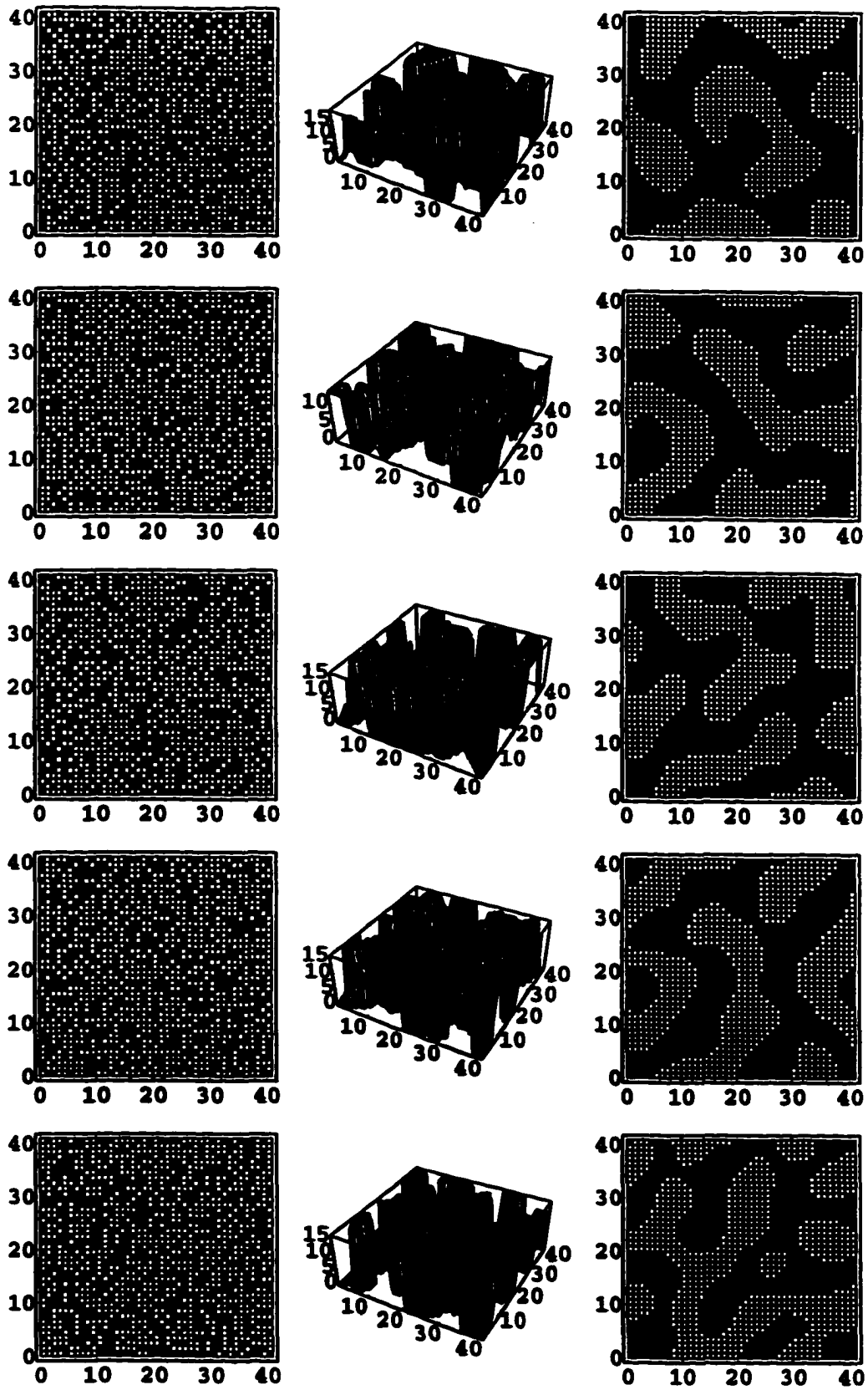


Figure B.2: Complete Function : Set 2

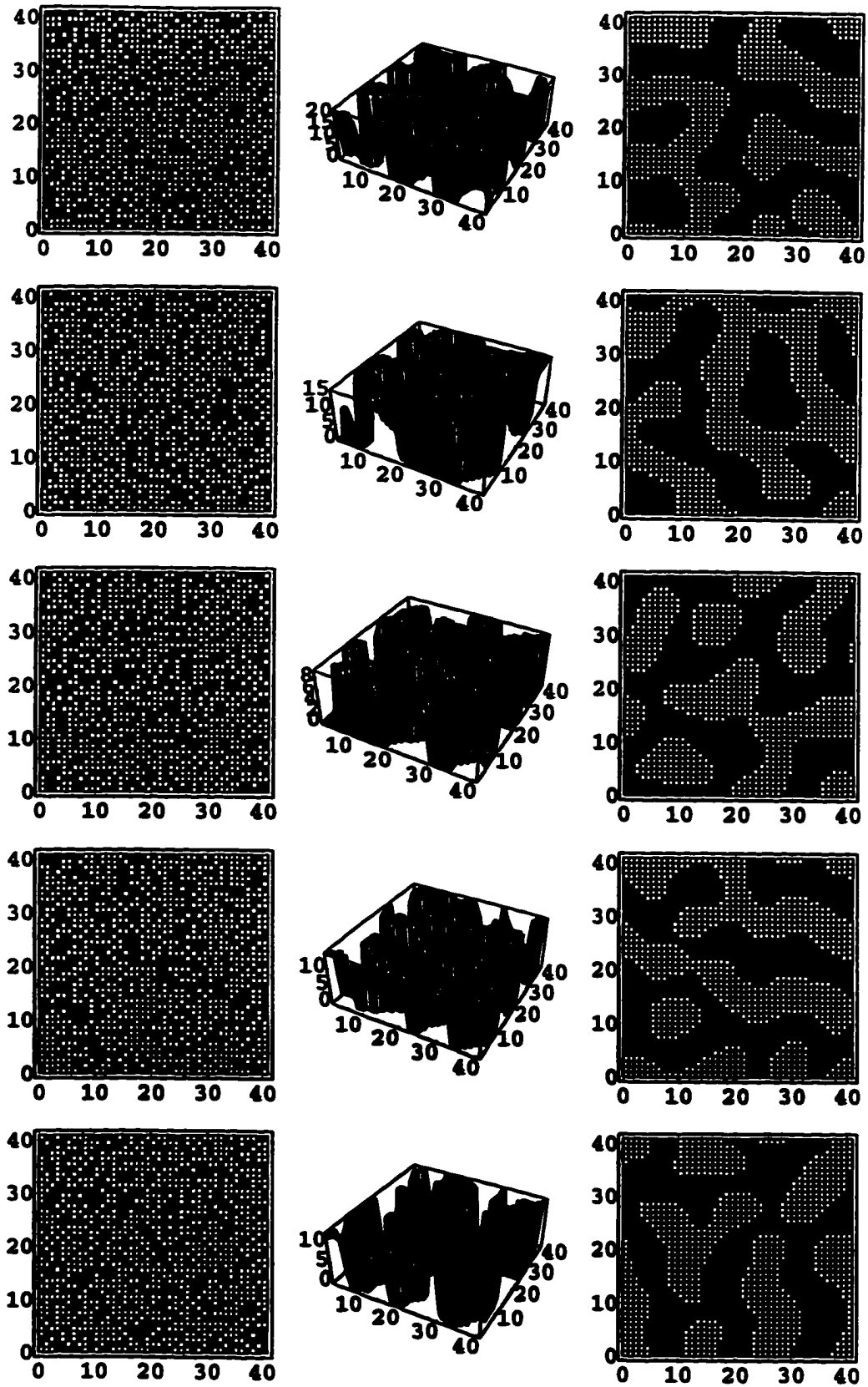


Figure B.3: Complete Function : Set 3

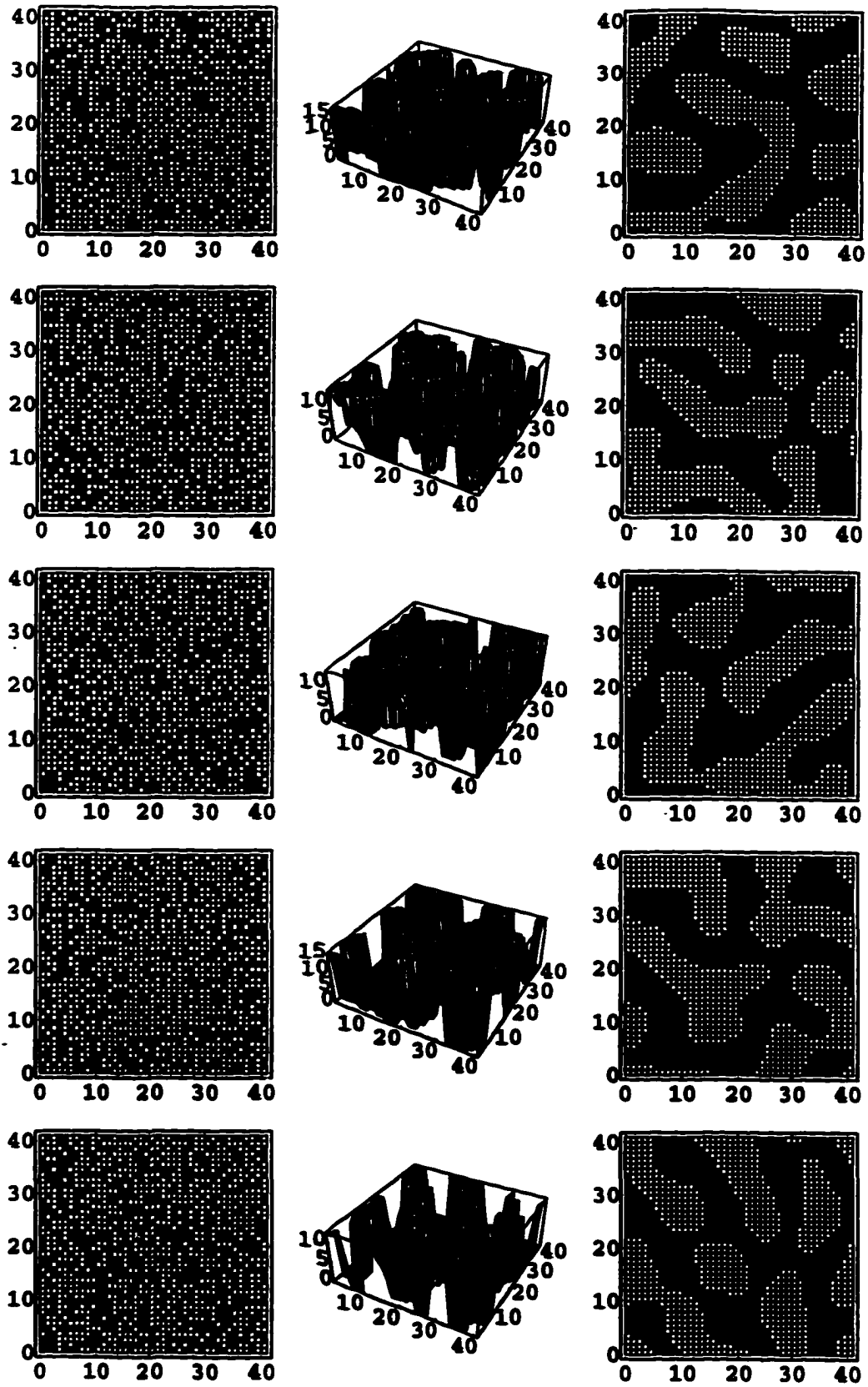


Figure B.4: Complete Function : Set 4

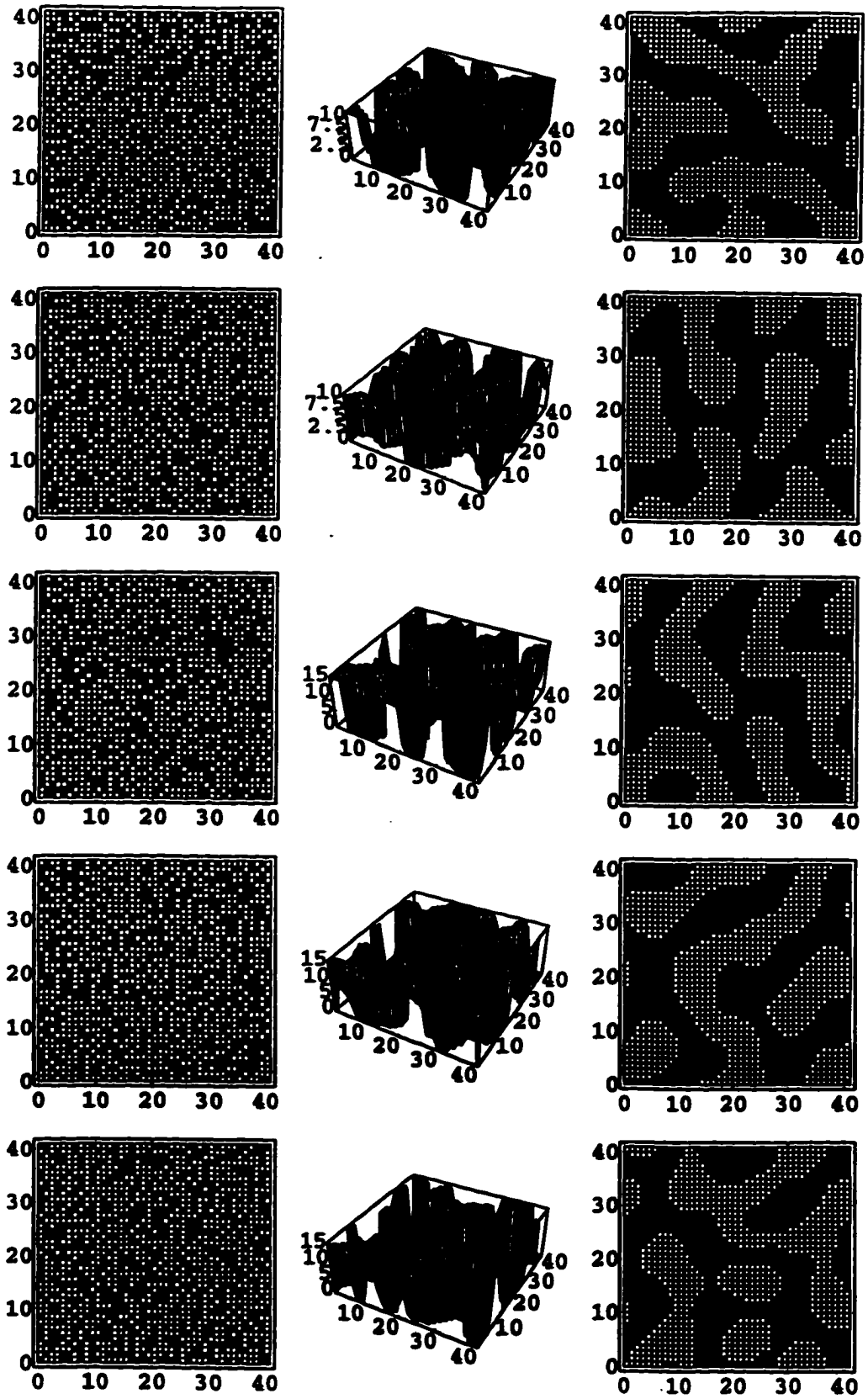


Figure B.5: Complete Function : Set 5

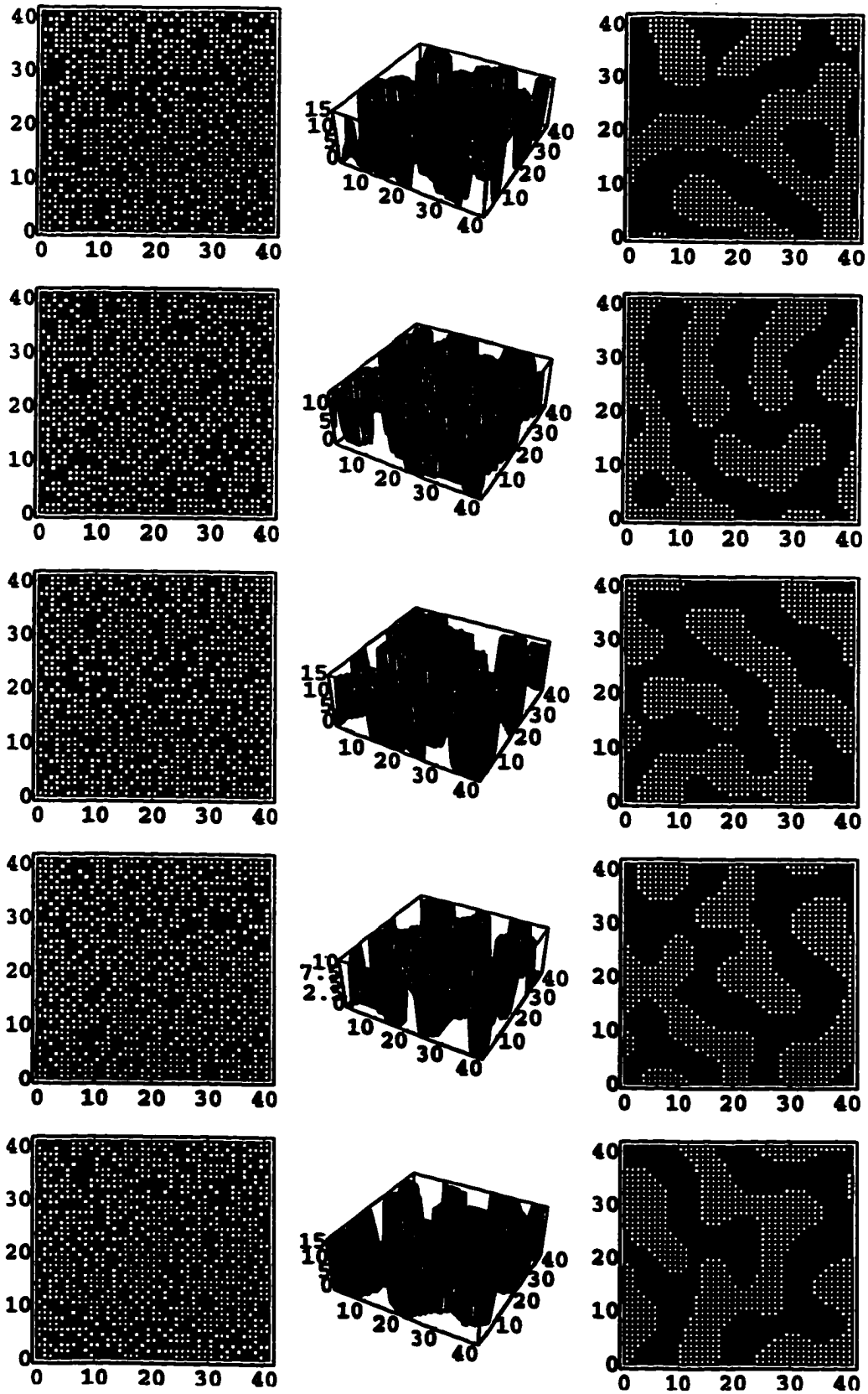


Figure B.6: Complete Function : Set 6

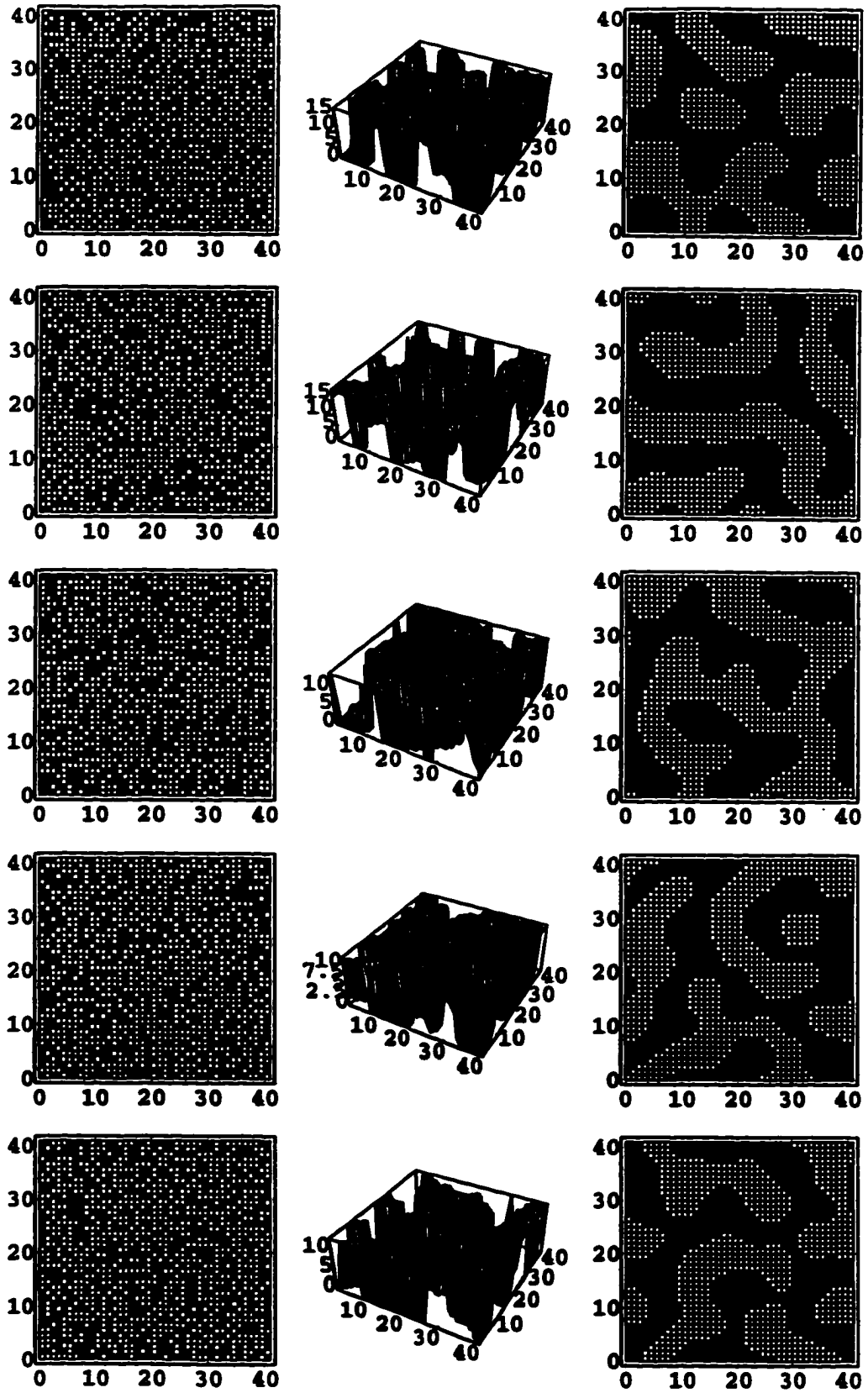


Figure B.7: Complete Function : Set 7

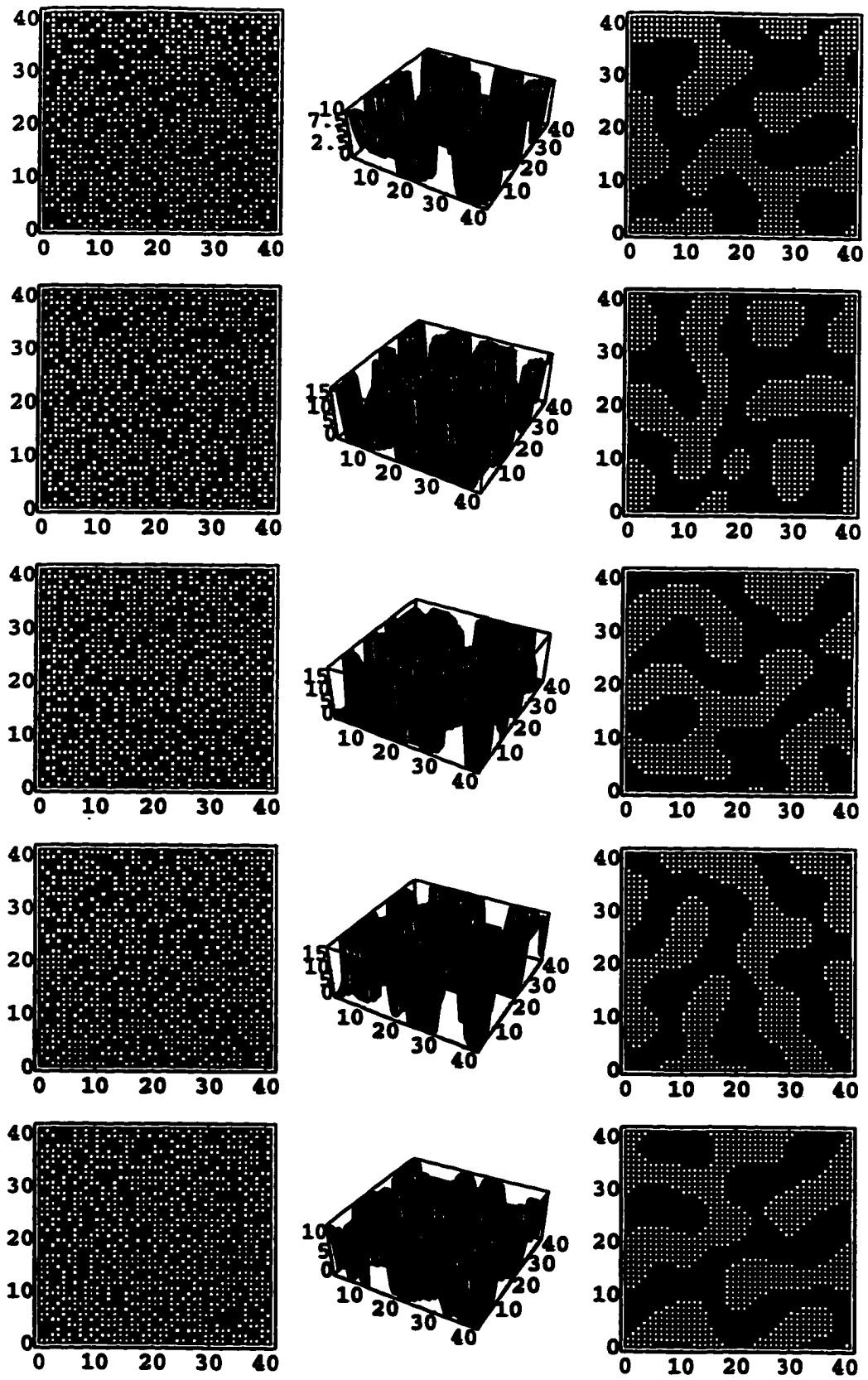


Figure B.8: Complete Function : Set 8

APPENDIX C

FUNCTION VARIATION : REDUCED

The following eight pages show the steady states reached in a series of simulations of automatic cluster formation. The simulation was run a total of 40 times with a different random initial state for each. The initial and final states of each run are shown flanking a three-dimensional chart. This chart indicates the number of iterations for which each array element was in the active state (+1) during that run.

A reduced lateral interaction function (two parts), described in Chapter 4, was used with $r_1 = 3$ and $r_2 = 14$. No bias was used and the threshold was set at zero.

The percent of the 41 by 41 array found to be active in the final steady state was on average 21.47 with a minimum of 5 and a maximum of 30. The number of iterations required to reach steady state was on average 29.58 with a minimum of 7 and a maximum of 99. Simulations were stopped at 99 iterations twice, indicating that a stable state was never reached for these two particular runs.

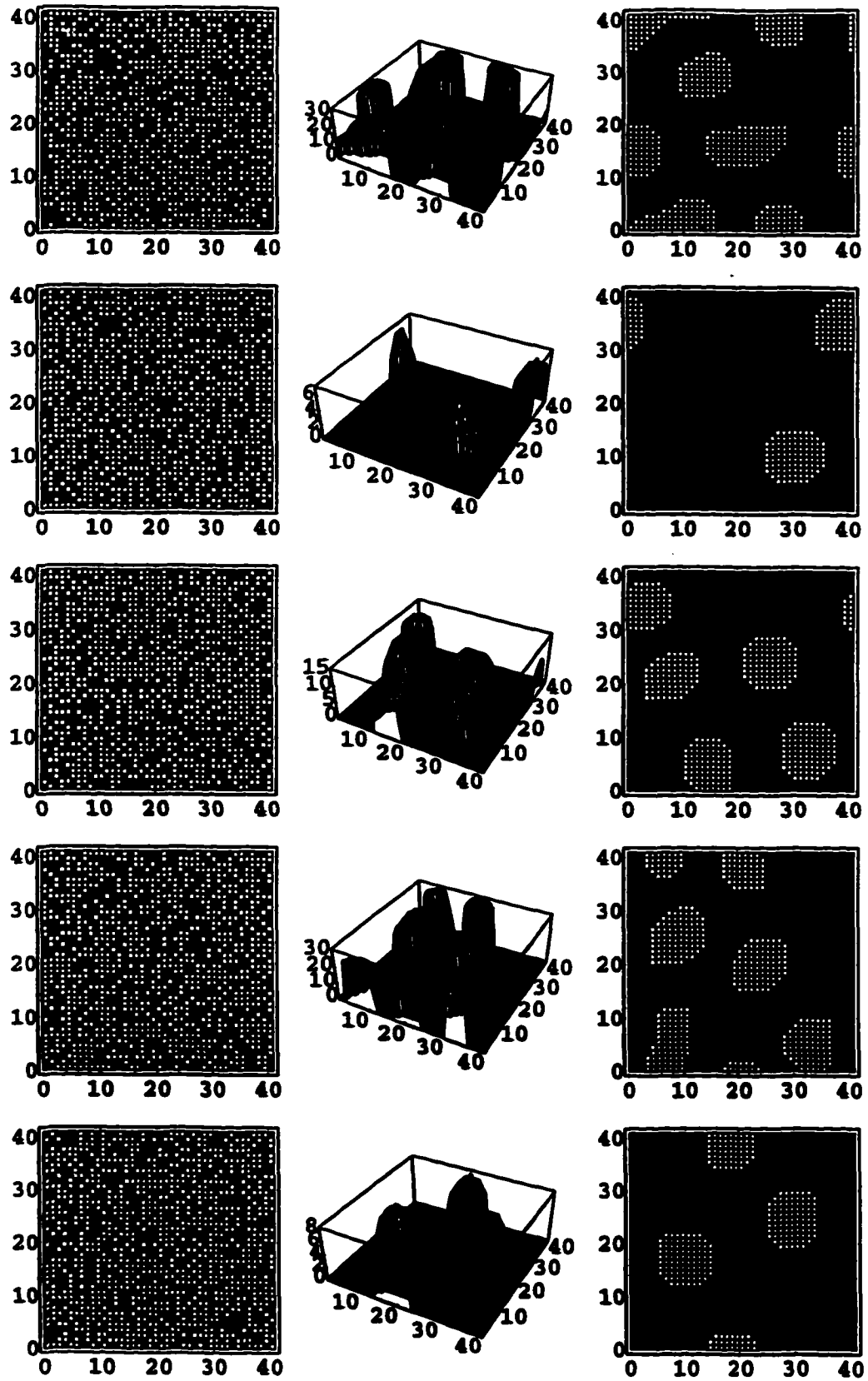


Figure C.1: Reduced Function : Set 1

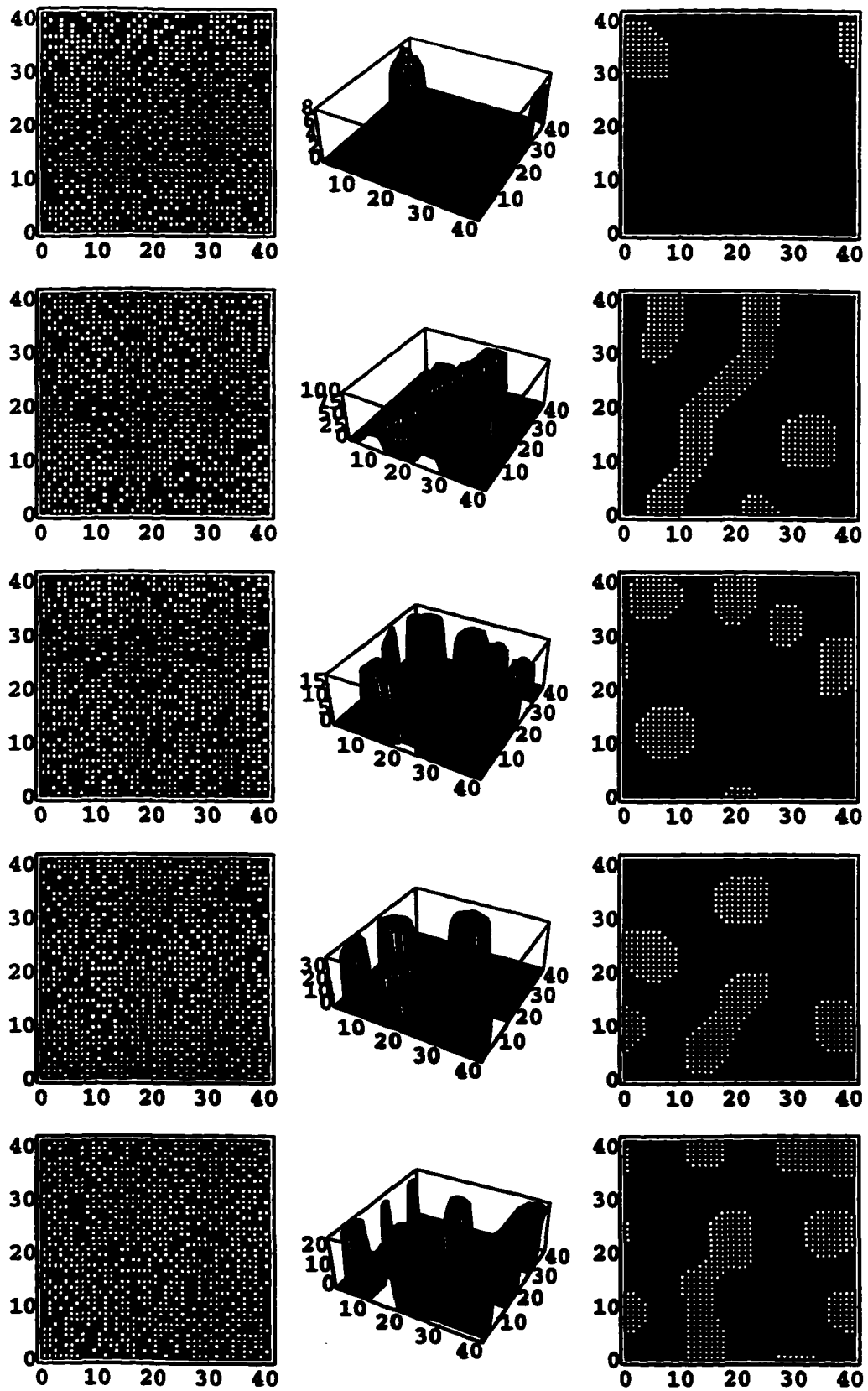


Figure C.2: Reduced Function : Set 2

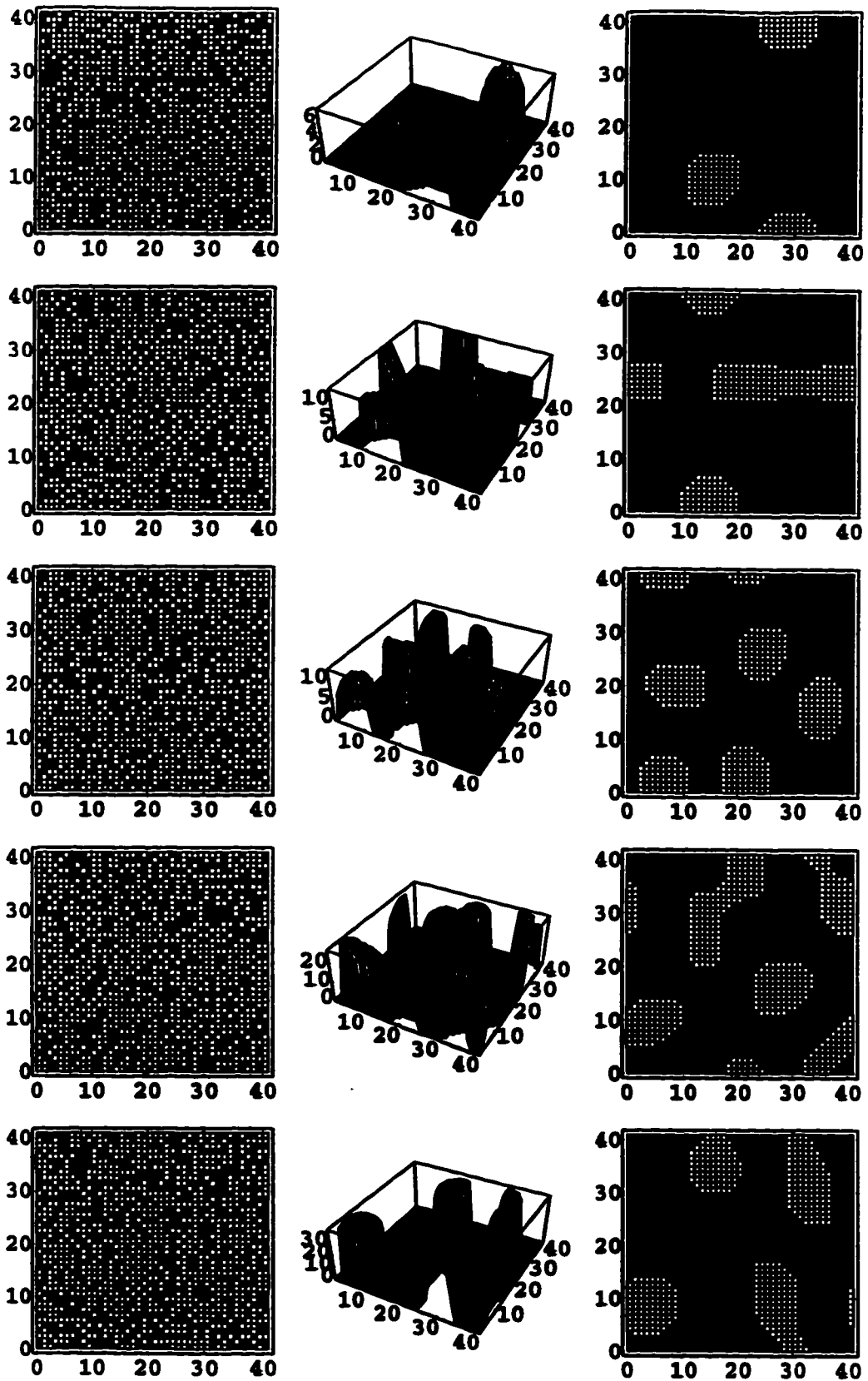


Figure C.3: Reduced Function : Set 3

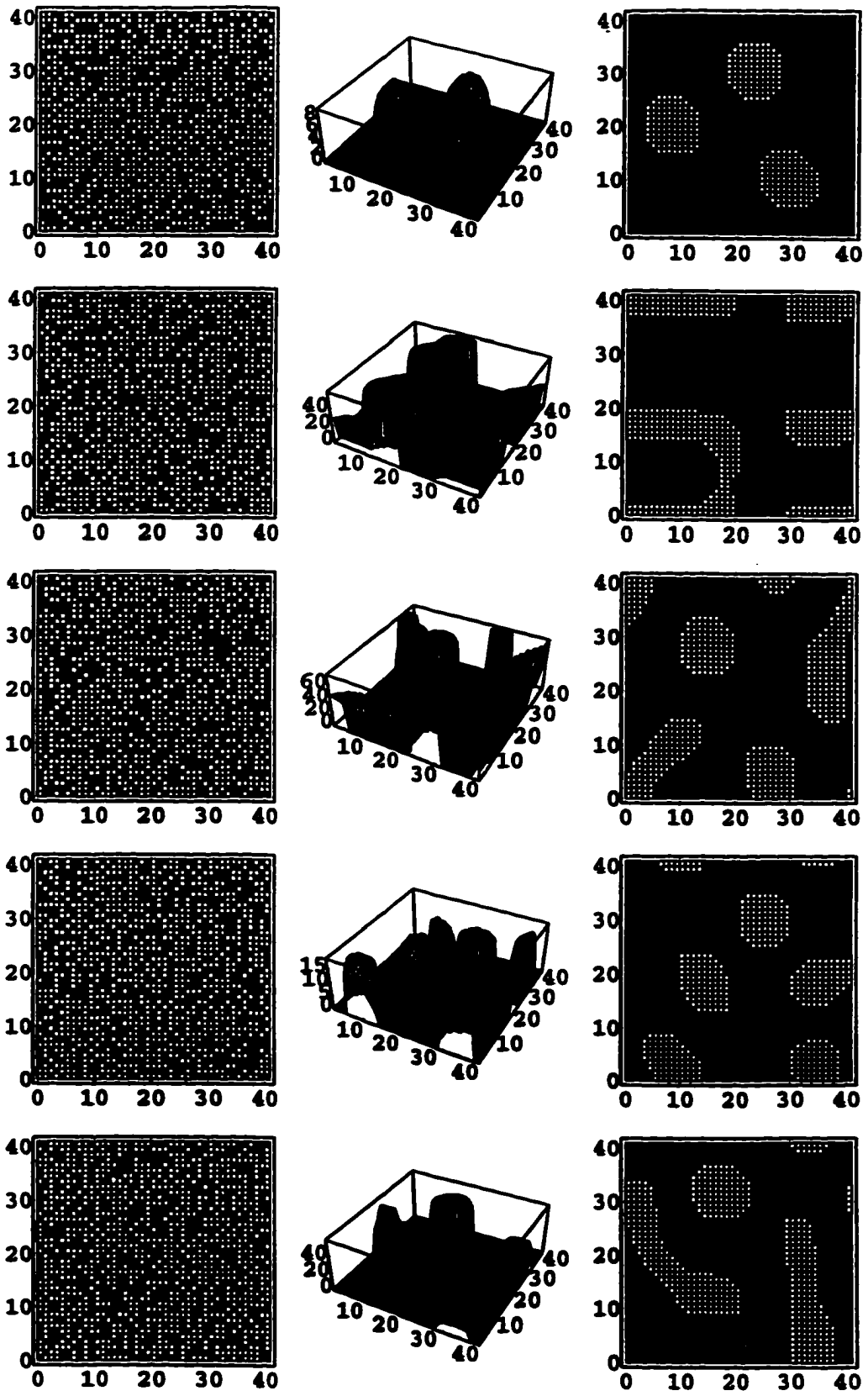


Figure C.4: Reduced Function : Set 4

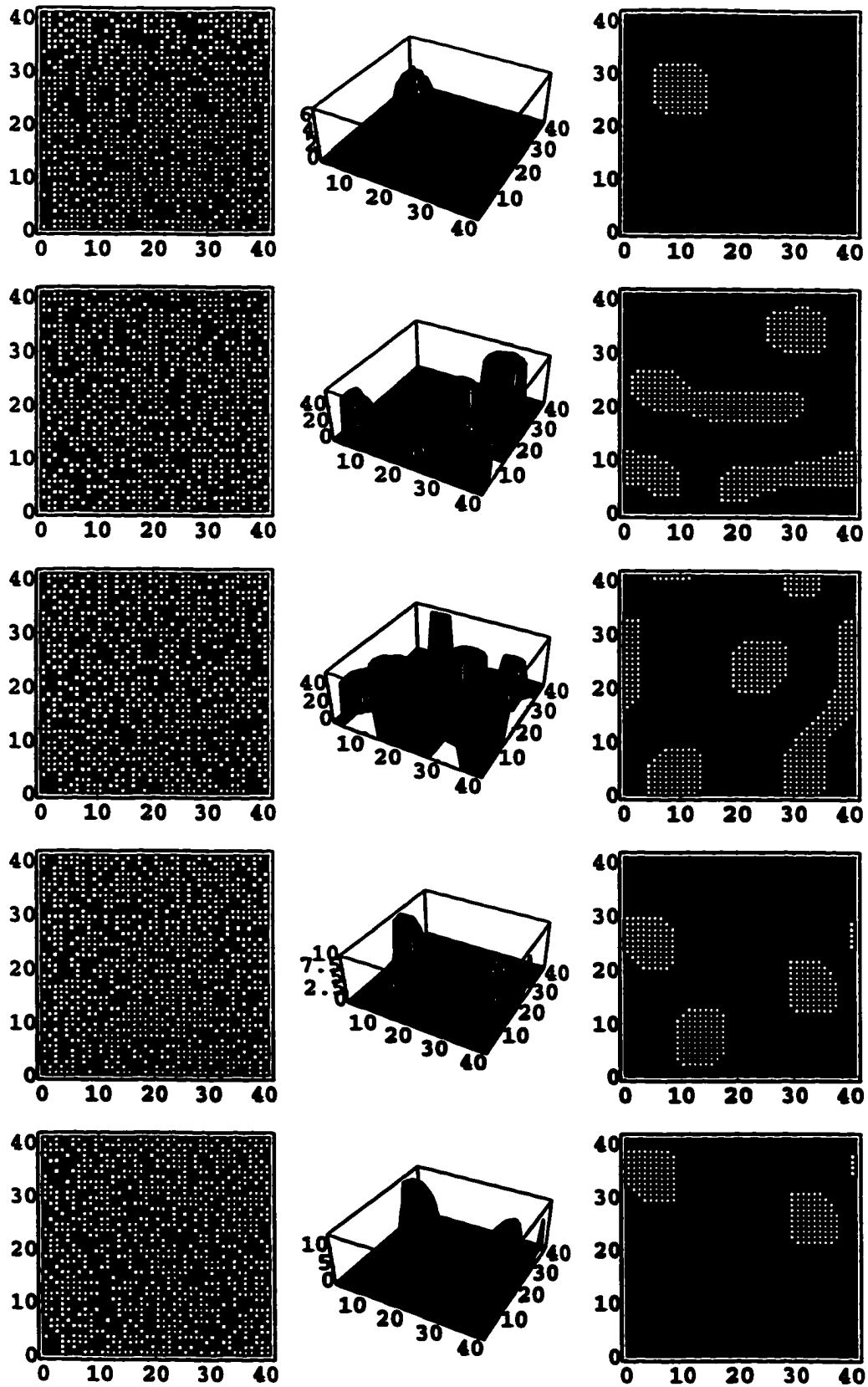


Figure C.5: Reduced Function : Set 5

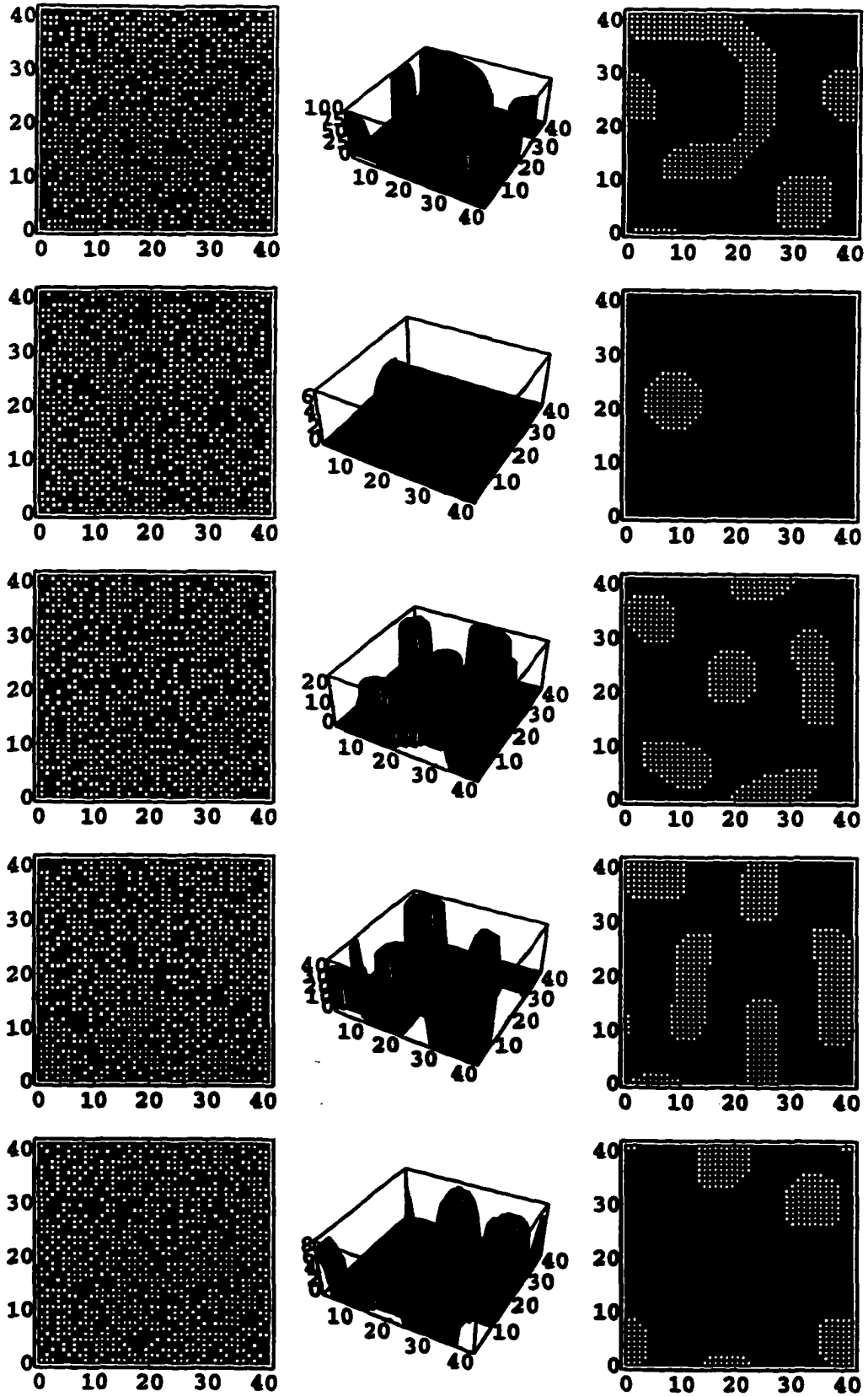


Figure C.6: Reduced Function : Set 6

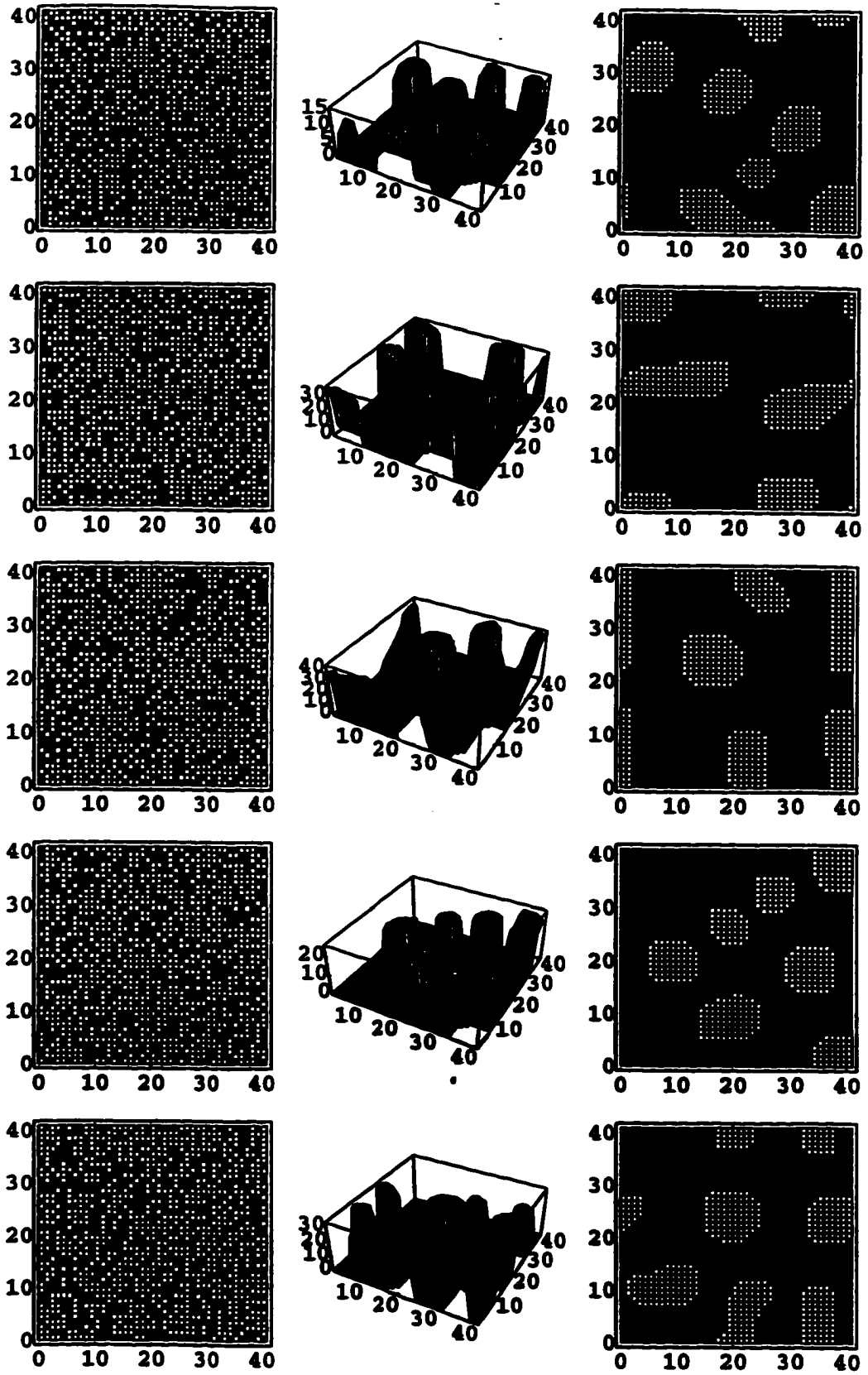


Figure C.7: Reduced Function : Set 7

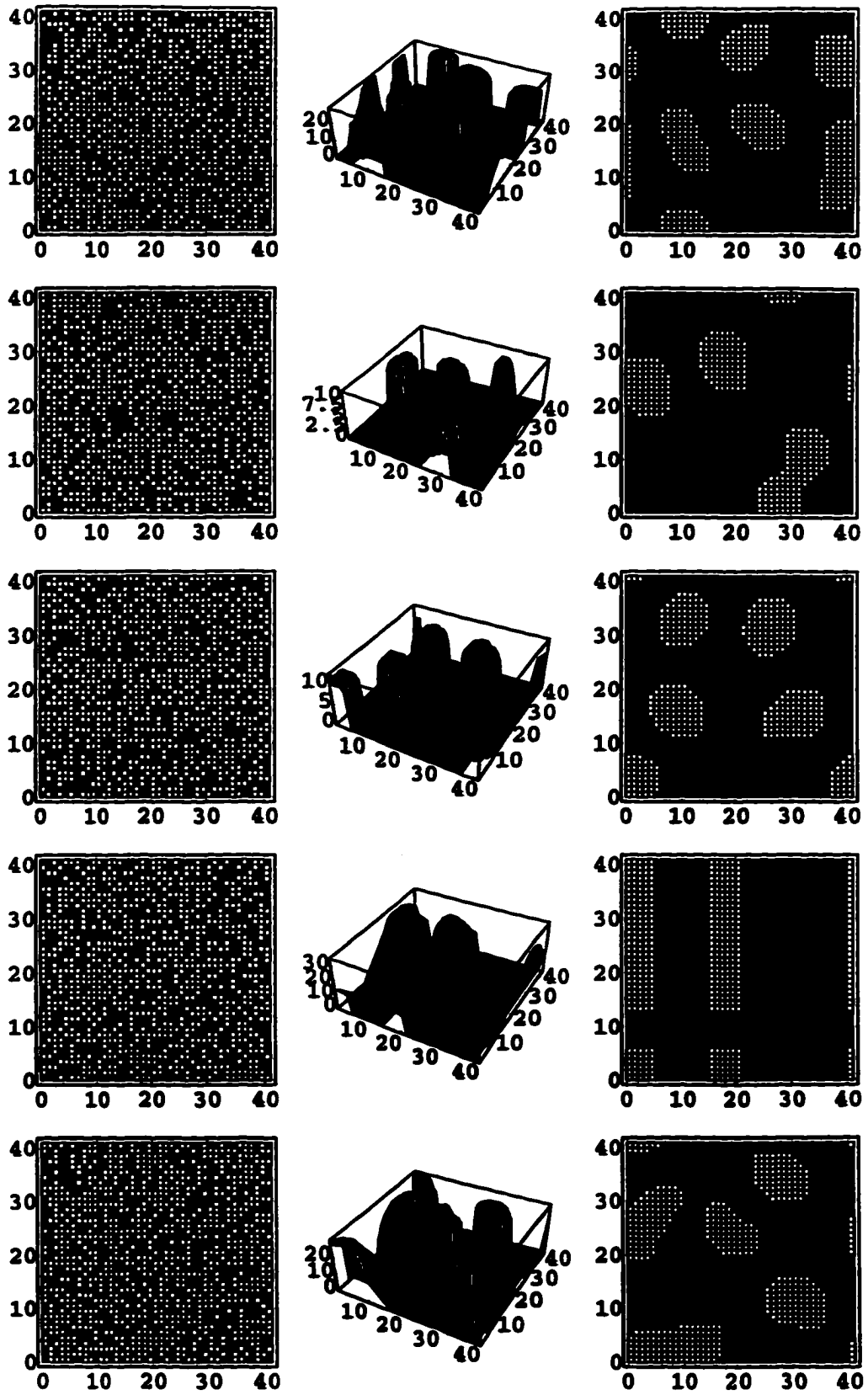


Figure C.8: Reduced Function : Set 8

APPENDIX D

SELF PARTITIONING ON WALSH PATTERNS

This appendix shows the steady states reached in a series of simulations of automatic cluster formation. A total of 136 regular patterns were selected from the set of Walsh patterns for a 41 by 41 binary array. Patterns not selected represent complementary patterns and diagonal reflections. Each page shows 10 initial states, except the last which shows 6. To the right of each initial state is a three-dimensional chart. The chart indicates the number of iterations for which each array element was in the active state (+1) during that particular run.

The complete lateral interaction function (all three parts), described in Chapter 4, was used with $r_1 = 3$, $r_2 = 14$ and $r_3 = 41$. No bias was used and the threshold was set at zero.

There were 7 runs that were not stable after 99 iterations, (the stopping point in the simulation) indicating that stability was never reached. The minimum number of iterations for a run was zero. It occurred for the all zero initial state which was immediately stable. Many cases required fewer than 5 iterations to reach stability.

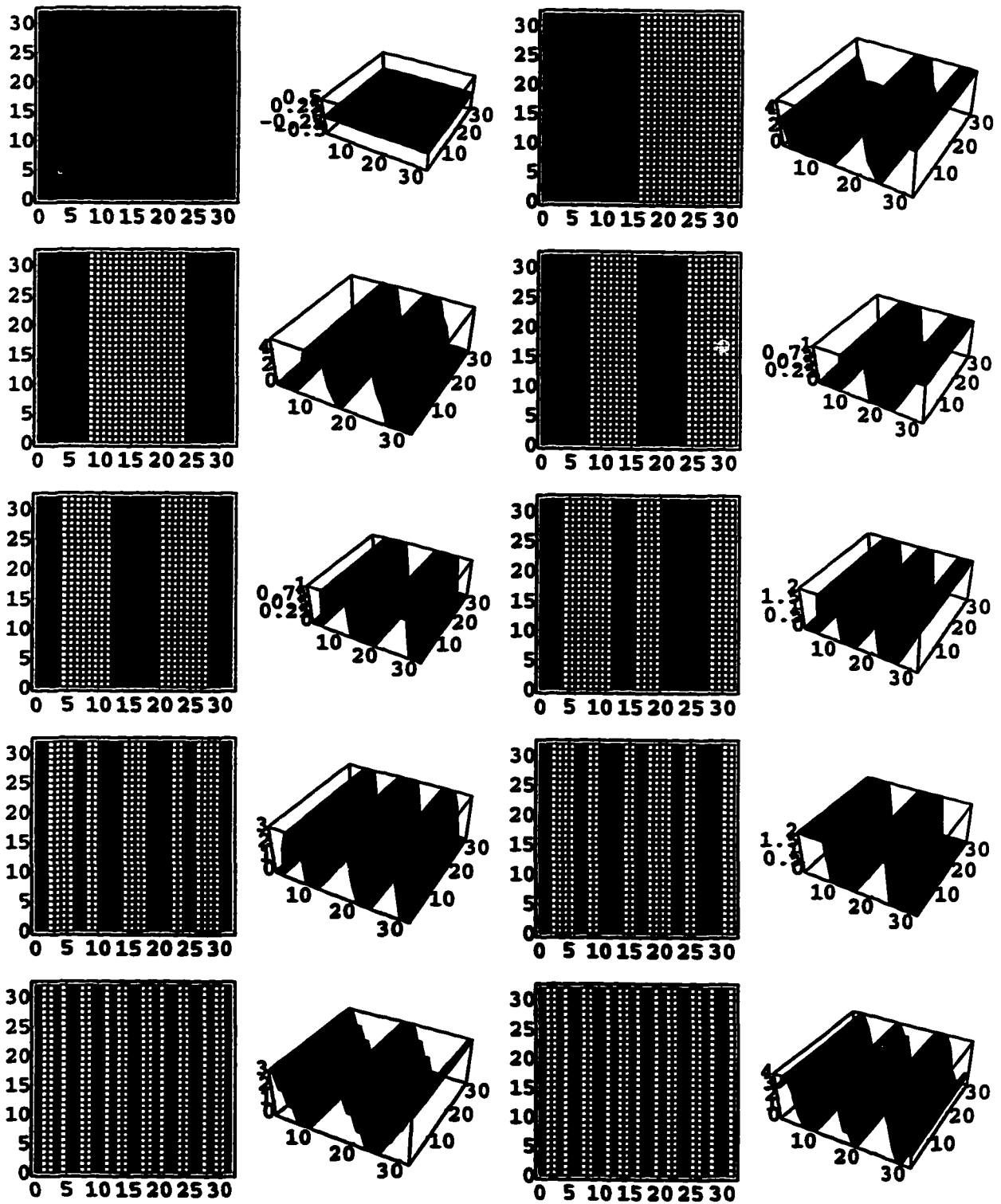


Figure D.1: Walsh Pattern Response : Set 1

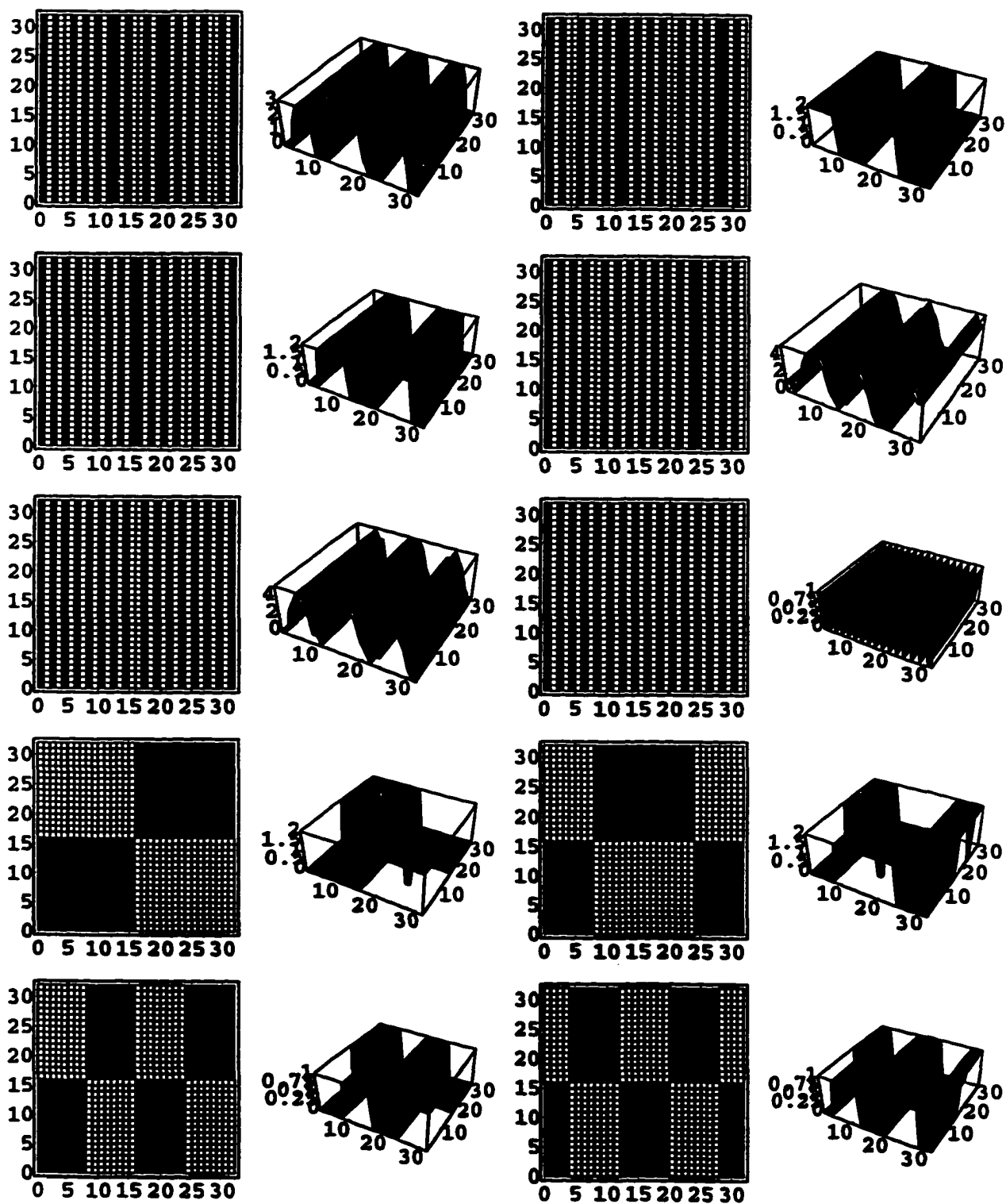


Figure D.2: Walsh Pattern Response : Set 2

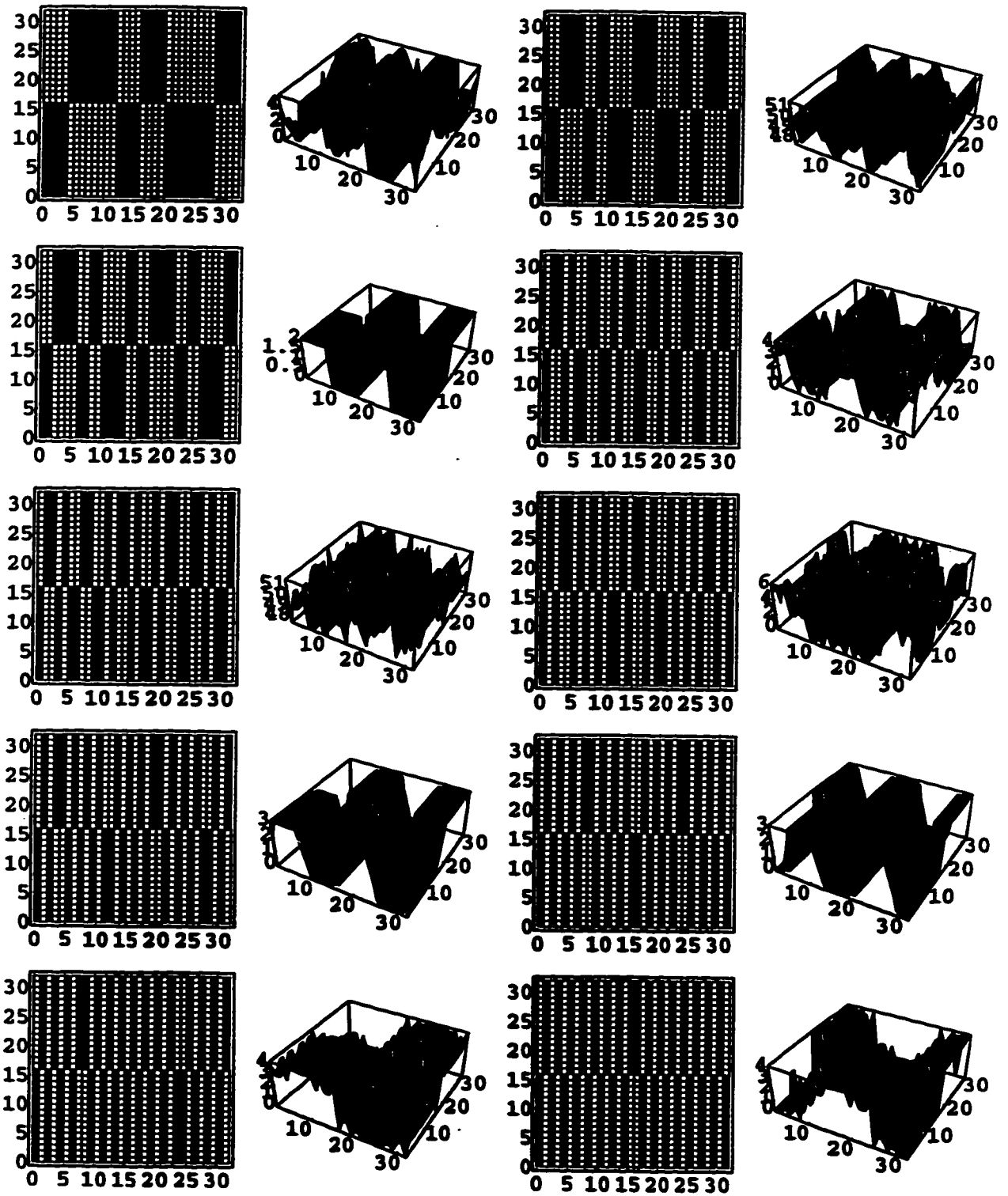


Figure D.3: Walsh Pattern Response : Set 3

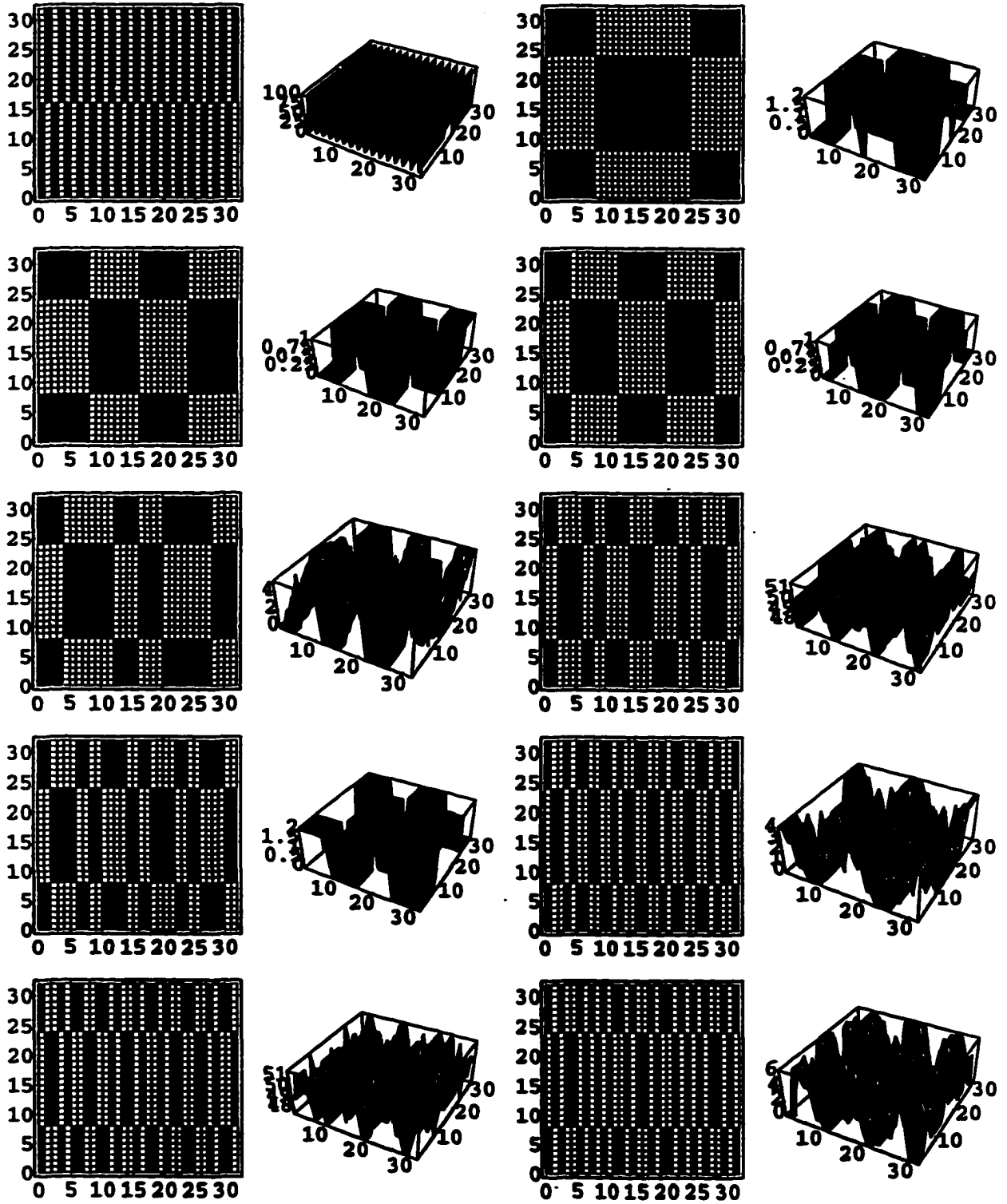


Figure D.4: Walsh Pattern Response : Set 4

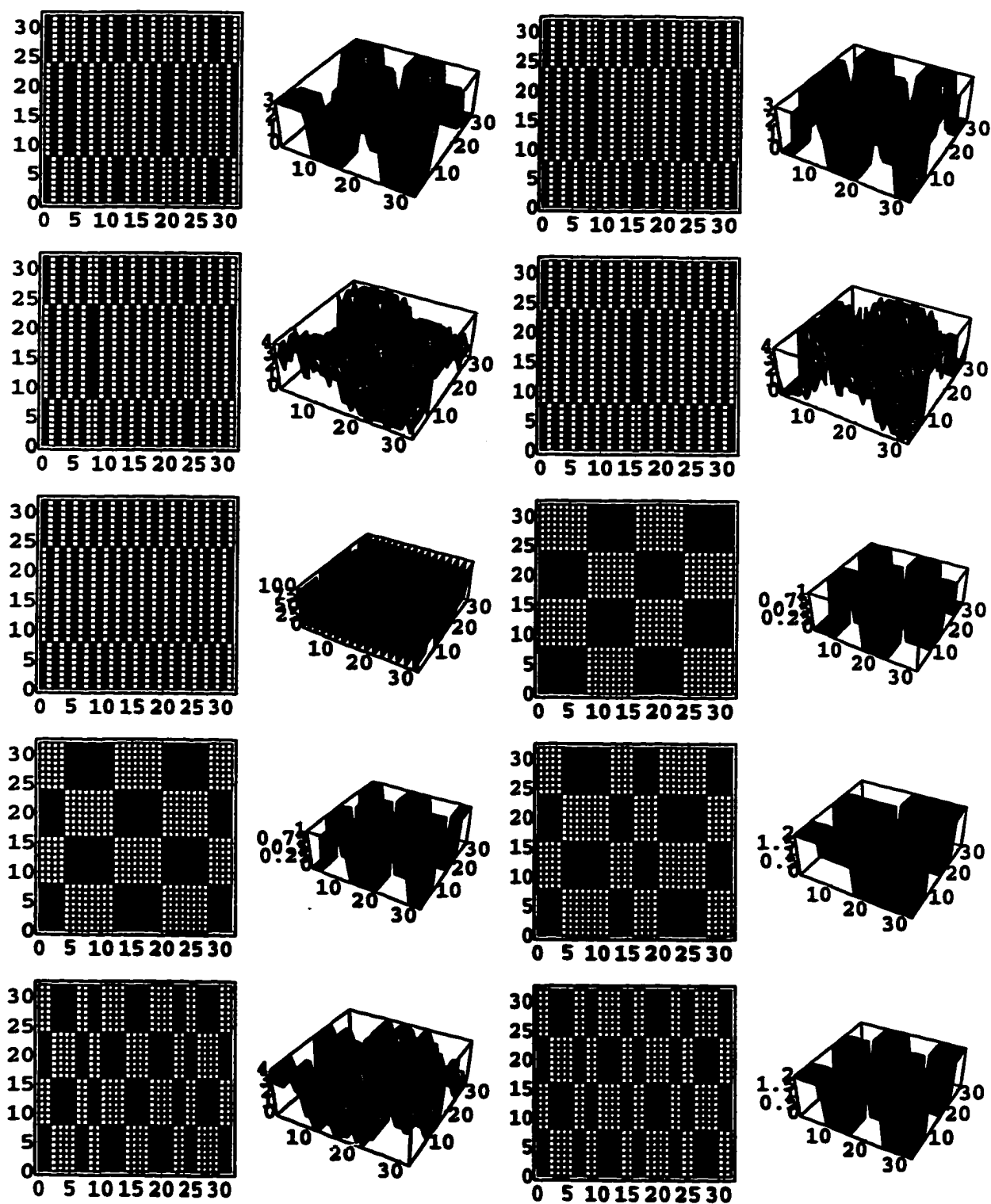


Figure D.5: Walsh Pattern Response : Set 5

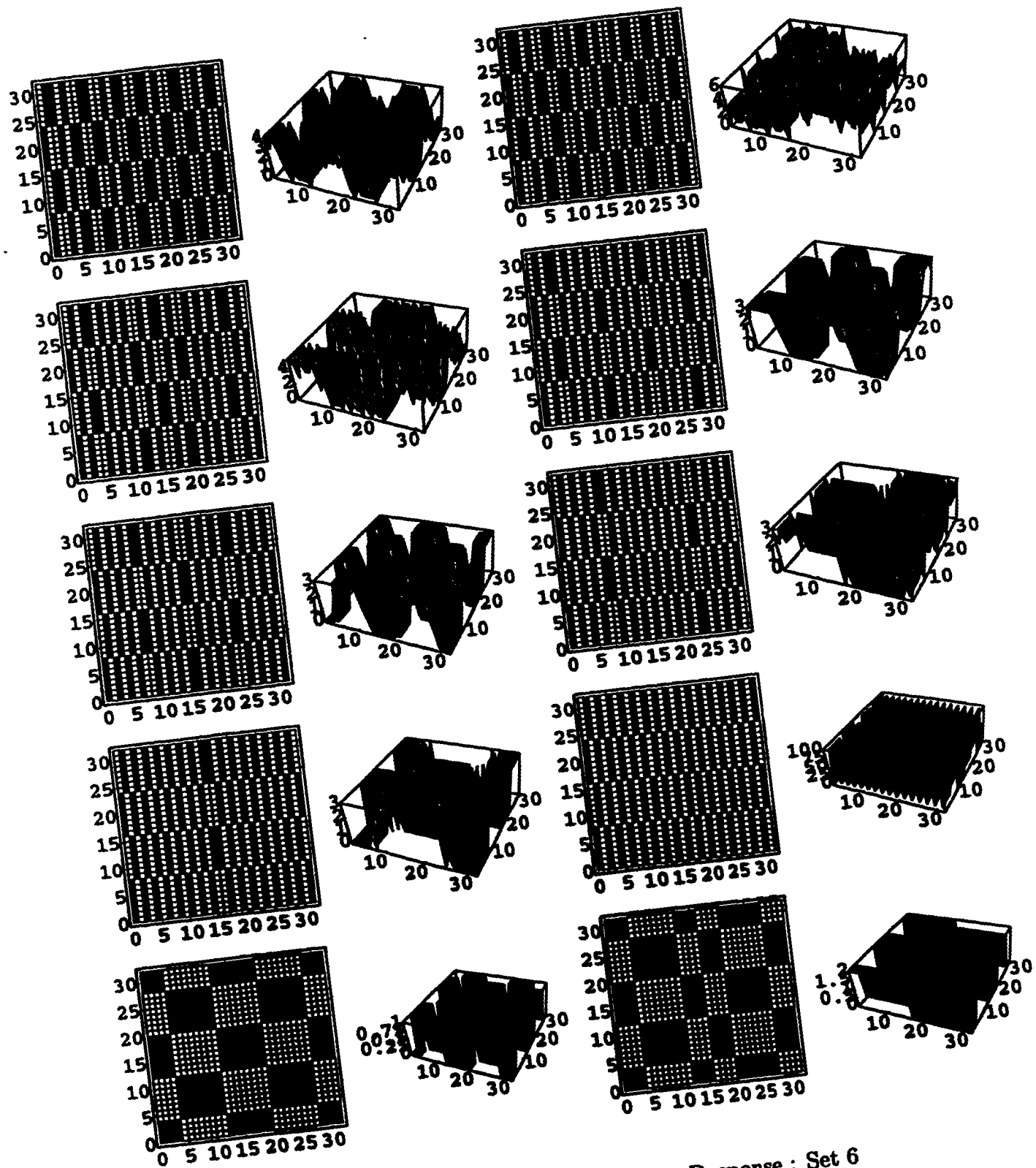


Figure D.6: Walsh Pattern Response : Set 6

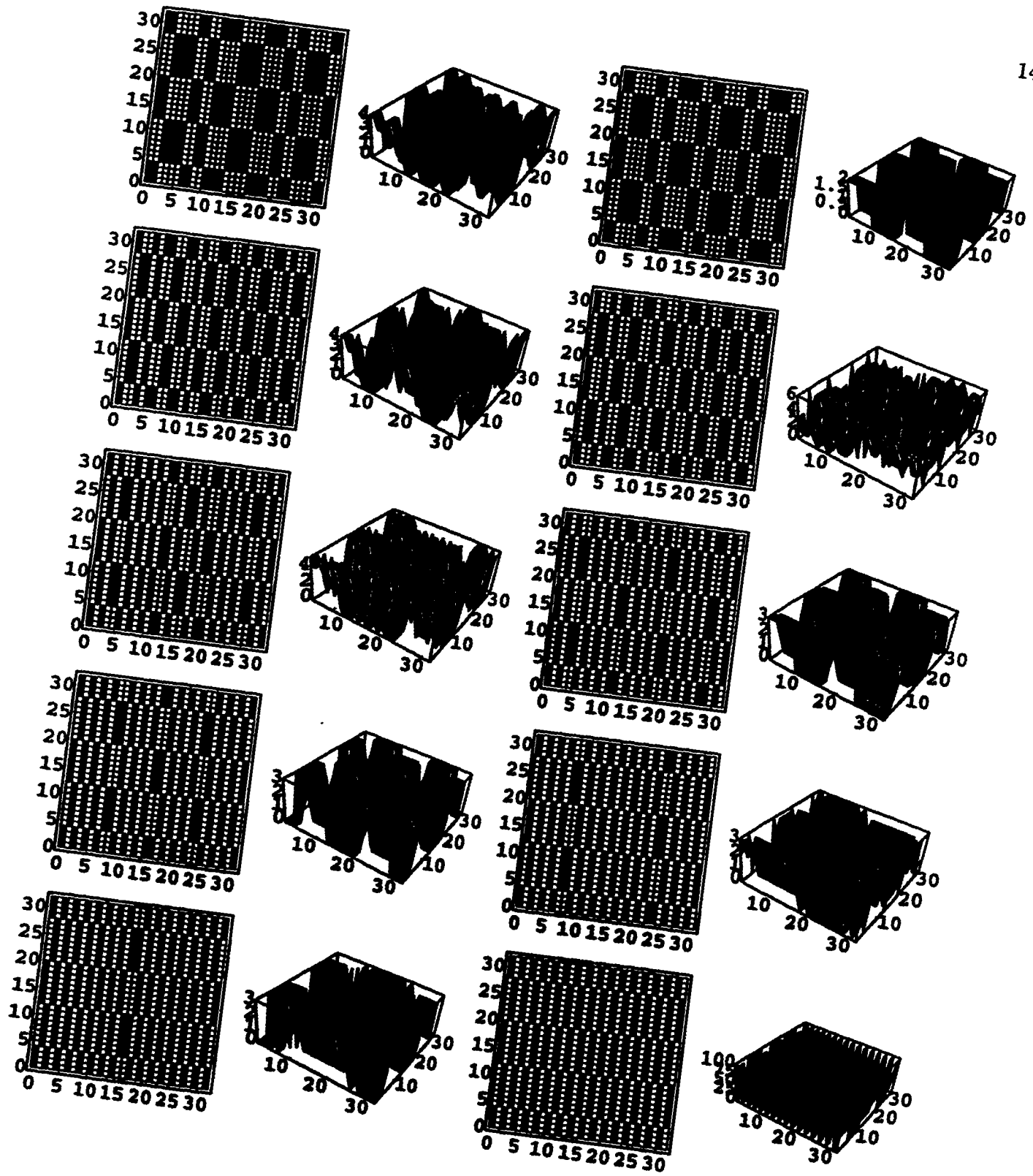


Figure D.7: Walsh Pattern Response : Set 7

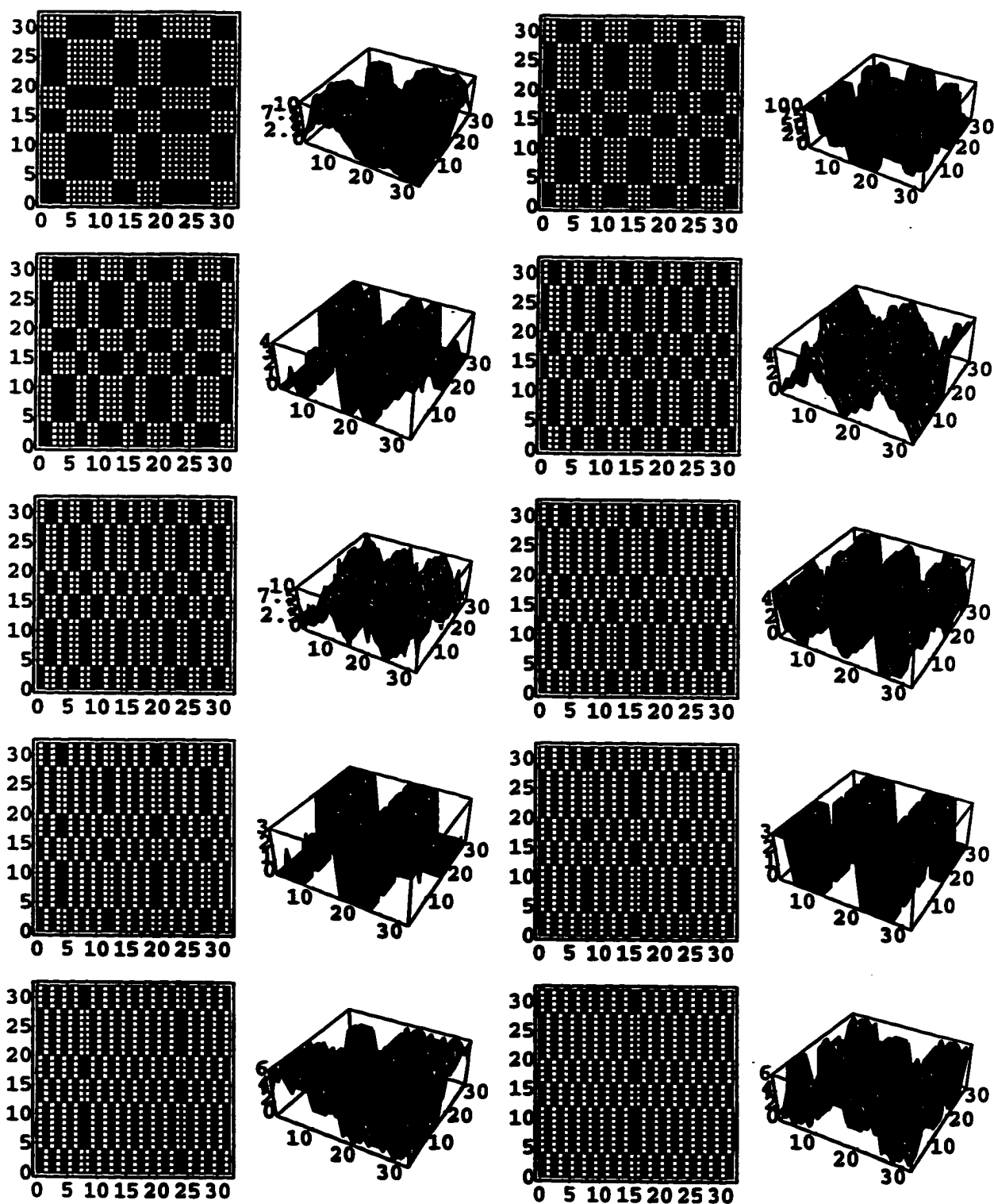


Figure D.8: Walsh Pattern Response : Set 8

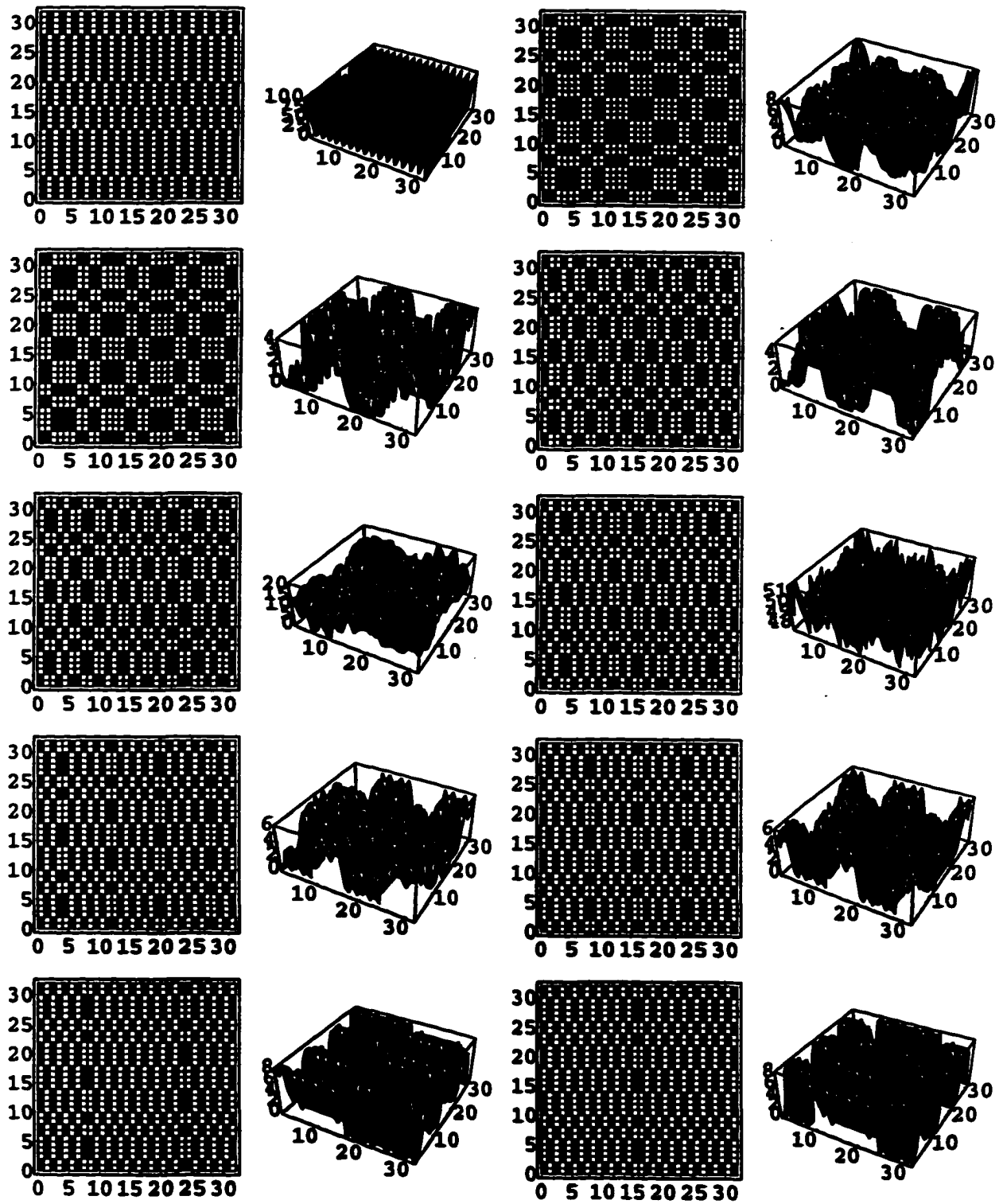


Figure D.9: Walsh Pattern Response : Set 9

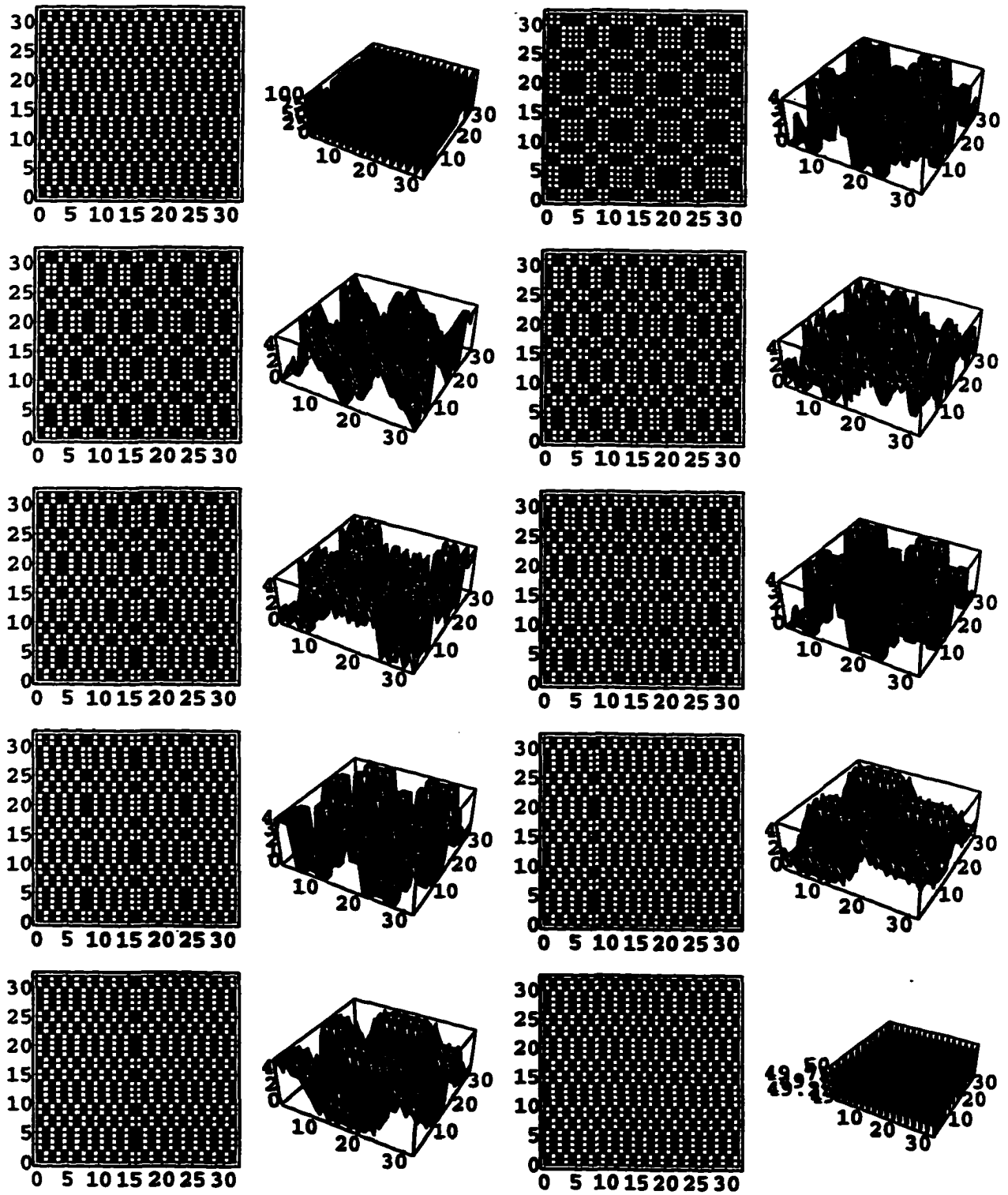


Figure D.10: Walsh Pattern Response : Set 10

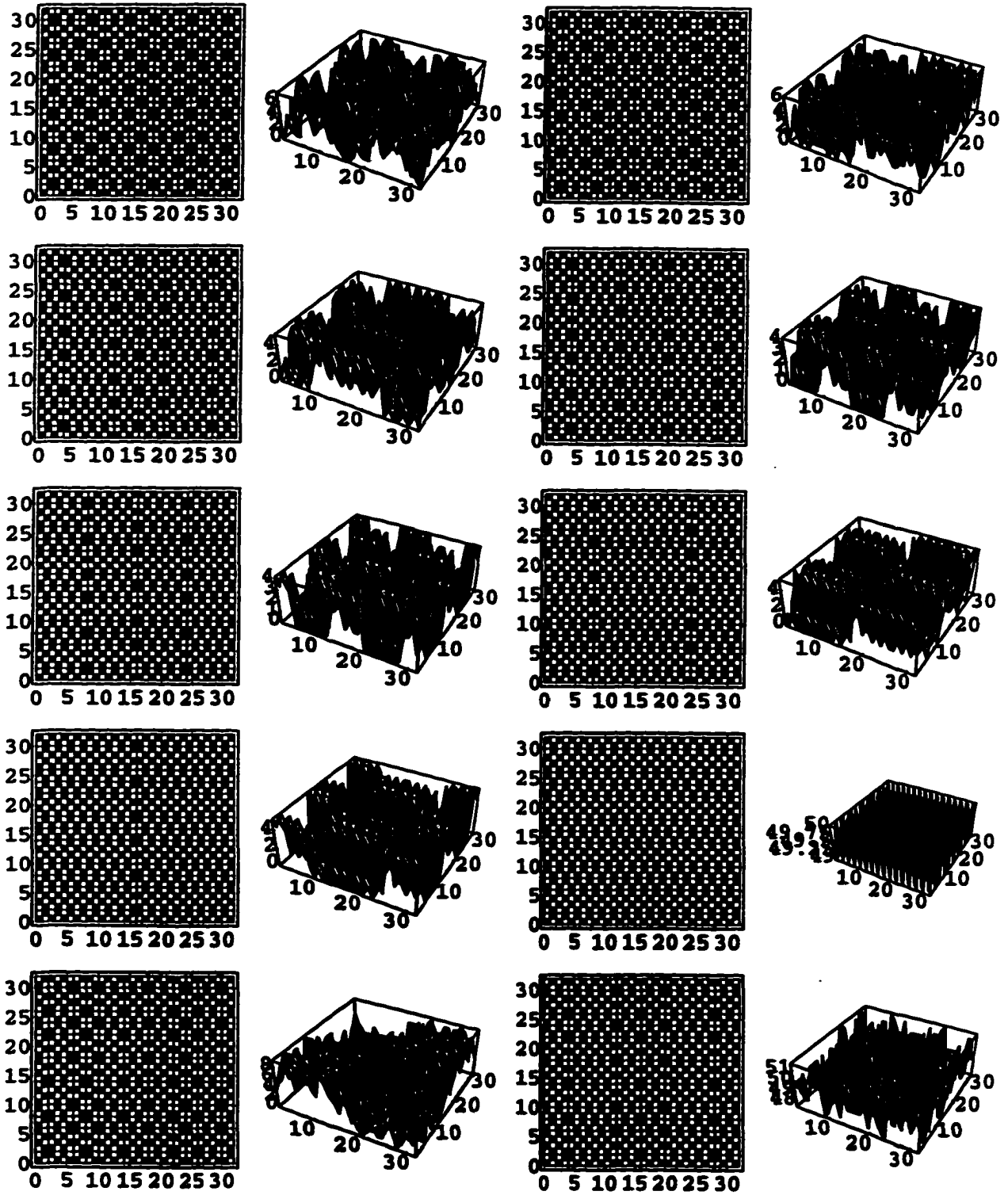


Figure D.11: Walsh Pattern Response : Set 11

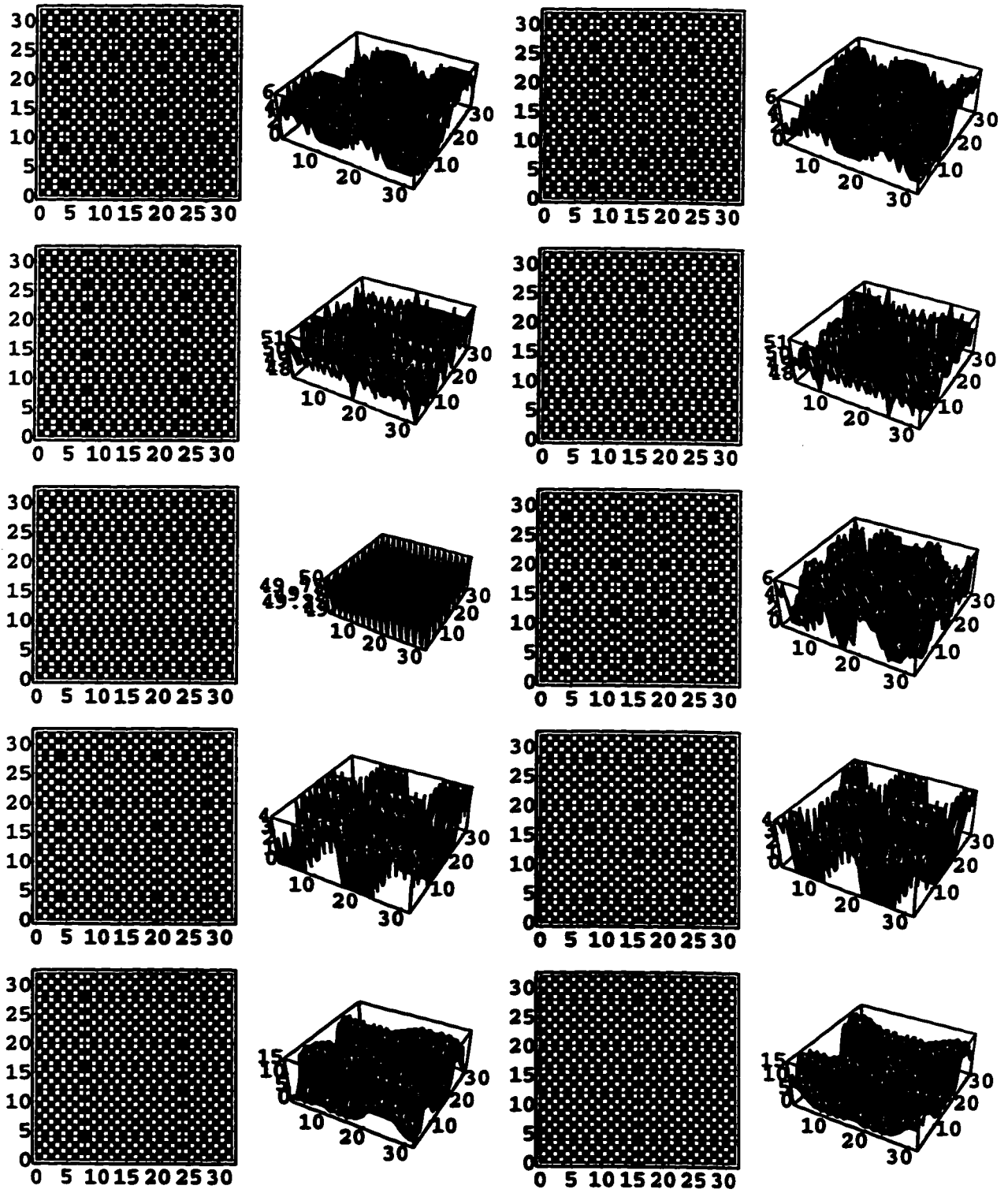


Figure D.12: Walsh Pattern Response : Set 12

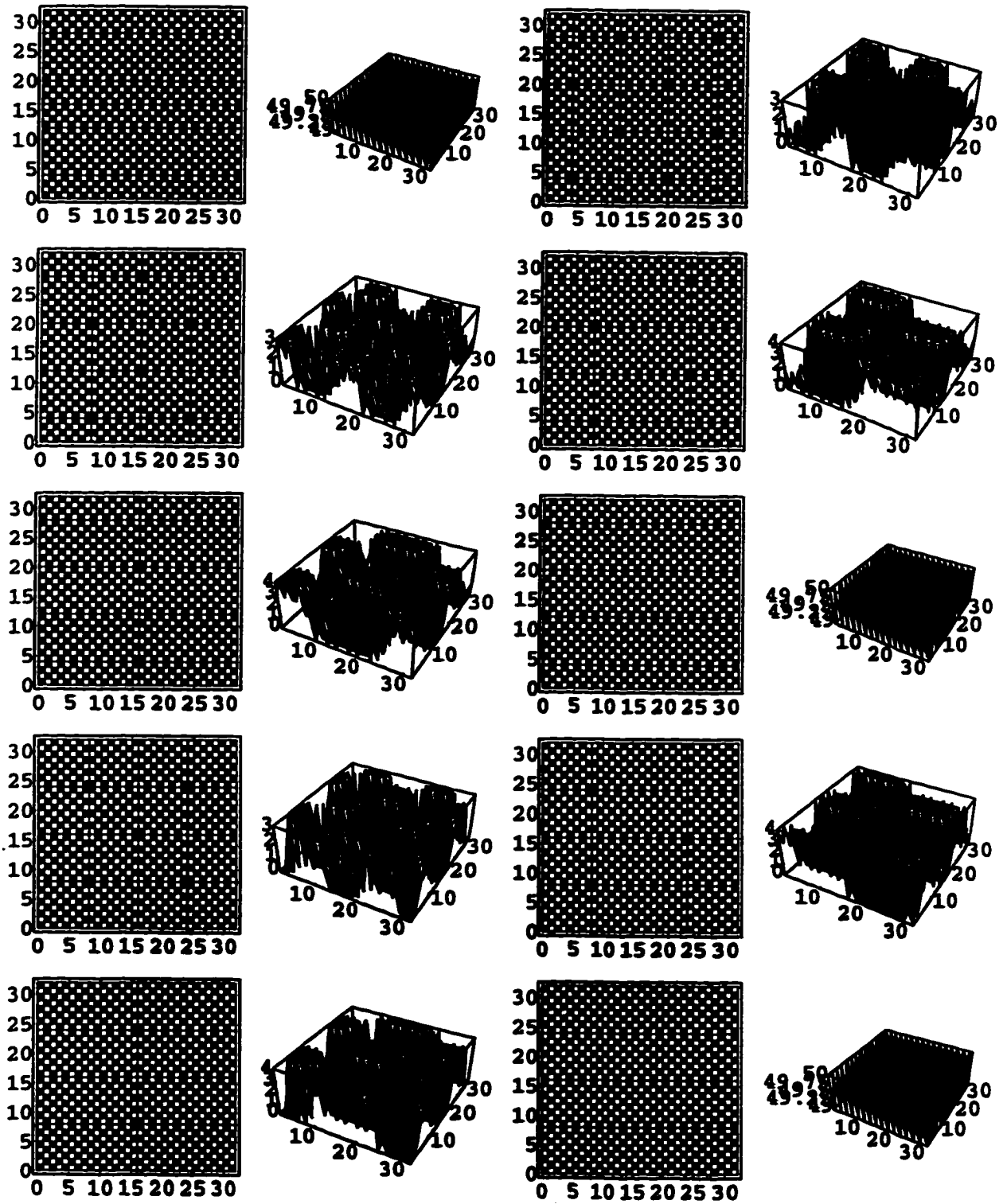


Figure D.13: Walsh Pattern Response : Set 13

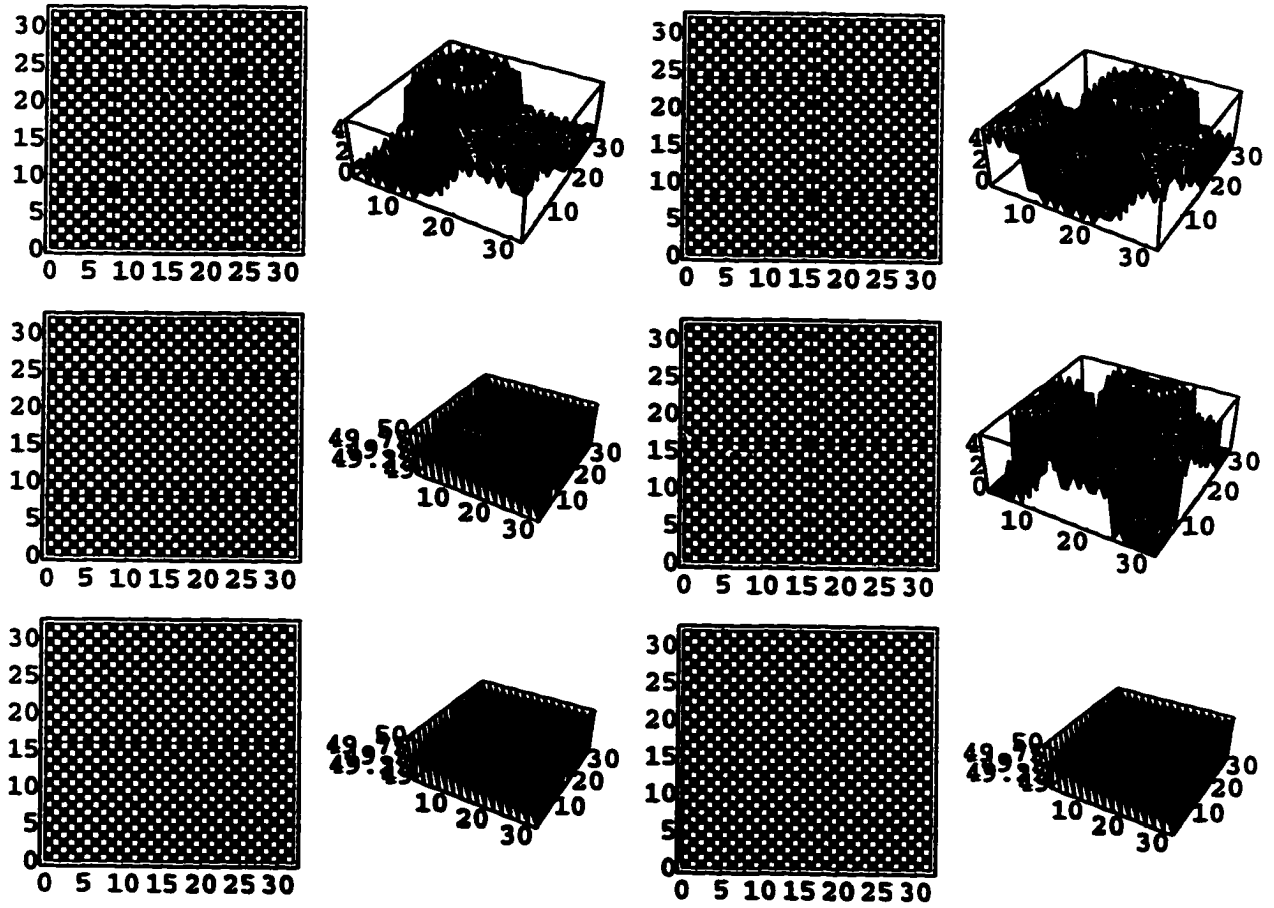


Figure D.14: Walsh Pattern Response : Set 14

APPENDIX E

FEATURE BASED RETRIEVAL RESULTS

The following three tables illustrate the response of our feature based retrieval model to probed input. A discussion of these tables is found in Chapter 5.

Table E.1: Probe Percent Correlations

	probe 1	probe 2	probe 3	probe 4	probe 5	probe 6
patt. 1	50.000	0.000	50.000	50.000	100.000	50.000
patt. 2	75.000	25.000	25.000	25.000	75.000	75.000
patt. 3	75.000	25.000	75.000	25.000	75.000	25.000
patt. 4	100.000	50.000	50.000	0.000	50.000	50.000
patt. 5	25.000	25.000	25.000	75.000	75.000	75.000
patt. 6	50.000	50.000	0.000	50.000	50.000	100.000
patt. 7	75.000	75.000	25.000	25.000	25.000	75.000
patt. 8	25.000	25.000	75.000	75.000	75.000	25.000
patt. 9	50.000	50.000	100.000	50.000	50.000	0.000
patt.10	75.000	75.000	75.000	25.000	25.000	25.000
patt.11	0.000	50.000	50.000	100.000	50.000	50.000
patt.12	25.000	75.000	25.000	75.000	25.000	75.000
patt.13	25.000	75.000	75.000	75.000	25.000	25.000
patt.14	50.000	100.000	50.000	50.000	0.000	50.000

Table E.2: Final Percent Correlations (Random)

	probe 1	probe 2	probe 3	probe 4	probe 5	probe 6
patt. 1	57.143	21.429	42.857	42.857	78.571	57.143
patt. 2	78.571	0.000	21.429	21.429	100.000	78.571
patt. 3	78.571	42.857	64.286	21.429	57.143	35.714
patt. 4	100.000	21.429	42.857	0.000	78.571	57.143
patt. 5	35.714	42.857	21.429	64.286	57.143	78.571
patt. 6	57.143	21.429	0.000	42.857	78.571	100.000
patt. 7	78.571	42.857	21.429	21.429	57.143	78.571
patt. 8	21.429	57.143	78.571	78.571	42.857	21.429
patt. 9	42.857	78.571	100.000	57.143	21.429	0.000
patt.10	64.286	57.143	78.571	35.714	42.857	21.429
patt.11	0.000	78.571	57.143	100.000	21.429	42.857
patt.12	21.429	57.143	35.714	78.571	42.857	64.286
patt.13	21.429	100.000	78.571	78.571	0.000	21.429
patt.14	42.857	78.571	57.143	57.143	21.429	42.857

Table E.3: Final Percent Correlations (FBR)

	probe 1	probe 2	probe 3	probe 4	probe 5	probe 6
patt. 1	57.143	0.000	42.857	42.857	100.000	57.143
patt. 2	78.571	21.429	21.429	21.429	78.571	78.571
patt. 3	78.571	21.429	64.286	21.429	78.571	35.714
patt. 4	100.000	42.857	42.857	0.000	57.143	57.143
patt. 5	35.714	21.429	21.429	64.286	78.571	78.571
patt. 6	57.143	42.857	0.000	42.857	57.143	100.000
patt. 7	78.571	64.286	21.429	21.429	35.714	78.571
patt. 8	21.429	35.714	78.571	78.571	64.286	21.429
patt. 9	42.857	57.143	100.000	57.143	42.857	0.000
patt.10	64.286	78.571	78.571	35.714	21.429	21.429
patt.11	0.000	57.143	57.143	100.000	42.857	42.857
patt.12	21.429	78.571	35.714	78.571	21.429	64.286
patt.13	21.429	78.571	78.571	78.571	21.429	21.429
patt.14	42.857	100.000	57.143	57.143	0.000	42.857

Vita

David Timothy Young was born August 11, 1965 in Oak Ridge, Tennessee. He is the son of Dr. Myron H. and Marlene S. Young. He graduated from Baton Rouge Magnet High School in 1983. Honorary societies of which he has been an active member include Tau Beta Pi, Pi Mu Epsilon and Gamma Beta Phi. He received the Bachelor of Science Degree and the Master of Science Degree in Computer Engineering from Louisiana State University in 1987 and 1989, respectively. Currently he is a candidate for the Degree of Doctor of Philosophy which will be conferred in August, 1997.


DOCTORAL EXAMINATION AND DISSERTATION REPORT

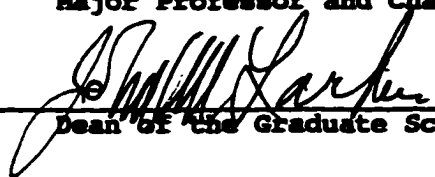
Candidate: David T. Young

Major Field: Electrical Engineering

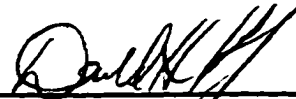
Title of Dissertation: A Theory of Cortical Neural Processing


Approved:


Major Professor and Chairman



Dean of the Graduate School

EXAMINING COMMITTEE:





J. R. _____



Mark J. Davidson

Date of Examination:

June 18, 1997